Characterization of exosomes as a diagnostic marker in neurodegenerative diseases

---

Dissertation

in partial fulfillment for the award of the degree

"Doctor rerum naturalium"

of the Georg-August University Göttingen

within the doctoral program "Molecular Physiology of the Brain"

of the Georg-August University School of Science (GAUSS)

submitted by

Anne-Katrin Stündl

from Giessen

Göttingen 2016

Thesis Committee

Prof. Dr. Mikael Simons (Reviewer)

Institute of Neuronal Cell Biology, Technical University Munich

Prof. Dr. Blanche Schwappach (Reviewer)

Department of Molecular Biology, University Medical Center Göttingen

Prof. Dr. Anja Schneider

German Center for Neurodegenerative Diseases (DZNE), Göttingen

Members of the Examination Board

Members of the Thesis Committee and

Prof. Dr. Dr. Hannelore Ehrenreich

Department of Clinical Neuroscience, Max-Planck Institute of Experimental Medicine, Göttingen

Prof. Dr. André Fischer

German Center for Neurodegenerative Diseases (DZNE), Göttingen and
Department of Psychiatry and Psychotherapy, University Medical Center Göttingen

Prof. Dr. Michael Hörner

Johann-Friedrich-Blumenbach Institute for Zoology and Anthropology, Georg-August University Göttingen

Date of oral examination: 16.08.2016

Affidavit

I hereby declare that I have written my doctoral thesis entitled “Characterization of exosomes as a diagnostic marker in neurodegenerative diseases” independently with no other sources and aids than quoted.

Göttingen, 31.05.2016 Anne Stündl

List of Contents

Acknowledgements

I am deeply grateful to the following persons who have – each in her or his own way – contributed to this thesis.

First, I want to thank my supervisor Prof. Dr. Anja Schneider for introducing me to the 'world of exosomes' and for guiding me throughout my PhD studies. Thank you for allowing me to work independently on interesting projects and collaborations, for your ideas, trust and your scientific input and advices. I really learned a lot.
I also want to thank my Thesis Committee members Prof. Dr. Mikael Simons and Prof. Dr. Blanche Schwappach for further support during my thesis with helpful comments and discussions. Furthermore, I would like to thank Prof. Dr. Dr. Hannelore Ehrenreich, Prof. Dr. André Fischer and Prof. Dr. Michael Hörner for being part of my examination board.

In addition, I am thankful to all the collaborators who contributed to complete my thesis. I would like to thank Dr. Niels Kruse for plenty of α-Synuclein measurements, Prof. Dr. Brit Mollenhauer for providing CSF and plasma samples and all patients who have given their consent to use their CSF and plasma for scientific research purpose. Furthermore, I thank Prof. Dr. Karin Danzer and her lab for performing the protein-fragment complementation assay.
Regarding the small RNA project, I would like to acknowledge Prof. Dr. André Fischer, Susanne Burkhardt who has sequenced all my samples and especially Gaurav Jain for processing NGS data, performing bioinformatic analyses and for his great (last-minute) help.

I also want to appreciate the Göttingen Graduate School for Neuroscience and Biophysics (GGNB) for offering an excellent learning environment, especially Michael Hörner for arranging interesting PhD seminars and retreats.

Special thanks go to:

… all formers and currents of the Schneider lab especially Angela (for taking care of my always spilling over waste bag on my bench and for refilling my buffers without asking), Petra (for the best triple-chocolate-cake of the world and lending an ear in each situation), Belisa (for being the best bench mate and horoscope reader), Beate (for providing peanut butter candies for me, even across the ocean), Marcel (for teaching me multiple methods when I came to the lab and for your diverse support and help) as well as Jing and Tao for the nice working atmosphere.

… Daniel and Uli from the DZNE for taking care of everything what is close to 'administrative work'.

... my friends from the Simons lab for allowing me to crash your coffee breaks, for cookie baking nights and for funny times outside the lab, especially Tina for your great help in many situations and for being my friend.

… my friends from outside Göttingen (you know who you are) who have accompanied me since school or university and still do so. Thank you for your immense support and for always being next to me.

Zudem gilt mein größter Dank meiner Familie für die unendliche Unterstützung, Förderung und Freiheit, die ihr mir all die Jahre gegeben habt.
Mama, danke für das schöne Gefühl nach Hause zu kommen…

List of Abbreviations

The International System of Units (SI) base units and prefixes for unit names have been used and are not specified in this list.

°C	degree Celsius
a.m.	*ante meridiem* (latin = before midday)
AD	Alzheimer`s disease
ALS	amyotrophic lateral sclerosis
ANOVA	analysis of variance
APP	Amyloid precursor protein
APS	ammonium persulfate
AUC	area under the curve
Aβ	β-amyloid peptide
BSA	bovine serum albumin
C	carboxy
CHAPS	3-[(3-cholamidopropyl)dimethylammonio]-1-propanesulfonate
CNS	central nervous system
CSF	cerebrospinal fluid
Ctr	control
CV	Coefficient of variance
DC	dendritic cell
DeNoPa	de novo Parkinson
dH_2O	distilled water
DLB	dementia with Lewy bodies
DMEM	Dulbecco`s modified eagle medium
ECL	electrochemiluminescence
EDTA	ethylenediaminetetraacetic acid
ELISA	enzyme-linked immunosorbent assay
EM	electron microscopy
ESCRT	endosomal sorting complex required for transport
et al.	*et alii* (Latin = and others)
EV	extracellular vesicles
FCS	fetal calf serum

FRET	fluorescence resonance energy transfer
H&Y	Hoehn and Yahr
HBSS	Hank`s buffered saline solution
hnRNPA2B1	heterogenous nuclear ribonucleoprotein A2B1
HRP	horseradish peroxidase
IgG	Immunoglobulin G
ILV	intraluminal vesicle
IRB	institutional review board
LB	Lewy body
MCI	mild cognitive impairment
MHC	major histocompatibility complex
min	minute(s)
miRNA	micro RNA
MMSE	mini-mental state examination
mRNA	messenger RNA
MSA	multiple system atrophy
MV	microvesicle
MVB	multivesiclular body
n	number of biological replicates
N	amino
ncRNA	non-coding RNA
Neurol. Ctrl.	neurological control(s)
NGS	next-generation sequencing
NTA	nanoparticle tracking analysis
PAGE	polyacrylamide gel electrophoresis
PBS	phosphate buffered saline
PBST	phosphate buffered saline supplemented with Tween-20
PD	Parkinson`s disease
PFA	paraformaldehyde
pH	potential hydrogen
piRNA	piwi-interacting RNA
PNP	polyneuropathy
PrP	prion protein
PSP	progressive supranuclear palsy

Rab	Ras-related in brain
RISC	RNA-induced silencing complex
RNA	ribonucleic acid
ROC	receiver operating characteristics
rpm	revolutions per minute
rRNA	ribosomal RNA
RT	room temperature
SDS	sodium dodecyl sulfate
SEC	size exclusion chromatography
SEM	standard error of the mean
snoRNA	small nucleolar RNA
snRNA	small nuclear RNA
SOP	standard operating procedure
TBS	tris buffered saline
TEMED	N'N'N'-tetramethylethylene diamine
Tris	tris(hydroxymethyl)aminomethane
tRNA	transfer RNA
UC	ultracentrifugation
v/v	volume per volume
w/v	weight per volume
WB	western blot
x g	Times gravitational acceleration

List of Figures

List of Tables

Summary

α-Synuclein pathology has been hypothesized to propagate in synucleinopathies by intercellular transfer of pathogenic seeds in a prion-like fashion. Extracellular release of α-Synuclein via small extracellular vesicles has been proposed as one of the mechanisms of cell-to-cell disease transmission. *In vitro*, extracellular α-Synuclein has been detected in exosomal vesicles and we have recently provided evidence that α-Synuclein is present in exosomes in the central nervous system *in vivo*.

We hypothesized that exosomes from patients with α-Synuclein related neurodegeneration serve as carriers for interneuronal disease transfer. In this study, we purified exosomes from cerebrospinal fluid from patients with synucleinopathies including Parkinson`s disease and dementia with Lewy bodies, progressive supranuclear palsy as an example of a disease that clinically overlaps with Parkinson`s disease but without underlying α-Synuclein pathology and other neurological controls without neurodegenerative diseases. Exosome numbers and exosomal α-Synuclein levels were quantified and their potential to induce aggregation of soluble α-Synuclein was evaluated. We observed differences in cerebrospinal fluid exosomal α-Synuclein levels between patients with Parkinson`s disease and dementia with Lewy bodies and between dementia with Lewy bodies and controls. In addition, exosomal α-Synuclein levels correlated with cognitive decline and Tau levels as a marker of neurodegeneration in dementia with Lewy bodies. By analyzing exosomal α-Synuclein levels and exosome numbers, we were able to distinguish Parkinson`s disease from dementia with Lewy bodies and controls as well as dementia with Lewy bodies from Parkinson`s disease and controls with high sensitivity and specificity. Importantly, cerebrospinal fluid exosomes from Parkinson`s disease and dementia with Lewy bodies disease patients induced aggregation of α-Synuclein in a reporter cell model, dependent on the amount of exosomal α-Synuclein. Thus, exosomal α-Synuclein could serve as a diagnostic biomarker for α-Synuclein related neurodegenerative diseases and as a progression marker in dementia with Lewy bodies.

These findings further indicate that cerebrospinal fluid derived exosomes from patients with Parkinson`s disease and dementia with Lewy bodies contain a pathogenic α-Synuclein species, which induces aggregation of endogenous α-Synuclein in recipient neurons and therefore could transmit disease pathology.

Since multiple recent therapy trials in Alzheimer`s disease have failed and therapeutic interventions are most promising in early and even preclinical stages, the accurate identification of patients with Alzheimer`s disease is indispensable. Therefore, diagnostic and prognostic biomarkers are required and identification of such markers would also give insight into the underlying molecular mechanisms of Alzheimer`s disease pathology.
Accumulating evidence suggests that dysregulation of processes, which physiologically regulate gene expression, plays an important role in the pathogenesis of neurodegenerative diseases. Additionally, dysregulation of small non-coding RNAs in Alzheimer`s disease brain has been shown in various studies.

In our second study, we analyzed the small non-coding RNA composition of exosomes derived from human cerebrospinal fluid in order to test whether exosomal small non-coding RNA profiles can be used as a disease signature for Alzheimer`s disease.
Here, we show that genome-wide profiling of cerebrospinal fluid exosomal small non-coding RNA expression reveals a specific small RNA signature which differentiates Alzheimer`s disease from cognitive healthy controls. Thus, our selected set of exosomal small non-coding RNAs could be used as a potential biomarker in the future, replication in a larger validation cohort provided.

1. Introduction

1.1. Extracellular vesicles

Extracellular vesicles (EVs) are membrane vesicles which are secreted from prokaryotic and eukaryotic cells into the extracellular space. According to their subcellular origin, they can be divided into several subclasses. Exosomes are 30 – 100 nm in diameter, generated within the endosomal system and secreted into the extracellular space upon fusion of late endosomes with the plasma membrane, first described during reticulocyte maturation (Harding et al., 1983; Johnstone et al., 1987; Pan et al., 1985). Shedding vesicles display another class of EVs and originate from the plasma membrane. This EV population includes microvesicles (MVs) with a heterogenous shape and size of approximately 50 – 1000 nm and apoptotic bodies or blebs, which are generally larger and display a size range of 1 – 4 µm (Schneider and Simons, 2013). The latter are released from dying cells during apoptotic processes.

It has been shown by now that many different cell types release EVs including cells of hematopoetic origin, e.g. B-lymphocytes and dendritic cells (DCs) (Raposo et al., 1996; Zitvogel et al., 1998) but also other cells, such as neurons (Faure et al., 2006), oligodendrocytes (Kramer-Albers et al., 2007) and intestinal epithelial cells (van Niel et al., 2001). Moreover, EVs were identified and isolated from diverse body fluids such as urine, blood (plasma and serum), saliva and cerebrospinal fluid (CSF) (Caby et al., 2005; Palanisamy et al., 2010; Pisitkun et al., 2004; Street et al., 2012), thus demonstrating their secretion *in vivo*.

1.1.1. Biogenesis and extracellular release of exosomes

Exosomes are generated along the endocytic pathway which comprises the uptake of extracellular or cellular cargo into early endosomes and further sorting to the degradation or to the recycling pathway (Gould and Lippincott-Schwartz, 2009). During maturation from early endosomes to late endosomes (Stoorvogel et al., 1991), intraluminal vesicles (ILVs) are formed by inward budding of the endosomal membrane (Figure 1.1). The lumina of these endosomes are then filled with ILVs, a characteristic feature giving them the name multivesicular bodies (MVBs). During the process of ILV formation, proteins, lipids and

nucleic acids are sorted into the vesicles. Depending on their fate, MVBs fuse with the lysosome for the degradation of their cargo or they fuse with the plasma membrane to release their ILVs into the extracellular space (Colombo et al., 2014). Released ILVs are then referred to exosomes.

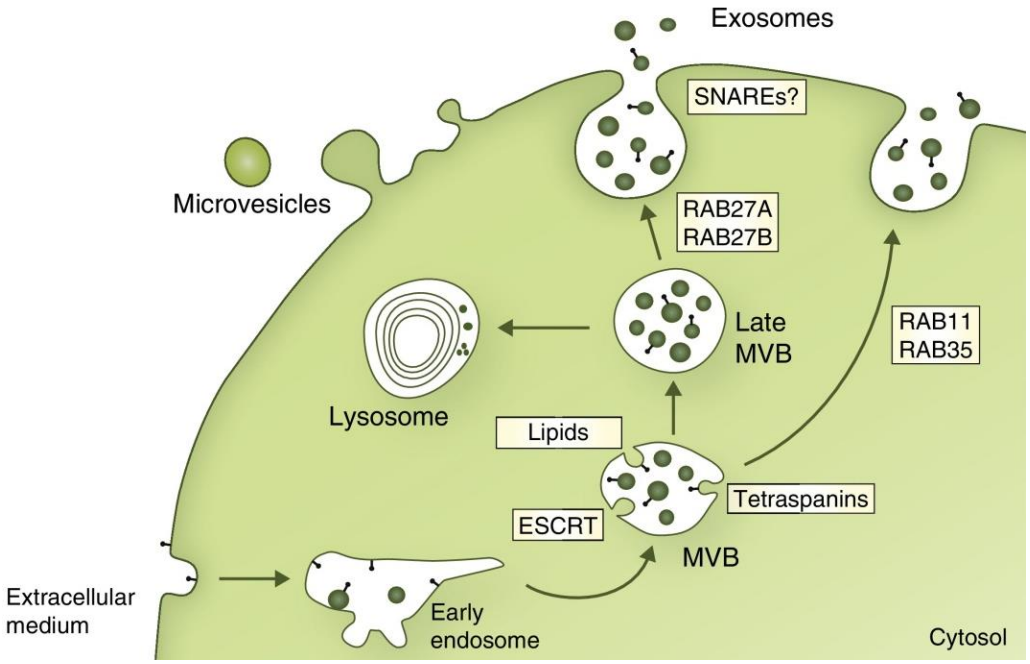

Figure 1.1: Biogenesis and release of exosomes from eukaryotic cells. Intraluminal vesicles (ILVs) are formed by invagination of the membrane of early endosomes and further budding into the endosomal lumen. Endosomal compartments filled with ILVs are named multivesicular bodies (MVB) and several molecules as ESCRT machinery proteins, tetraspanins and cermamide lipids might be involved in the biogenesis of ILVs. Depending on their fate, MVBs can fuse either with the lysosome for intracellular degradation or with the plasma membrane to secrete their ILVs as exosomes into the extracellular space. Several Rab proteins seem to be involved in the transport process of MVBs to the plasma membrane. In contrast, MVs bud directly from the plasma membrane. Adopted and modified image from Kowal et al. (2014).

1.1.1.1. ESCRT-dependent exosome biogenesis

The molecular mechanism for the formation of ILVs is driven by the endosomal sorting complex required for transport (ESCRT) machinery (Williams and Urbe, 2007). The complex is organized by four multiprotein subcomplexes named ESCRT-0, -I, -II, and -III and associated proteins such as Alix and VPS4. The ESCRT-0, -I and -II complexes are responsible for the recognition and recruitment of ubiquitinated proteins in the endosomal membrane and are involved in membrane deformation (Babst et al., 2002b; Katzmann et al., 2001; Mayers et al., 2011). Further budding and vesicle scission is then mediated by ESCRT-III components followed by the recruitment of the VPS4 ATPase that drives disassembly and recycling of the ESCRT components (Babst et al., 2002a). It has been also argued whether VPS4 directly contributes to ILV scission (Babst, 2011; Henne et al., 2011). The enrichment of the ESCRT associated proteins Alix and Tsg101 in exosome preparations (Thery et al., 2001) strengthen the assumption that the biogenesis of exosomes is processed by the ESCRT pathway. However, several studies discussed the hypothesis of involvement of ESCRT-independent mechanisms in the formation of ILVs and exosome biogenesis.

1.1.1.2. ESCRT-independent exosome biogenesis and protein sorting

ESCRT-independent mechanism of ILV formation and ILV sorting of proteins was proposed based on the finding that ILV and MVB formation as well as exosomal protein release still take place when ESCRT subcomplexes are inactivated (Stuffers et al., 2009). Besides ESCRT mediated sorting, several mechanisms of ILV formation and protein loading into ILVs have been described, which involve lipids, tetraspanins or heat shock proteins.

Lipid dependent mechanisms

Trajkovic and co-workers demonstrated that sorting of proteolipid protein PLP into ILVs is not mediated via ESCRT proteins but instead requires the synthesis of the sphingolipid ceramide in an oligodendroglial cell line. The authors showed that the cone-shaped ceramide induced the inward budding of the endosomal membrane (Trajkovic et al., 2008). Exosomes contain lipid-enriched microdomains composed of cholesterol and glycosphingolipids termed lipid rafts which were suggested to be involved in targeting of lipid raft associated proteins to exosomes (de Gassart et al., 2003).

Strauss et al. (2010) additionally showed that cholesterol increases the release of exosomes in a flotillin-dependent manner.

Tetraspanin dependent mechanisms

Sorting of premelanosomal protein PMEL into ILVs, in human melanoma cells, is not driven by ceramide and does not require the ESCRT pathway, but is regulated by interaction of PMEL with the tetraspanin CD63 (van Niel et al., 2011). Moreover, an alternative mechanism was reported in which budding of CD63 positive ILVs into MVBs, including protein packaging, is controlled by the interaction of syntenin with Alix dependent on heparan sulfate and several ESCRT proteins (Baietti et al., 2012).

Expression of the tetraspanin TSPAN8 resulted in modified exosomal mRNA content and protein composition in rat adenocarcinoma cells (Nazarenko et al., 2010) and CD81 enriched microdomains were shown to target certain ligands to exosomes (Perez-Hernandez et al., 2013).

Heat shock proteins

It was demonstrated that the chaperone HSC70 recruits the transferrin receptor to exosomes through a specific binding sequence in the receptor (Geminard et al., 2004).

Oligomerization dependent mechanisms

Moreover, an alternative process that facilitates exosomal sorting was reported in Jurkat T cells, where plasma membrane proteins were targeted to exosomes through higher-order protein oligomerization (Fang et al., 2007). Similarily, antibody-induced cross-linking of membrane proteins enhanced their incorporation into exosomes as reported for the transferrin receptor in reticulocytes (Vidal et al., 1997) and for major histocompatibility complex (MHC) II in lymphocytes (Muntasell et al., 2007).

Release of exosomes

The release of ILVs into the extracellular space as exosomes comprises the guidance of MVBs to the plasma membrane and the docking and fusion of the MVB membrane with the plasma membrane. MVB trafficking is mainly mediated by proteins of the cytoskeleton (actin and microtubules) and Rab family small GTPase proteins, which have been identified as important mediators of intracellular vesicle transport and docking events (Stenmark, 2009). Rab11 was the first family member that was observed to be involved in exosome release (Savina et al., 2005; Savina et al., 2002). Rab27 (Ostrowski et al., 2010) and Rab35 (Hsu et al., 2010) were also shown to control secretion of exosomes in different cell types. Since Rab11 and Rab35 associate to early and recycling endosomes whereas Rab27 is mainly found in late endosomes, it was hypothesized that different subtypes of exosomal vesicles exist, with some of them being released from early or recycling endosomes and some from late endosomes (Figure 1.1) (Colombo et al., 2014). The final fusion machinery includes soluble N-ethylmaleimide-sensitive-factor attachment protein receptor (SNARE) proteins localized to both, the MVB and the plasma membrane, which then form complexes to facilitate membrane fusion (Fader et al., 2009; Gross et al., 2012).

1.1.2. Biophysical properties of exosomes

Exosomes are characterized by their morphology, size, density and molecular composition and these properties are commonly used to discriminate them from other EVs. The morphology and size of exosomes were intensively studied by subjecting purified exosome preparations to electron microscopy (EM), where they appear as 40 – 120 nm vesicles encapsulated by a lipid bilayer. They exhibit a cup-shaped form (Raposo et al., 1996), which was later identified as a methodically induced artifact due to collapsing of the vesicle membrane. However, by using cryo-EM it has been demonstrated, that the natural appearance of exosomes is a round shape (Conde-Vancells et al., 2008; Raposo and Stoorvogel, 2013). As all lipid-containing vesicles, exosomes have the ability to float in sucrose gradients with reported densities of 1.13 g/ml to 1.19 g/ml (Thery et al., 2006) whereas bigger vesicles as apoptotic bodies float at higher densities ranging from 1.24 – 1.28 g/ml (Thery et al., 2001).

1.1.3. Nucleic acids in exosomes

In addition to their protein and lipid content, exosomes contain messenger RNA (mRNA) and small non-coding RNA species (ncRNA) as first reported by Valadi et al. (2007). These authors and others could show that exosomal mRNA and micro RNA (miRNA) molecules can be transported to host cells where they can modulate protein expression levels. (Mittelbrunn et al., 2011; Skog et al., 2008; Valadi et al., 2007). Next-generation sequencing (NGS) of exosomal RNA content revealed the presence of mRNA, small ncRNA species as miRNA, piwi-interacting RNA (piRNA), small nucleolar RNA (snoRNA) and small nuclear RNA (snRNA) as well as transfer RNAs (tRNA) within exosome preparations (Bellingham et al., 2012a; Cheng et al., 2014b; Huang et al., 2013; Nolte-'t Hoen et al., 2012). Exosomes can be enriched in certain RNA species compared to cellular RNA and their RNA composition can be distinct from the one of the parental cell, indicating specific targeting to sort RNAs into exosomes (Guduric-Fuchs et al., 2012; Montecalvo et al., 2012). However, as exosomes derived from various cell types were found to carry similar miRNA cargo, a common mechanism for targeting miRNAs to exosomes could also exist (Guduric-Fuchs et al., 2012).

1.1.3.1. Exosomal RNA sorting

While the loading of specific RNA species into exosomes is not fully clarified, several molecular mechanisms have been proposed. One process involves specific lipid-raft like structures within the endosomal membrane, which promote the binding of cytosolic RNA molecules depending on their affinity (Janas et al., 2015). The affinity of a RNA molecule to bind to lipid bilayers is probably given by a specific membrane binding motif within the RNA sequence as suggested for miRNA (Villarroya-Beltri et al., 2013) and mRNA molecules (Batagov et al., 2011). In addition, hydrophobic modifications of RNA molecules were shown to enhance the affinity of tRNAs to raft-like structures (Janas and Yarus, 2012) suggesting an alternative recognition signal. There is also evidence of involvement of RNA-binding proteins in the incorporation processes of RNAs as described by Villarroya-Beltri et al. (2013). Here, the heterogenous nuclear ribonucleoprotein A2B1 (hnRNPA2B1) was found to control the loading of miRNAs into exosomes through binding to short RNA sequence motifs.

1.1.4. Function of exosomes

1.1.4.1. Physiological function of exosomes

Initially, exosomes were considered as cellular garbage cans to discard unnecessary or obsolete plasma membrane or cytoplasmic proteins (Johnstone et al., 1987). It was shown that the transferrin receptor is transported from the plasma membrane to the extracellular space by a MVB/exosome involved mechanism during the maturation of reticulocytes into erythrocytes (Chitambar et al., 1991; Johnstone et al., 1987). In 1996, Raposo et al. proposed for the first time a signaling role of exosomes in cell-to-cell communication when they demonstrated that B lymphocytes secrete MHC II enriched exosomes leading to the specific activation of $CD4^+$ T cells and therefore mediate immune response (Raposo et al., 1996). Furthermore, exosomes can trigger immune response by activating immune cells including direct peptide/MHC complex presentation to T cells or DCs or antigen transfer to DCs. Inhibitory effects on immume response mediated by exosomes include inhibition of T cell activation, inhibition of T cell and natural killer cell cytotoxicity and promotion of regulatory T cell activity (Thery et al., 2009). In addition, exosomes were discussed to be involved in morphogenesis processes due to their association to Wnt (Beckett et al., 2013; Luga et al., 2012), thus confirming their function on signal transduction.

Moreover, multiple studies focused on potential functions of exosomes in the central nervous system (CNS). It has been observed that multiple cell types, as neurons, oligodendroglial cells and microglia release exosomes which might be transferred to target cells (Faure et al., 2006; Kramer-Albers et al., 2007; Lachenal et al., 2011). Secreted exosomes from oligodendrocytes are involved in the regulation of myelin formation due to an autoinhibitory effect as shown by Bakhti et al. (2011). Exosomes released from glia cells were enriched in Synapsin I and appeared to promote neurite outgrowth in hippocampal neurons and neuronal survival of cortical neurons under cellular stress conditions (Wang et al., 2011). Furthermore, the study from Lachenal et al. (2011) considered a potential role of exosomes in synaptic function, since the release of exosomes from the somato-dendritic part of cortical neurons is regulated by a Calcium influx and glutamatergic synaptic activity.

Besides the transfer of proteins, exosomes were shown to transport mRNA molecules which are taken up by target cells and are translated into the corresponding proteins or small RNA species which act on their target mRNA and thereby interfere and modulate gene

expression. Horizontal transfer of genetic information via exosomes as a new mechanism of intercellular communication was reported in multiple cell models, such as embryonic stem cells (Ratajczak et al., 2006), mast cells (Valadi et al., 2007), glioblastoma cells (Skog et al., 2008), endothelial cells (Deregibus et al., 2007) or primary cortical neurons (Morel et al., 2013).

1.1.4.2. Exosomes in pathological processes: Role in neurodegenerative diseases

In addition to their biological function, exosomes are hypothesized to be involved in various pathological processes and disease pathogenesis including cancer, virus infection and neurodegenerative diseases such as Alzheimer`s diseases (AD), Parkinson`s disease (PD), prion disease and amyotrophic lateral sclerosis (ALS). Despite differences in clinical symptoms and molecular pathology, most neurodegenerative diseases share common properties, such as oligomerization and aggregation of disease-specific proteins leading to intra- or extracellular deposits in the brain. These include, among many others, β-amyloid and Tau in AD, α-Synuclein in PD, Prion proteins (PrP) in prion diseases and superoxide dismutase (SOD) in ALS. Interestingly, all of these proteins were found to be released from cells in association with exosomes *in vitro* (Emmanouilidou et al., 2010; Fevrier et al., 2004; Gomes et al., 2007; Rajendran et al., 2006). A second common feature of these disorders is that the protein related pathology spreads throughout the brain over time following anatomical connections (Braak and Braak, 1991; Braak et al., 2003; Brettschneider et al., 2015). Among several alternative modes of action, exosomes were hypothesized to contribute to the propagation of pathological protein species by transferring them between different cells.

Exosomes in Alzheimer`s disease

The pathological characteristics of AD are represented by insoluble extracellular senile plaques composed of accumulated β-amyloid protein (Aβ) and by intracellular tangles composed of hyperphosphorylated Tau protein. Aβ is generated by proteolytic processing of the transmembrane protein amyloid precursor protein (APP). Interestingly, the APP cleaving secretases β- and γ-secretase were not only found at the plasma membrane but also localized to early endosomes indicating that Aβ might be synthesized intracellular with the endocytic pathway as an important site of generation (Kaether et al., 2006).

Aβ peptides, C-terminal fragments of APP or even full-length APP were detected in exosomal preparations as demonstrated in SY5Y and CHO cells overexpressing wild-type APP (Sharples et al., 2008; Vingtdeux et al., 2007) or in HeLa and N2a cells stably expressing the swedish mutant of APP (Rajendran et al., 2006). The first *in vivo* evidence of Aβ associated exosomes came from exosome-enriched preparations derived from brains of transgenic mice overexpressing human APP where an enrichment of Aβ, full-length and fragmentated APP was observed compared to exosome-enriched preparations from wild-type control brains (Perez-Gonzalez et al., 2012).

It is possible that exosome-associated Aβ may help to regulate intracellular Aβ levels. The insulin-degrading enzyme, a protease that is involved in the degradation of extracellular Aβ, was reported to be sorted and released via exosomes (Bulloj et al., 2010), suggesting that exosomes might exhibit a neuroprotective role in AD. Moreover, neuron-derived exosomes were observed to promote conformational changes of extracellular Aβ42 into non-toxic fibrils and facilitate Aβ uptake and clearance by microglia *in vitro* (Yuyama et al., 2012). In contrast, exosomes derived from primary astrocytes and injected into 5xFAD AD mouse brains were reported to promote the aggregation of Aβ42 *in vivo* (Dinkins et al., 2014). However, whether this leads to increased toxicity in neurons was not reported.

In addition to the presence of Aβ in exosomes, the intracellular hyperphosphorylated Tau protein was observed to be exported from Tau overexpressing cells in association with exosome-like membrane vesicles (Simon et al., 2012). It was recently demonstrated by using a fluorescence resonance energy transfer (FRET) Tau biosensor cell model, that exosome enriched fractions prepared from brain tissue of Tau transgenic mice can seed Tau aggregation in recipient cells (Polanco et al., 2016). Interestingly, an enrichment of several

phosphorylated Tau species, which are known to be implicated in AD pathology, was reported in exosomes derived from blood of AD patients compared to controls with further specification of neuronal derived exosomes by cell adhesion molecule L1 (L1CAM) immunodetection (Fiandaca et al., 2015).

Exosomes in Parkinson`s disease

The protein pathology in PD and other neurodegenerative diseases including dementia with Lewy bodies (DLB) or multiple system atrophy (MSA) is characterized by intracellular inclusions named Lewy bodies (LBs), which are mainly composed of aberrantly aggregated α-Synuclein protein. Since soluble and aggregated α-Synuclein species were detected in cell culture supernatant and body fluids including plasma, CSF and brain interstitial fluid (Borghi et al., 2000; El-Agnaf et al., 2003; 2006; Emmanouilidou et al., 2011; Lee et al., 2005; Tokuda et al., 2010), it became evident that α-Synuclein can be released from cells which could be one potential mechanism of disease propagation between cells. The first evidence of exosome mediated α-Synuclein secretion was provided by Emmanouilidou et al. (2010) who reported exosomal α-Synuclein release from α-Synuclein overexpressing cells. This was further supported by Danzer et al. (2012), who could additionally show that oligomeric α-Synuclein is present in exosomes of neuronal cells. We could recently demonstrate for the first time that exosomal α-Synuclein exists *in vivo* by analyzing exosomes derived from human CSF (Kunadt et al., 2015). Moreover, exosomes isolated from plasma also contain α-Synuclein (Shi et al., 2014).

In 2011, it was demonstrated that α-Synuclein containing exosomes released from α-Synuclein overexpressing SH-SY5Y cells could be transferred to untransfected SH-SY5Y cells where they are internalized (Alvarez-Erviti et al., 2011). Moreover, exosomal α-Synuclein oligomers are taken up by recipient cells more efficiently compared to free α-Synuclein species (Danzer et al., 2012). These results support the hypothesis of exosome mediated spreading of α-Synuclein between different cells with a potential transfer of toxic oligomeric species.

It has been shown that the autophagy pathway can modulate exosome release whereby induction of autophagy promotes the interaction of MVBs and autophagosomes and thereby inhibits exosome release (Fader et al., 2008). Interestingly, sporadic as well as genetic forms

of PD are associated with impaired autophagy processes (Damme et al., 2015) and cells treated with the autophagy inhibitor bafilomycin in fact released more exosomal α-Synuclein (Alvarez-Erviti et al., 2011; Danzer et al., 2012). Poehler and co-workers additionally reported that blocking of the autophagy pathway in α-Synuclein expressing H4 cells resulted in less intracellular α-Synuclein aggregates but enhanced release of small α-Synuclein oligomers via exosomes (Poehler et al., 2014). These studies suggest that α-Synuclein could be secreted into the extracellular space via exosomes as an alternative mechanism when other cellular degradation pathways are impaired.

The protein ATP13A2 (also named PARK9), which is linked to an inherited form of PD (Ramirez et al., 2006) and is physiologically localized to lysosomes and MVBs, was recently shown to be implicated in exosome biogenesis (Kong et al., 2014; Tsunemi et al., 2014). ATP13A2 overexpression in H4 cells and mouse cortical neurons led to an increase in α-Synuclein secretion via exosomes, whereas loss of function mutations in *ATP13A2* resulted in decreased exosome secretion due to a reduced number of ILVs in MVBs and thereby elevated intracellular α-Synuclein levels (Kong et al., 2014; Tsunemi et al., 2014). Interestingly, *ATP13A2* mutations are accompanied by decreased protein expression in PD, but ATP13A2 protein levels were found to be higher in surviving dopaminergic neurons of sporadic PD patients (Dehay et al., 2012).

1.1.5. Purification of EVs

All currently available methods to purify EVs are generally based on vesicle separation in accordance to their biophysical properties including size, morphology and density. The most common protocol to purify exosomes from tissue culture supernatants or biological fluids is a serial centrifugation step protocol at increasing speeds to remove cellular debris and larger plasma membrane derived vesicles followed by sedimentation of exosomes by ultracentrifugation (UC) at 100,000 x g (Thery et al., 2006). To overcome problems with co-purification of protein aggregates of similar size, exosome preparations might be subjected to sucrose density gradient UC where they float at characteristic densities (see section 1.1.2). However, separation of EVs in the size range of exosomes from MVs of similar size is impossible.

Further isolation methods, which are based on vesicle separation by size, are size exclusion chromatography (SEC) columns and membrane ultrafiltration. SEC purification resulted in pure EV fractions (Boing et al., 2014) whereas ultrafiltration often results in co-isolation of macromolecular aggregates that stick to the membranes (Abramowicz et al., 2016). In addition, EVs can be isolated by using immunocapture approaches such as magnetic beads coupled to a specific antibody that recognizes a surface marker protein of EVs (Shi et al., 2014).

Within this study, the term exosomes is used to describe EVs with the size of 40 – 100 nm which are obtained via UC purification and therefore might also contain shedding vesicles of similar size.

1.2. Biomarkers

Biomarkers (biological markers) are basically defined as indicators of biological conditions including healthy and pathological processes (Hulka and Wilcosky, 1988). They are measurable in tissues and body fluids and a reliable biomarker is characterized by its accurate, reproducible and robust quantification. Multiple molecules including proteins, metabolites, DNA and RNA species are used as biomarkers to facilitate diagnosis and prognosis of a current disease (Boukouris and Mathivanan, 2015). The identification and validation of circulating biomarkers in body fluids, such as blood (plasma and serum), urine, saliva and CSF raised immense attention due to the non-invasive and quick sample drawing, thus enabling early diagnosis and therapy.

Pathophysiological changes including protein misfolding, aggregation and further loss of neuronal function and integrity are processes which start years before the first clinical symptoms of neurodegeneration arise. Currently, pharmacological treatment is only symptomatic and no treatment exists that prevents these diseases or influences their progression. Further, accurate diagnosis of a specific disease is often hampered due to an overlap of clinical symptoms and neuropathological changes. These obstacles point out that there is a strong need for reliable biomarkers to predict and diagnose disorders in a preclinical stage in order to target and/or monitor early changes in the brain when they are potentially reversible.

1.2.1. Alzheimer`s disease

AD is the most common neurodegenerative disorder and the main cause of dementia worldwide (Blennow et al., 2006). Epidemiological studies have estimated that 40 million persons over 60 years are living with dementia and this is expected to double every 20 years (Scheltens et al., 2016). Clinically, AD is characterized by a progressive loss of cognitive function and daily-life activities.

Onset of clinical symptoms is preceded by a preclinical stage, which may start decades earlier (Jack and Holtzman, 2013). Mild cognitive impairment (MCI) is a possible prodromal stage with subtle cognitive symptoms, which do not fulfill the criteria of dementia (Petersen, 2004; Winblad et al., 2004). MCI patients have an increased probability of progression towards AD, which depends further on the presence or absence of biomarkers indicative of AD pathology (Albert et al., 2011). Despite the availability of biomarkers such as CSF Aβ, CSF Tau and amyloid positron emission tomography (PET) imaging, there is still a risk of false positive or false negative test results (Coart et al., 2015). Predictive testing has far-reaching consequences, especially in light of the notion that any disease-modifying therapy should start in the earliest possible disease stage (Cummings et al., 2007). However, better markers are needed to unequivocally identify those patients which MCI who will later progress to AD.

1.2.2. Parkinson`s disease and dementia with Lewy bodies

PD is the second most common neurodegenerative disorder that affects 1 – 2% of the population older than 65 years (Goedert, 2001). It is a progressive disorder characterized by the specific loss of midbrain dopaminergic neurons in the substantia nigra and the presence of intracellular protein deposits named Lewy bodies which predominantly consist of pathologically aggregated α-Synuclein (Spillantini et al., 1998). The core clinical symptoms include bradykinesia, tremor in rest and rigidity that is often accompanied by postural instabilities in later disease stages (Jankovic, 2008; Postuma et al., 2015). In addition, non-motor symptoms such as autonomic dysfunction, hyposmia, sleep disturbances and psychiatric disorders e.g. depression are present in many patients.

While 90% of PD patients are sporadically diseased (de Lau and Breteler, 2006), a small portion belongs to the familiar form which is usually characterized by an earlier disease

onset. Genetic studies have identified mutations in several genes encoding for proteins linked to PD including α-Synuclein (Kruger et al., 1998; Polymeropoulos et al., 1997), Parkin (Kitada et al., 1998)or DJ-1 (Bonifati et al., 2003).

DLB is characterized by Lewy bodies which, in contrast to PD, are also present in higher cortical regions (Kosaka, 1990). The disease is clinically defined by Parkinson syndrome plus cognitive impairment, fluctuating attention, visual hallucinations and often sleep disturbances within one year of onset of Parkinson syndrome (McKeith et al., 2005). A high proportion of PD patients also develop cognitive impairment during the disease progression which can result in a difficult differential diagnosis between both diseases (Fahn, 2003), even among specialized motor centers.

Similar to AD, PD and DLB are characterized by a preclinical phase in which neuropathological changes occur in the absence of clinical symtoms. At clinical disease onset, already 60 – 70% of the dopaminergic neurons are lost in PD (Lang and Lozano, 1998). As in AD, a disease modifying therapy is not yet available but there is a broad consensus that such a therapy would need to start as early as possible, ideally in the preclinical stage.

1.2.2.1. CSF biomarkers

CSF represents a nearly optimal source of neurodegenerative disease biomarkers due to its close proximity to the extracellular space of the brain, thus providing potential conditions to reflect and track biochemical changes in the brain. In AD, CSF biomarkers already found their way into clinical practice, whereas CSF biomarkers in PD and α-Synuclein pathology related diseases are currently restricted to clinical studies and trials (Lleo et al., 2015).

Several studies evaluated the potential of extracellular α-Synuclein in CSF as a diagnostic biomarker in PD and other synucleinopathies, such as DLB. Most studies reported reduced CSF total α-Synuclein levels of patients with PD and DLB compared to AD patients or neurological controls (Mollenhauer et al., 2011; Parnetti et al., 2011; Tokuda et al., 2006). However, CSF total α-Synuclein levels of PD and DLB patients were found to overlap with those levels of patient groups suffering from non α-Synuclein related Parkinson syndrome (Aerts et al., 2012). In addition, several studies have detected similar α-Synuclein concentrations when comparing DLB patients with other dementias as AD or frontotemporal

dementia (Noguchi-Shinohara et al., 2009; Reesink et al., 2010; Spies et al., 2009). Thus, extracellular (CSF) α-Synuclein has not been approved as a biomarker for clinical use (Gao et al., 2015).

1.2.2.2. Plasma biomarkers

Blood based biomarkers are highly attractive since blood is easy to obtain and allows follow-up investigations in long-term studies to track the course of the disease. Regarding synucleinopathies, α-Synuclein levels were predominantly examined in plasma samples with variable results. α-Synuclein levels were found to be increased in plasma derived from PD patients compared to controls (Duran et al., 2010; Lee et al., 2006) as were α-Synuclein oligomers (El-Agnaf et al., 2006). In another study, α-Synuclein levels were decreased in PD patients compared to controls (Li et al., 2007). Interestingly, α-Synuclein was also lower in PD plasma after the inhibition of heterophilic antibodies, which are present in human blood and might produce false positive signals due to their potential binding to the antibodies used in α-Synuclein ELISAs (Ishii et al., 2015). Furthermore, overlapping α-Synuclein levels were reported in plasma of PD, AD and control samples (Shi et al., 2010).

Overall, extracellular α-Synuclein has not been approved as a biomarker in human body fluids and a neurochemical biomarker of disease state and trait in PD is missing.

1.2.3. Small ncRNAs as potential biomarkers in neurodegenerative diseases

The human genome project revealed that protein-coding sequences only represent approximately 1.5% of the entire genome (Lander et al., 2001) with a huge portion of the genome being transcribed into non-coding RNAs (ncRNAs). These RNA species comprise a class of regulatory small/short RNAs with up to 200 nucleotides (Kapranov et al., 2007), which is further divided into miRNA, small interfering RNA (siRNA), snRNA, snoRNA, piRNA, tRNA and ribosomal RNA (rRNA) (Huttenhofer et al., 2005).

The best characterized small ncRNAs are represented by the members of the miRNA family, which are approximately 22 nucleotides long. miRNAs regulate gene expression post-transcriptionally either by cleaving their target mRNA followed by further degradation or by blocking protein translation. The biogenesis of miRNAs is a complex multistep process that

involes the RNAse enzymes Drosha and Dicer, which are responsible for the processing of long primary miRNAs to premature miRNAs and further into mature miRNA molecules, respectively. The mature miRNA is then loaded into the RNA-induced silencing complex (RISC) which then recognizes and binds to a complementary sequence in the target mRNA (Esteller, 2011).

Besides their physiological regulatory functions on proliferation, differentiation, development and apoptotic processes (Esteller, 2011), miRNAs seem to be involved in multiple diseases where their expression level is often significantly altered. miRNAs were found to be highly abundant in the CNS and dysregulated miRNA expression was observed in specific brain regions of patients with neurodegenerative disorders including PD (Alvarez-Erviti et al., 2013; Cardo et al., 2014; Kim and Kim, 2007) and AD (Geekiyanage and Chan, 2011; Shioya et al., 2010; Smith et al., 2011). Hence, disease specific miRNA expression pattern were proposed to provide important information regarding disease diagnosis and progression. Extracellular miRNAs circulate in body fluids and are characterized by a high stability with relatively slow turnover rates (Zhang et al., 2012), thus raising the possibility to use them as biomarkers.

Patient fluids have been screened to identifiy specific miRNA signatures by using different techniques such as microarray, NGS or real-time PCR. Several studies investigated whole blood-, plasma-, serum- and CSF-based miRNAs in PD patients (Burgos et al., 2014; Cardo et al., 2013; Khoo et al., 2012; Margis and Rieder, 2011; Vallelunga et al., 2014) as well as in AD patients (Cogswell et al., 2008; Kumar et al., 2013; Leidinger et al., 2013). All of them found dysregulated expression levels of several miRNAs with putative target genes involved in PD and AD, nevertheless analyses also resulted in diverging miRNA profiles even for the same disease.

In addition, miRNA signatures in body fluids did not correlate well with those found in brain tissue of patients suffering from neurodegenerative diseases (Goodall et al., 2013).

1.2.3.1. Exosomal small ncRNAs as potential biomarkers

Exosomes are detectable in body fluids and contain specific cargo molecules, such as proteins and RNA. Thus, they bear the potential to be used as diagnostic and prognostic biomarkers in various diseases including neurodegenerative disorders (Vella et al., 2016). Exosomes provide a protective envelope for their cargo, such as RNA (Cheng et al., 2014a).
NGS of exosomal RNA released from prion-infected neuronal mouse cells revealed differentially expressed miRNAs compared to exosomes from non-infected cells (Bellingham et al., 2012a). Moreover, the diagnostic potential of a serum exosomal miRNA expression pattern was tested and could differentiate AD patients from controls in serum of AD patients (Cheng et al., 2015). Recently, Gui et al. (2015) identified altered miRNA expression levels in CSF exosomes from patients with PD compared to controls by using microarray analysis.

These studies strongly suggest that exosomal RNA may be suitable to discriminate between diseased patients and healthy controls and other neurodegenerative diseases. However, as for free extracellular small ncRNA, the diagnostic signatures identified by different studies did not overlap, thus precluding their use as a biomarker.

1.3. α-Synuclein

α-Synuclein is an intracellular soluble protein of 140 amino acids and member of the Synuclein family which additionally comprises β-Synuclein and γ-Synuclein. All Synuclein proteins are abundantly expressed in the brain (George, 2002).

1.3.1. Structure and function

α-Synuclein contains an amphipathic N-terminal region with a conserved repeat sequence that was shown to bind to phospholipids (Perrin et al., 2000) followed by a highly hydrophobic domain which was suggested to be sufficient for α-Synuclein aggregation and fibril formation (Bodles et al., 2001; Giasson et al., 2001). C-terminal truncated α-Synuclein was shown to seed and facilitate the aggregation of full-length α-Synuclein *in vitro* (Murray et al., 2003).

In solution, α-Synuclein is a native unfolded protein (Weinreb et al., 1996), however it was found to be stabilized in an α-helical conformation upon binding to lipid membranes (Davidson et al., 1998; Eliezer et al., 2001; Jo et al., 2000). It has been suggested that endogenous α-Synuclein could occur natively as a helical folded tetramer that resists aggregation and co-exists in equilibrium with unfolded monomers (Bartels et al., 2011; Dettmer et al., 2015). However, the natively tetrameric structure seems to be controversial since α-Synuclein purified from mouse and human brains was reported to predominantly consists of unfolded monomers (Burre et al., 2013; Fauvet et al., 2012).

α-Synuclein is primaly localized to the synapse (Iwai et al., 1995) and was found in association to synaptic vesicles (Maroteaux and Scheller, 1991). Evidence from several studies suggests that α-Synuclein plays a role in synaptic transmission through influence on the synaptic vesicle cycle including vesicle endocytosis, recycling and exocytosis (Lundblad et al., 2012; Scott and Roy, 2012; Vargas et al., 2014). α-Synuclein overexpression leads to decreased neurotransmitter release (Lundblad et al., 2012; Nemani et al., 2010) and the size of the vesicle recycling pool is reduced (Nemani et al., 2010) whereas an absence of α-Synuclein results in larger recycling pools and enhanced synaptic trafficking (Scott and Roy, 2012). These results indicate that α-Synuclein might be a potential negative regulator of synaptic transmission.

1.3.2. α-Synuclein pathology

The pathological relevance of α-Synuclein became evident when different missense mutations in, or triplicates of the α-Synuclein gene were found to cause familiar PD (Kruger et al., 1998; Polymeropoulos et al., 1997; Singleton et al., 2003; Zarranz et al., 2004). Multiple animal models (e.g. transgenic mouse and fly models) further supported the pathogenic role of α-Synuclein in PD (Benskey et al., 2016). α-Synuclein represents the major component of LBs (Spillantini et al., 1997) which are found to spread in a topographical pattern in the brain during disease course (Brettschneider et al., 2015).

1.4. Aims of the study

1.4.1. Characterization of CSF and plasma exosomal α-Synuclein in PD and DLB patients

Based on the finding that extracellular α-Synuclein exists *in vivo* where it is partially localized in exosomes and that exosomes might contribute to the dissemination of aberrant proteins in neurodegenerative diseases, we characterized exosomal α-Synuclein purified from CSF and plasma of patients with α-Synuclein related neurodegeneration (PD and DLB), patients with no α-Synuclein related Parkinson syndrome (progressive supranuclear palsy, PSP) and neurological controls with no indication of neurodegeneration. The present study includes the quantification of exosome numbers as well as exosomal α-Synuclein levels in all patient groups and the first evaluation of CSF exosomal α-Synuclein to serve as a biomarker for differential diagnostic purpose. Furthermore, the impact of CSF exosomes from these diagnostic groups on the aggregation of soluble α-Synuclein was investigated in a reporter cell assay.

1.4.2. CSF exosomal small ncRNAs as a biomarker for AD

The aim of the second study was to analyze the exososomal small ncRNA composition of exosomes prepared from human CSF and determine whether CSF exosomal small ncRNA profiles may distinguish AD from cognitively healthy controls. In particular, our study investigated (a) whether exosomal small ncRNAs reflect neuronal small ncRNA composition and (b) whether these profiles can be used as a diagnostic biomarker to distinguish between AD and controls.

2. Materials and Methods

2.1. Materials

2.1.1. Chemicals and consumables

Unless indicated otherwise, chemicals were purchased from AppliChem GmbH (Darmstadt, Germany), Merck KGaA (Darmstadt, Germany) or Sigma-Aldrich Chemie GmbH (Munich, Germany). Plastic consumables were purchased from BD Falcon™ (BD Biosciences, Le Pont de Claix, France), Greiner bio-One GmbH (Frickenhausen, Germany), Starlab GmbH (Hamburg, Germany), and Eppendorf AG (Hamburg, Germany).

2.1.2. Antibodies

Primary antibodies are listed in Table 2.1. Horseradish peroxidase (HRP) conjugated secondary antibodies against mouse, rabbit, and human Immunoglobulin G (IgG) were obtained from Dako (Hamburg, Germany), Dianova GmbH (Hamburg, Germany), and Invitrogen (Thermo Fisher Scientific, Waltham, MA, USA).

Table 2.1: List of primary antibodies

Antibody	Host species	Company, catalog number	Dilution
Anti-Flotillin-2	mouse	BD Biosciences, 610384	1:1000 (WB)
Anti-Calnexin	rabbit	Sigma-Aldrich, C4731	1:1000 (WB)
Anti-α-Synuclein clone Syn 211	mouse	Invitrogen, 32-8100	1:1000 (WB)
Anti-α-Synuclein clone 42/α-Synuclein	mouse	BD Biosciences, 610787	1:250 (ECL assay)
Anti-α-Synuclein MJF-1 clone 12.1	rabbit	kindly provided by Dr. Liyu Wu (Epitomics, Burlingame, USA)	3 µg/ml (ECL assay)

2.1.3. Plasmids

α-Synuclein-hGLuc1 (S1) and α-Synuclein-hGLuc2 (S2) plasmids were described in Outeiro et al. (2008). In short, α-Synuclein was subcloned into the Not1/Cla1 sites of constructs containing specific fragments of humanized *Gaussia* Luciferase (kindly provided by Dr. Stephen Michnick, University of Montreal) to generate α-Synuclein-hGLuc1 (S1) and α-Synuclein-hGLuc2 (S2) fusion constructs. Construct S1 contains the N-terminal fragment of hGLuc (aa 1 – 93) and S2 contains the C-terminal fragment of hGLuc (aa 94 – 185).

2.1.4. Buffer and solutions

Phosphate buffered saline (PBS)

10x stock solution

1.37 M	NaCl
27 mM	KCl
100 mM	Na_2HPO_4
18 mM	KH_2PO_4

The final volume was filled up to 1 liter with dH_2O and the pH was adjusted to 7.4

PBS-Citrate 0.32%

PBS was prepared as decribed above and diluted to 1x PBS solution in dH_2O. 0.32% Trisodium citrate (w/v) was then added and the pH was adjusted to 7.4 followed by filtration through a 0.22 µm filter.

PBS-0.05% or 0.025% Tween-20 (PBST)

PBS was prepared as decribed above and diluted to 1x PBS solution in dH_2O. 0.05% or 0.025% Tween-20 (MP Biomedicals LLC; Santa Ana, CA, USA) was added and the solution was mixed well.

Tris buffered saline (TBS)

10x stock solution

1.37 M	NaCl
27 mM	KCl
248 mM	Tris base

The final volume was filled up to 1 liter with dH_2O and the pH was adjusted to 7.4

CHAPS lysis buffer

10% stock solution

10% (w/v)	3-[(3-cholamidopropyl)dimethylammonio]-1-propanesulfonate (CHAPS)
5 mM	EDTA (Ethylenediaminetetraacetic acid)
50 mM	Tris-HCl [Tris(hydroxymethyl)aminomethane]

The pH was adjusted to 8.0. To obtain 1% or 2% CHAPS lysis buffer, 10% stock solution was further diluted in 50 mM Tris-HCl/5 mM EDTA.

Protein loading buffer

5x loading buffer

312.5 mM	Tris-HCl, pH 6.8
5 mM	EDTA, pH 8.0
10% (w/v)	Sodium dodecyl sulfate (SDS)
0.05% (w/v)	Bromphenol Blue
50% (v/v)	Glycerol
0.5%	β-Mercaptoethanol

2.1.5. Commercial solutions, media and components

Commercial available solutions, media and components used during this study are listed in Table 2.2.

Table 2.2: Commercial solutions, media and components

Solution/Medium	Company
cOmplete™ Protease inhibitor cocktail	Roche Diagnostics, Rotkreuz, Switzerland
Dulbecco`s Modified Eagle Medium (DMEM)	Gibco®, Thermo Fisher Scientific, Waltham, MA, USA
Fetal Calf Serum (FCS)	GE Healthcare Life Sciences, Little Chalfont, United Kingdom and Gibco®, Thermo Fisher Scientific, Waltham, MA, USA
GlutaMAX™	Gibco®, Thermo Fisher Scientific, Waltham, MA, USA
Hank`s buffered saline solution (HBSS)	Gibco®, Thermo Fisher Scientific, Waltham, MA, USA
Minimum essential medium (MEM)	Gibco®, Thermo Fisher Scientific, Waltham, MA, USA
Opti-MEM® I reduced serum	Gibco®, Thermo Fisher Scientific, Waltham, MA, USA
PBS	Gibco®, Thermo Fisher Scientific, Waltham, MA, USA
Penicillin/Streptomycin (Pen/Strep), 100 x	Gibco®, Thermo Fisher Scientific, Waltham, MA, USA
SuperFect® transfection reagent	Qiagen GmbH, Hilden, Germany
Trypsin-EDTA, 0.25%	Gibco®, Thermo Fisher Scientific, Waltham, MA, USA

2.1.6. Commercial kits

Table 2.3 depicts commercial kits used in this study.

Table 2.3: Commercial kits

Kit	Application	Company
Agilent RNA 6000 Pico Kit	RNA quality and quantity	Agilent Technologies, Santa Clara, CA, USA
INNOTEST® hTAU Ag ELISA Kit	Detection of Tau protein in human CSF	Innogenetics N.V., Ghent, Belgium
TruSeq Small RNA Library Preparation Kit	Small RNA library preparation	Illumina Inc., San Diego, CA, USA

2.1.7. Software

The software used in this sudy are stated in Table 2.4

Table 2.4: Software

Software	Application	Source
Adobe Illustrator CS5.1	Illustration of figures	Adobe Systems Inc.
EndNote X5	Bibliography managing	Thomson Reuters
GraphPad Prism® 6	Statistical analysis and graph illustration	GraphPad Software Inc.
MS Office Excel 2010	Statistical analysis and graph illustration	Microsoft
MS Office Word 2010	Text writing and editing	Microsoft
NanoSight Tracking Analysis 2.3	Number and concentration of exosomes in liquids	Malvern Instruments
SPSS Statistics 17.0	Statistical analysis	IBM Corporation

2.2. Methods

2.2.1. Patient material

2.2.1.1. Cerebrospinal fluid collection

CSF samples were obtained from the Paracelsus-Elena Klinik Kassel, Germany and the Memory Clinic of the University Medical Center Göttingen, Department of Psychiatry, Germany after written informed consent was given by the participants. The use of CSF samples was approved by the Institutional review board (IRB) of the local board of Hessen, Germany (IRB 09/07/04 and 26/07/02) and the Ethics committee of the University Medical Center Göttingen (IRB 02/05/09). Samples used in this study were collected between 2009 and 2012 in polypropylene tubes by lumbar puncture between 9 and 12 a.m. followed by centrifugation at 2000 x g for 10 minutes (min) at room temperature (RT). The CSF supernatant was aliquoted and flash frozen at −80°C within 30 min of completion of the procedure. Samples with erythrocyte counts > 50/mm^3 were excluded from the study. All samples were obtained according to the ethical principles as defined in the Declaration of Helsinki (1964).

2.2.1.2. Plasma collection

Plasma samples were also obtained from the Paracelsus-Elena Klinik Kassel (IRB 09/07/04 and 26/07/02) and the Memory Clinic of the University Medical Center Göttingen, Department of Psychiatry (IRB 02/05/09), Germany. After written informed consent was given by the participants blood was drawn and collected in plasma monovettes supplied with lithium heparin. Samples were centrifuged at 2000 x g for 10 min at RT within 1 hour after blood draw. The supernatant was then aliquoted and immediately stored at −80°C until further use.

2.2.2. Patient cohorts

2.2.2.1. The cross-sectional Kassel cohort

The cross-sectional Kassel cohort comprises patients suffering from multiple neurological disorders including DLB, PD and PSP and is described in detail in Mollenhauer et al. (2011). DLB was clinically diagnosed in accordance with the McKeith consensus criteria (McKeith et al., 2005). All patients diagnosed with PD fulfilled UK Brain Bank criteria and patients with PSP fulfilled the National Institute of Neurological Disorders and Stroke Society for Progressive Supranuclear Palsy (NINDS-SPSP) criteria for possible or probable disease (Litvan et al., 1996). None of the neurological control patients who were selected from the cohort suffered from PD or dementia. For this study, CSF and plasma samples were obtained from the Kassel cohort. Demographic information of the analyzed samples is given in Table 6.2 for CSF and in Table 6.3 for plasma samples.

2.2.2.2. The DeNoPa cohort

The longitudinal *de novo* Parkinson (DeNoPa) cohort consists of 159 PD patients who have been diagnosed according to the UK Brain Bank criteria and were drug naïve at enrollment. In addition, 150 neurologically healthy controls matching for age, gender and educational levels were included in the study in parallel. Controls had no family history of PD. Study enrollment was completed between 9/2009 and 1/2012 and the cohort will be followed for several years with follow-up investigations every two years. 94% of participants returned for

the first follow-up and clinical baseline diagnosis was confirmed in 84%. CSF was obtained by lumbar puncture between 8 and 9 a.m. and collected in polypropylene tubes followed by further processing (centrifugation and freezing) within 30 min according to a protocol from Mollenhauer et al. (2010). For this study, 76 patients with PD and 58 healthy controls who had completed their first follow-up with normal routine CSF parameters including haemoglobin and protein content, were randomly chosen from the DeNoPa cohort. Demographic information of the analyzed CSF samples is displayed in Table 6.1.

2.2.2.3. Cohorts for small ncRNA sequencing

The test cohort

Samples of the CSF test cohort used for small ncRNA sequencing were obtained from the University Medical Center Göttingen and collected between 2012 and 2013. The cohort comprises 24 AD patients who have been diagnosed according to the criteria of the National Institute of Neurological and Communicative Disorders and Stroke and the Alzheimer`s disease and related Disorders Association (NINCDS-ADRDA) (McKhann et al., 1984) after clinical assessment including neuropsychological testing, neurological examination and CSF parameter diagnostics. In addition, 18 control samples, which were provided by the Department of Psychiatry, Göttingen were included. None of the control patients suffered from dementia or neurodegeneration. Further demographic information of the used samples is specified in Table 6.4.

The replication cohort

The replication cohort comprises 21 patients diagnosed with AD and 20 control patients. 19 AD samples were collected in Göttingen (identical to the test cohort) and 2 AD samples were collected at the Department of Neurology, University Hospital Tübingen. The control samples were obtained from three different centers including Göttingen (10 samples), Tübingen (2 samples) and the Paracelsus-Elena Klinik Kassel (6 samples). Collection, storage and processing of the samples were performed by using the same protocol. Further demographic information of the analyzed samples is given in Table 6.5.

2.2.3. Purification of exosomes from CSF and plasma

Exosomes were purified from frozen CSF or plasma samples (see also section 2.2.1.1 and 2.2.1.2).

2.2.3.1. Purification of exosomes by ultracentrifugation

Exosome isolation from CSF or plasma was performed according to a protocol from Strauss et al. (2010). CSF or plasma was thawed on ice and subjected to serial centrifugation steps at 4°C with the supernatant collected and the pellet discarded each time: 3,500 x g for 10 min, two times 4,500 x g for 10 min and 10,000 x g for 30 min. The supernatant was finally subjected to UC at 100,000 x g for 60 min to obtain the exosome pellet. The pellet was washed once with PBS at 100,000 x g for 60 min followed by resuspension in appropriate buffers or solutions.

For Western blot (WB) analysis, exosomes were prepared from 2.5 ml CSF and resuspended in 5x protein loading buffer (for protocol, see section 2.1.4). For α-Synuclein measurements, exosomes were prepared from 500 µl CSF or plasma and dissolved in 50 µl 1% CHAPS lysis buffer (see 2.1.4 for protocol). Exosomes for the *Gaussia* luciferase protein-fragment complementation assay were purified from CSF under sterile conditions and dissolved in 50 µl PBS for further use. For exosomal RNA isolation, exosomes were purified from 500 µl CSF and resuspended in 200 µl TRI Reagent®. Samples were then stored at −80°C until RNA extraction was performed (section 2.2.8).

2.2.3.2. Purification of plasma exosomes by Size Exclusion Chromatography (SEC)

In addition to the UC based isolation method, exosomes from 1 ml plasma were purified by single-step SEC. This method is based on vesicle separation by size and was used for the isolation of EVs from body fluids as described previously (Boing et al., 2014; Muller et al., 2014). Plasma samples were processed according to the serial centrifugation protocol at 4°C (see also 2.2.3.1): one time 3,500 x g, two times 4,500 x g (10 min each) and one time 10,000 x g for 30 min centrifugation steps were performed before SEC. The supernatant was immediately applied to a commercial qEV column (Izon Science Limited, Cambridge, MA, USA) that was equilibrated with 10 ml of PBS containing 0.32% Trisodium citrate (PBS-Citrate, pH 7.4) before, in accordance to the protocol from Boing et al. (2014).

Subsequently, the applied sample was eluted with PBS-Citrate and 24 fractions of 500 µl were collected followed by washing of the column with at least 30 ml PBS before reuse. All SEC steps were carried out at RT and 0.22 µm filtered buffers were used.

For each fraction, the number of particles was measured by nanoparticle tracking analysis (NTA, section 2.2.4.1). Fractions containing the highest concentrations of particles were pooled as the exosome fraction and concentrated to 90 µl by centrifugation at 4,000 x g and 4°C in an Amicon Ultra centrifugal filter with a 3 kD cut-off (Merck Millipore, Darmstadt, Germany). 10 µl of 10% CHAPS lysis buffer were added and samples were stored at −20°C until α-Synuclein quantification (see 2.2.6.3). For WB analysis, SEC fractions were diluted 1:100 in PBS and supplied with 5x protein loading buffer.

2.2.4. Analysis of exosomes

2.2.4.1. Nanoparticle tracking analysis (NTA)

The NTA technique allows rapid measurements of size distribution and concentration of vesicles in solution (Dragovic et al., 2011). Here, particles are illuminated by laser light and their individual movement is tracked followed by the determination of each vesicle`s diameter based on Bronian motion. Concentration and size distribution of particles in CSF and plasma were analyzed with a NanoSight LM10-HS instrument equipped with a high sensitivity CMOS camera and a LM14 viewing unit comprising a 532 nm laser (NanoSight, part of Malvern Instruments Ltd, Malvern, UK).

Exosomes in unprocessed fractions or in the UC preparation from CSF as well as exosomes in SEC derived plasma fractions were analyzed in appropriate dilutions to keep the particles in the field of view below 100 per image. More specific, total CSF samples were diluted 1:4 to 1:40 in PBS and total plasma samples were diluted 1:10,000 in PBST-0.025% prior to analysis. UC pellets derived from 500 µl CSF were resuspended in 50 µl PBS and diluted 1:40 in PBS. SEC fractions derived from 1 ml plasma were diluted 1:800 in PBST-0.025%. Samples were applied to the laser chamber by using a syringe and 30 sec videos were taken under automated settings. Samples were recorded in triplicates (DeNoPa cohort) or six times (all other samples). Particle numbers and size distribution were then automatically analyzed

with the NanoSight Tracking Analysis 2.3 software. A minimum of 200 tracks per video was analyzed and a cut-off at 120 nm was used for the quantification of exosome numbers.

2.2.4.2. Electron microscopy (EM)

Exosomes were prepared from 4 ml CSF as described in section 2.2.3.1 followed by fixation of the 100,000 x g pellet in 4% Paraformaldehyde (PFA). Then, exosomes were layered onto glow discharged Formvar-carbon-coated copper grids and the grids were negatively stained with 2% uranyl acetate containing 0.7 M oxalate, pH 7.0. Imaging was performed with a LEO EM912 Omega electron microscope (Carl Zeiss, Oberkochen, Germany) and digital micrographs were captured with an on-axis 2048 x 2048 pixel CCD camera (Proscan Special Instruments Ltd., Minsk, Belarus).
EM of CSF exosomes was kindly performed by Dr. Wiebke Möbius (MPI of Experimental Medicine, Göttingen).

2.2.5. Cell culture

2.2.5.1. Maintenance of cell lines

Cells were grown at 37°C and 5% CO_2 in humidified incubators in 75 cm^2 cell culture flasks or 10 cm petri dishes (both obtained from BD), respectively.

Mouse neuroblastoma N2a cells were maintained in Dulbecco`s Modified Eagle Medium (DMEM; Gibco®, Thermo Fisher Scientific, Waltham, MA, USA) containing 4.5 g/L glucose and supplemented with 10% fetal calf serum (FCS; GE Healthcare Life Sciences, Little Chalfont, United Kingdom), 1% GlutaMAX™ and 1% Penicillin/Streptomycin (both from Gibco®, Thermo Fisher Scientific, Waltham, MA, USA).

Human neuroglioma H4 cells (Cell Lines Service GmbH, Eppelheim, Germany) were maintained in Opti-MEM® I reduced serum medium supplemented with 10% FCS (both from Gibco®, Thermo Fisher Scientific, Waltham, MA, USA).

2.2.5.2. Transfection of H4 cells and treatment with CSF derived exosomes

H4 cells were plated on 96 well plates 24 hours prior to transfection which was performed at 80 – 90% cell confluency using SuperFect® transfection reagent (Qiagen GmbH, Hilden, Germany). Cells were transiently transfected with equimolar ratios of the plasmids α-Synuclein-hGLuc1 (S1) and α-Synuclein-hGLuc2 (S2, see also 2.1.3) according to the manufacturer`s instructions. After 2 hours of incubation under normal growth conditions the transfection mix was removed from the cells and fresh Opti-MEM® medium supplemented with 10% FCS containing purified CSF exosomes derived from DLB patients, PD patients and neurological control patients was added. After 12 hours the split-luciferase protein fragment complementation assay was performed to measure the aggregation of α-Synuclein in the cells as described in section 2.2.6.5.

Transfection of H4 cells, treatment with purified CSF exosomes and the split-luciferase protein fragment complementation assay were kindly performed by the group of Prof. Dr. Karin Danzer (Department of Neurology, Ulm University).

2.2.5.3. Primary mouse cortical and hippocampal neuronal cultures

Primary cell cultures were generated from the cerebral cortex or hippocampus of mouse embryos at embryonic day 16.5. To this end, a pregnant NMRI mouse was sacrificed and embryos were removed immediately from the amniotic sac. Cortices or hippocampi were then dissected and collected in sterile Hank`s buffered saline solution (HBSS; Gibco®, Thermo Fisher Scientific, Waltham, MA, USA) at RT. After transferring hippocampal or cortical tissue from all embryos into a sterile tube, 500 µl of 0.05% Trypsin-EDTA was added and the mixture was incubated for 10 min at 37°C in the incubator. Trypsination was then stopped with DMEM supplemented with 10% FCS, 1% GlutaMAX™ and 1% Penicillin/Streptomycin. To obtain a single cell suspension, the mixture was homogenized by resuspending with a glass pipette. 1 ml of growth medium MEM-B27 [Minimum essential medium (MEM) with 0.2% sodium bicarbonate solution, 0.6% glucose, 1% sodium pyruvate (100x), 1% Penicillin/Streptomycin, 1% GlutaMAX™ and 2% B27 supplement 50x (all obtained from Gibco®, Thermo Fisher Scientific, Waltham, MA, USA)] was added per brain followed by the filtration of the cell suspension through a cell strainer (BD Falcon™). 30 µl cell suspension

was plated in each well of a 12 well plate precoated with poly-L-lysine and cultures were grown for up to 2 weeks in 1 ml growth medium MEM-B27 per well.

One day before exosome purification, the growth medium was changed to 500 µl medium and exosomes were collected for 16 hours. For exosome isolation, the medium was removed from the cells and subjected to UC purification as described in section 2.2.3.1. Cells were washed once with PBS before scraping them in 200 µl TRI Reagent®. Cell lysates were then stored at −80°C until further processing for RNA extraction (see section 2.2.8).

2.2.6. Protein biochemistry

2.2.6.1. Preparation of cell lysates for protein analysis

For protein analysis, N2a cells were cultured in 10 cm petri dishes for at least 24 hours and scraped in 400 µl 1% CHAPS lysis buffer supplemented with cOmplete™ Protease inhibitor cocktail 1:25 (Roche Diagnostics, Rotkreuz, Switzerland). Cell lysates were centrifuged at 4,500 x g for 10 min at 4°C to remove cellular debris and 400 µl supernatant was diluted with 160 µl 5x protein loading buffer for western blot analysis.

2.2.6.2. Western Blot Analysis

Protein detection by WB analysis was performed to detect Flotillin-2 in CSF exosomes, Calnexin in total CSF and IgG in total plasma.

SDS-PAGE

Proteins of CSF exosomes, total CSF and N2a cell lysates were separated by sodium dodecyl sulfate polyacrylamide gel electrophoresis (SDS-PAGE) (Laemmli, 1970) under denaturating conditions by using the Bio-Rad Mini-PROTEAN® Tetra electrophoresis system (Bio-Rad Laboratories GmbH, Munich, Germany). 12% resolving gels and 4% stacking gels were prepared as depicted in Table 2.5.

Table 2.5: Composition of stacking and resolving gel for SDS-PAGE

Stacking gel (4%)		**Resolving gel (12%)**	
4%	Acrylamide/Bis Solution 30% (37.5:1)	12%	Acrylamide/Bis Solution 30% (37.5:1)
125 mM	Tris-HCl pH 6.8	375 mM	Tris-HCl pH 8.8
0.1%	SDS	0.1%	SDS
0.1%	Ammonium persulfate (APS)	0.1%	APS
0.15%	N'N'N'-tetramethylethylene diamine (TEMED)	0.04%	TEMED

UC purified CSF exosomes were resuspended in 20 µl 5x protein sample buffer, UC plasma exosomes and plasma SEC fractions were diluted 1:100 prior adding protein sample buffer and total CSF/plasma and N2a cell lysates were diluted 1:5 in protein sample buffer followed by incubation at 95°C for 5 min. 20 µl of UC CSF/plasma exosomes, total CSF/plasma or N2a cell lysate and 15 µl of plasma SEC fractions were loaded on the gel together with 3 µl of the protein marker PageRuler™ Plus Prestained Protein Ladder (Thermo Fisher Scientific, Waltham, MA, USA). Electrophoresis was performed in one time running buffer (25 mM Tris, 190 mM Glycine, 0.1% SDS) at 100 V for 120 min.

Protein transfer to membrane and immunodetection of proteins

Proteins were transferred from the gel onto an Amersham™ Protran™ nitrocellulose membrane (GE Healthcare Life Sciences, Little Chalfont, United Kingdom) by using the Mini Trans-Blot® tank blot system (Bio-Rad Laboratories GmbH, Munich, Germany). Blotting was performed at 100 V for 55 min in one time transfer buffer (25 mM Tris, 190 mM Glycine, 20% Methanol). After protein transfer, the nitrocellulose membrane was treated with Ponceau S solution [0.1% (w/v) Ponceau S in 5% (v/v) acetic acid (Sigma-Aldrich Chemie GmbH, Munich, Germany)] for 5 min to reversibly stain protein bands and therefore confirm correct protein transfer. After destaining of proteins by washing with dH_2O, the membrane was blocked in 4% non-fat milk powder (AppliChem, Darmstadt, Germany) in PBS for 1 hour at RT followed by incubation with the appropriate primary antibody diluted in 1% milk in PBST-0.05% overnight at 4°C. Specific dilutions of primary antibodies are listed in Table 2.1. The membrane was then washed three times in PBST for 10 min at RT followed by incubation with the appropriate HRP conjugated secondary antibody 1:2000 in PBST for 1 hour at RT. After three washing steps in PBST for 20 min each, proteins were detected by enhanced chemiluminesence using Pierce™ ECL Western Blotting Substrate (Thermo Fisher

Scientific, Waltham, MA, USA) or Amersham™ ECL Prime Western Blotting Detection Reagent (GE Healthcare Life Sciences, Little Chalfont, United Kingdom) when higher sensitivity was needed. The emitted light signal was subsequently visualized on CL-XPosure™ X-ray films (Thermo Fisher Scientific, Waltham, MA, USA).

2.2.6.3. Electrochemiluminescence (ECL) assay for α-Synuclein quantification

α-Synuclein was quantified in total CSF and plasma and in exosomes derived from both fluids by using an electrochemiluminescence assay according to Kruse et al. (2012). The technology of this assay is based on a sandwich enzyme-linked immunosorbent assay (ELISA) technique with high sensitivity due to the ECL based detection system.

96-well standard plates (Meso Scale Discovery™, Gaithersburg, MD, USA) were coated with 30 µl capture antibody MJF-1 clone 12.1 (kindly provided by Dr. Liyu Wu; Epitomics, Burlingame, USA) at 3 µg/ml in PBS and incubated overnight at 4°C. Plates were then washed three times with 150 µl PBST followed by blocking with 150 µl 1% bovine serum albumin (BSA) in PBST (BSA; SeraCare Life Sciences, Milford, MA, USA) for 1 hour at RT with shaking at 300 rounds per minute (rpm). After three times washing, 25 µl of recombinant α-Synuclein standards (kindly provided by Dr. Omar El-Agnaf, Hamad Bin Khalifa University, Doha, Qatar) and samples were applied to the wells in duplicates and incubated for 1 hour at RT and under shaking at 700 rpm. More specific, total CSF and plasma samples were diluted 1:8 and a 1:4 serial dilution of recombinant α-Synuclein starting at 25 ng/ml was prepared in 1% BSA. Purified exosome samples were applied without further dilution. Plates were washed again three times and Sulfo-TAG-labelled anti-α-Synuclein clone 42 (BD Biosciences, Le Pont de Claix, France) was applied at 1 µg/ml for 1 hour at RT and shaking at 700 rpm. After three times washing 150 µl of 2x Read Buffer T (Meso Scale Discovery™) was added to each well and plates were measured at 620 nm in a Sector Imager 6000 (Meso Scale Discovery™). Data analysis was performed with the MSD Discovery Workbench 3.0 Data Analysis Toolbox (Meso Scale Discovery™).

2.2.6.4. Quantification of CSF Tau levels

The concentration of total CSF Tau protein was determined by using the commercial available INNOTEST® hTAU Ag sandwich ELISA kit (Innogenetics N.V., Ghent, Belgium). The assay was performed according to the manufacturer`s instructions.

2.2.6.5. *Gaussia* luciferase protein-fragment complementation assay

The fusion constructs α-Synuclein-hGLuc1 (S1) and α-Synuclein-hGLuc2 (S2) were transfected into H4 cells followed by treatment with CSF derived exosomes as described in section 2.2.5.2. After 12 h of transfection, cells were washed once with PBS and fresh serum- and phenol red free medium was added. Luciferase activity resulting from protein complementation was measured in live cells in an automated plate reader at 480 nm immediately after adding 20 µM of the cell permeable substrate Coelenterazine (PJK GmbH, Kleinblittersdorf, Germany) to each well. Luminescence signals were integrated for 2 seconds. The protein-fragment complementation assay (including cell transfection and treatment with exosomes) was performed by Prof. Dr. Karin Danzer`s research group (Department of Neurology, Ulm University).

2.2.7. Data and statistical analysis

Data and statistical analyses were performed with MS Office Excel 2010 software (Microsoft, Redmond, WA, USA), GraphPad Prism® 6 software (GraphPad Software Inc., San Diego, CA, USA) and SPSS Statistics 17.0 software (IBM Corporation, Armonk, NY, USA). For normally distributed data sets the Student`s t test or one-way ANOVA followed by Games-Howell post hoc test (for data resulting from unequal sample size and variance) were performed. The nonparametric Mann-Whitney U-test was used when normal distribution was not given. P values less than 0.05 were regarded as significantly different. Results were shown as the mean and the standard error of the mean (SEM) and were illustrated with MS Office Excel and GraphPad Prism®. Correlation analysis was performed by using Pearson`s correlation and Receiver Operating Characteristics (ROC) curves were used to evaluate the diagnostic performance of exosomal α-Synuclein as a diagnostic marker. Data were analyzed blinded to the diagnosis.

2.2.8. RNA extraction from exosomes

Total RNA was extracted from purified CSF exosomes or primary neuronal culture exosomes under RNAse-free conditions using TRI Reagent® (Sigma-Aldrich Chemie GmbH, Munich, Germany). Exosome pellets (dissolved in 200 µl TRI Reagent®, see section 2.2.3.1 and 2.2.5.3) were filled up to 1 ml with TRI Reagent® followed by the addition of 3 µl Glycogen [25 µg/ml in diethylpyrocarbonate (DEPC) treated water]. The mixture was incubated for 5 min at RT. 200 µl of Chloroform was then added, samples were mixed by vigorous shaking and incubated for 5 min at RT. For phase separation, samples were centrifuged for 15 min at 12,000 x g and 4°C. The RNA containing aqueous upper phase was carefully transferred into a fresh tube followed by precipitation with 500 µl Isopropanol overnight at −20°C. The following steps were all carried out at 4°C. After centrifugation for 30 min at 12,000 x g, the supernatant was carefully discarded and the pellet was washed two times in 750 µl 75% Ethanol. The RNA pellet was air-dried until it was invisible and dissolved in 10 µl RNAse-free water.

Exosomal RNA yield was measured by NanoDrop 2000 spectrophotometer (Thermo Scientific, Waltham, MA, USA) and RNA quality was analyzed with an Agilent 2100 Bioanalyzer by using RNA 6000 Pico Chips on the appropriate total Eukaryotic pico 6000 RNA assay (all from Agilent Technologies, Santa Clara, CA, USA) in accordance to the manufacturer`s instructions. RNA samples were then stored at −80°C until sequencing.

2.2.9. Next Generation Sequencing (NGS) of small ncRNAs

NGS sequencing of small ncRNAs was carried out using a HighSeq™ 2000 system (Illumina, San Diego, USA). Small RNA libraries were prepared from total RNA extracted from CSF or primary cortical/hippocampal neuronal exosomes using the TruSeq Small RNA Library Kit according to the provided protocols from Illumina. Since exosomes contain relatively low amounts of RNA and the starting volume of CSF was 500 µl, a minimum of 0.5 ng of total RNA was used as starting material.

2.2.9.1. Bioinformatics and statistical analysis

Raw data obtained from NGS sequencing and the generation of small ncRNA reads were performed by the group of Dr. Stefan Bonn, German Center for Neurodegenerative Diseases, Göttingen, Germany. In short, quality assessment of RNA libraries and detection of small ncRNAs was performed using Oasis web platform (Capece et al., 2015) and comprised lengths filtering (15 – 32 nucleotides) of reads followed by their mapping to the reference genome.

All statistical and functional analyses, including feature selection via the application of machine learning approaches and statistical methods and further development and application of an algorithm that can differentiate AD patients from controls, were performed by Gaurav Jain under supervision of Prof. Dr. André Fischer, German Center for Neurodegenerative Diseases, Göttingen, Germany.

3. Results

3.1. Characterization of exosomal α-Synuclein in CSF and plasma from patients with Parkinson`s disease and dementia with Lewy bodies

We analyzed CSF and plasma exosomal α-Synuclein as a potential biomarker in different diseases with and without α-Synuclein related neurodegeneration. The characterization of CSF and plasma exosomal α-Synuclein from patients with PD, DLB, PSP as an example of a non-α-Synuclein related neurodegenerative disease with Parkinson syndrome and neurological, non-neurodegenerative controls included the quantification of exosome numbers and exosomal α-Synuclein protein concentrations as well as determination of the potential of CSF exosomes to induce the aggregation of soluble α-Synuclein in a reporter cell assay.

Most of the results from section 3.1 have been published in:

Induction of α-Synuclein aggregate formation by CSF exosomes from patients with Parkinson`s disease and dementia with Lewy bodies

Anne Stuendl, Marcel Kunadt, Niels Kruse, Claudia Bartels, Wiebke Moebius, Karin M. Danzer, Brit Mollenhauer and Anja Schneider

Brain: a journal of neurology (2016) *139*, 481-494.

3.1.1. Purification of exosomes from cerebrospinal fluid

Exosomes were purified from CSF by serial centrifugation rounds including a final UC step at 100,000 x g as described previously (Kunadt et al., 2015). The 100,000 x g pellet and total CSF were analyzed for exosome numbers and α-Synuclein concentrations (Figure 3.1A). Analysis of the UC pellet by electron microscopy revealed vesicles of 40 to 120 nm diameter and the typical cup shaped morphology of exosomes (Figure 3.1B). Next, purified CSF exosome and total CSF fractions were tested by WB analysis for the presence of the exosomal marker protein Flotillin-2 which was detectable in the exosome fraction but absent

in total CSF (Figure 3.1C, *left panel*). In contrast, the heavy and light chains of IgG were detected in total CSF but not in the exosome fraction (Figure 3.1C, *middle panel*) indicating that the UC pellet was not contaminated by protein complexes. To further verify the purity of the isolated exosomes and to rule out microsomal contaminations, exosomes and total CSF as well as a N2a cell lysate were immunostained against the endoplasmatic reticulum marker protein Calnexin. Calnexin was absent in the exosomal fraction (Figure 3.1C, *right panel*).

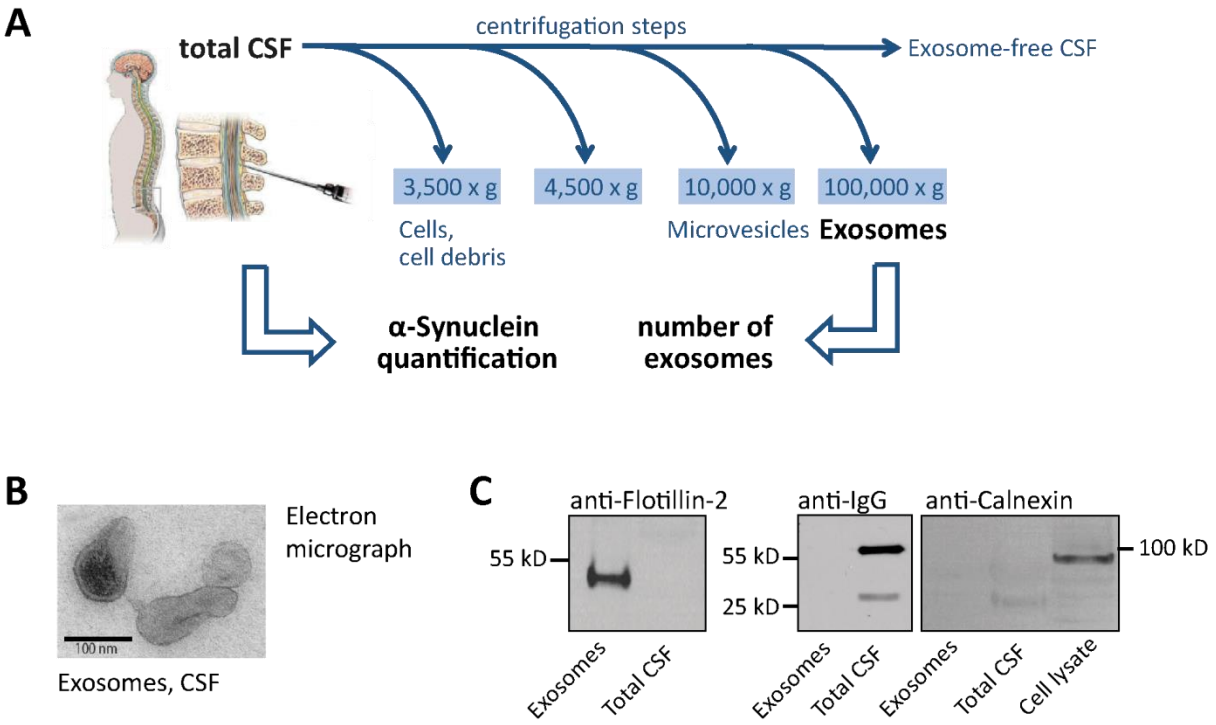

Figure 3.1: Purification and characterization of exosomes from CSF. (**A**) Exosomes were purified from 500 µl CSF by serial centrifugation rounds with a final ultracentrifugation step at 100,000 x g. Exosome numbers and α-Synuclein concentrations were quantified in total CSF and exosome fractions by NTA and ECL assay. (**B**) The exosome pellet derived from 4 ml CSF was subjected to electron microscopy and individual exosomes showed the typical cup shaped morphology. Scale bar = 100 nm. (**C**) Western Blot analysis of exosomes derived from 2.5 ml CSF and the corresponding total CSF fraction. The exosome pellet was resuspended in 20 µl 5x protein sample buffer and total CSF was diluted 1:5 in sample buffer. 20 µl of the exosome preparation and 20 µl of total CSF were immunostained against the exosomal marker protein Flotillin-2 (*left panel*) and with a secondary antibody against human IgG as a negative control (*middle panel*). 20 µl of the exosome pellet, total CSF and N2a cell lysate were probed with an antibody against the edoplasmatic reticulum protein Calnexin to exclude microsomal contaminations in the exosome fraction (*right panel*).

3.1.2. Quantification of CSF exosomes and exosomal α-Synuclein concentrations

To quantitatively analyse exosome numbers and their size in total CSF as well as in CSF exosome preparations, we used nanoparticle tracking analysis. Exosomes were purified from 500 µl CSF, dissolved in PBS and measured in triplicates. Figure 3.2A shows a representative graph of total CSF (red line) and the corresponding exosome preparation (blue line). Vesicle size in total CSF ranged from zero to 550 nm with several peak fractions. In contrast, the purified exosome sample predominantely contained vesicles in the size range of exosomes with a single peak at 102 nm.

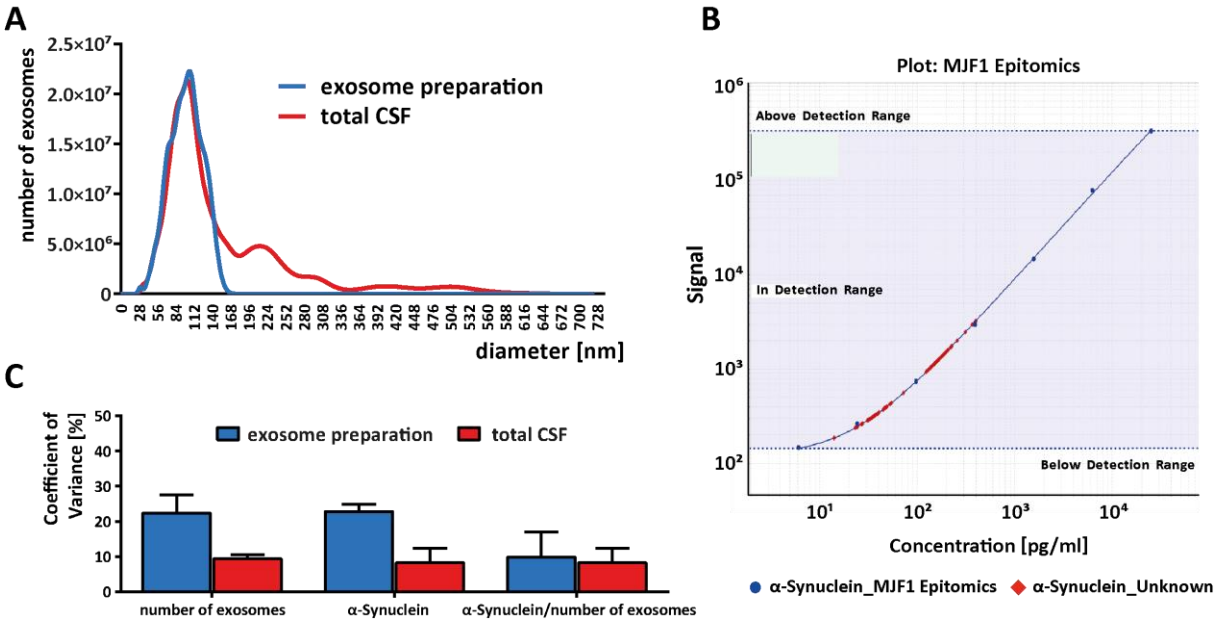

Figure 3.2: Quantitative analysis of CSF exosomes. (**A**) Size distribution profile showing vesicle numbers of a CSF exosome preparation from 500 µl CSF and the corresponding total CSF measured by NTA (total CSF: red line; exosome pellet: blue line; peak at 102 nm). The values were adjusted for the particular dilution factors and calculated to represent the absolute vesicle numbers in 1 ml CSF and in exosomes derived from the same CSF volume. (**B**) α-Synuclein levels in total CSF and CSF exosomes were quantified by using a highly sensitive ECL assay. A resulting plot of α-Synuclein standards (blue circles, standard curve = blue line) and CSF exosome samples (red diamonds) is shown and reveals that α-Synuclein levels in exosome samples are found in the linear detection range of the assay. (**C**) The coefficient of variance was calculated for the number of exosomes, α-Synuclein levels and the ratio of exosomal α-Synuclein protein levels to the number of exosomes in both, the exosome preparation and in total CSF. Therefore, CSF replicate samples of n = 3 and n = 4 from two different patients were analyzed. Values are given as mean ± SEM.

In order to use CSF exosomes as a potential biomarker in synucleinopathies, the necessary CSF volume should not exceed a maximum of 500 to 1000 µl and should allow for automated and quantitative analysis. To this end, we used an optimized ELISA, based on an ECL platform, that allows α-Synuclein quantification with high sensitivity and in a large dynamic range (Kruse et al., 2012). The ECL assay has an average lower detection limit of 5 pg/ml and, as shown in Figure 3.2B, all measured α-Synuclein levels in exosome preparations derived from 500 µl CSF (red dots) were found in the detection range of the assay. To verify the reproducibility of the NTA and ECL quantification methods, exosomes were purified from three or four aliquots of the same CSF sample (two different CSF samples in total) and quantified for exosome numbers and α-Synuclein levels. Measurements were also performed for the corresponding total CSF. The coefficient of variance (CV) was below 10% for the number of exosomes (9.4%) and α-Synuclein levels (8.2%) in total CSF whereas CV values for the same measurements in the exosome fraction were 22.3% for the number of exosomes as well as for α-Synuclein levels (Figure 3.2C). Further, CV calculations for the ratio of exosomal α-synuclein levels to the number of exosomes revealed values of 9.9% in the exosome preparation and 8.2% in the total CSF fraction. These values indicate that the exosome preparation is suitable for quantitative analysis in patient samples.

3.1.3. Quantification of CSF exosomal α-Synuclein in early stage PD patients

First, we analyzed exosomal α-Synuclein protein levels from CSF samples obtained from drug naïve patients with early stage PD and healthy controls. 76 patients diagnosed with PD and 58 age- and gender-matched healthy controls were obtained from the longitudinal DeNoPa cohort (Mollenhauer et al., 2013a) (see section 2.2.2.2 for detailed description of the cohort and Table 6.1 for demographic information of the analyzed CSF samples). Exosomes were purified from 500 µl CSF followed by the quantification of α-Synuclein protein levels in total CSF (Figure 3.3A) and in the exosome fraction (Figure 3.3B). All values were normalized to 1 ml CSF starting volume. α-Synuclein levels in total CSF were significantly lower in PD patients compared to the healthy control group (PD mean α-Synuclein = 647.88 pg/ml, SEM = 26.95 pg/ml, n = 76; healthy controls mean α-Synuclein = 774.64 pg/ml, SEM = 36.13 pg/ml, n = 58; * $p < 0.05$, Student`s two-sided t-test; Figure 3.3A).

This observation is consistent to the findings previously described in Mollenhauer et al. (2013b). In addition, we observed a significant lower amount of absolute α-Synuclein in CSF exosomes derived from PD patients compared to healthy controls (Figure 3.3B; PD mean = 13.04 pg α-Synuclein in exosomes derived from 1 ml CSF, SEM = 0.61 pg, n = 76; healthy controls mean = 16.01 pg α-Synuclein derived from 1 ml CSF, SEM = 0.98 pg, n = 58; * $p < 0.05$, Student`s two-sided t-test). Furthermore, we calculated the ratio of α-Synuclein in exosomes to total α-Synuclein in the CSF starting volume (Figure 3.3C). Here, we observed that only a small portion (2.17%) of total CSF α-Synuclein is localized in exosomes with no significant difference between PD patients and the healthy control group (PD mean = 2.17%, SEM =0.12%, n = 76; healthy controls mean = 2.17%, SEM = 0.12%, n = 58, Student`s two-sided t-test).

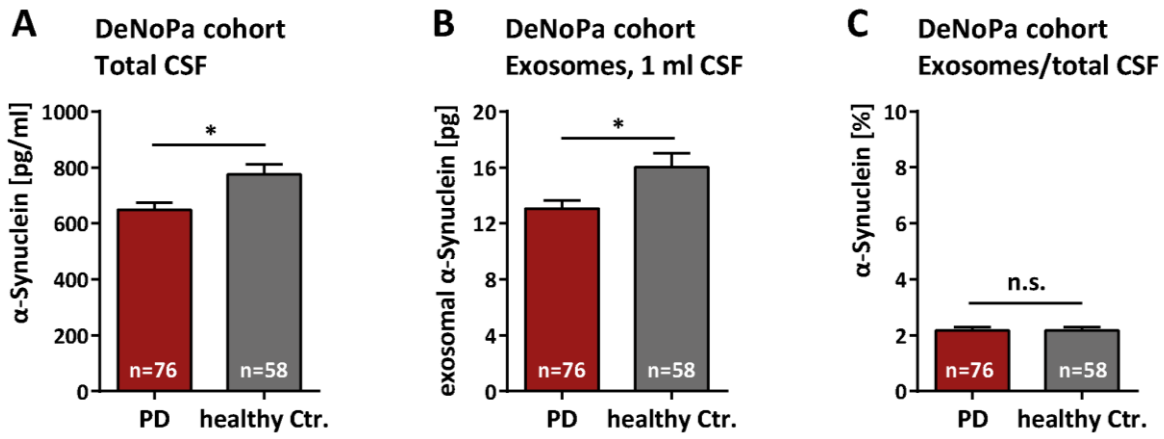

Figure 3.3: Quantification of exosomal α-Synuclein in CSF from patients with PD and healthy controls from the DeNoPa cohort. (**A**) α-Synuclein concentrations in total CSF from PD patients (red bar) are lower as α-Synuclein levels in healthy control patients (grey bar), n = 76 PD patients, n = 58 healthy control patients, * $p < 0.05$, two-sided t-test. (**B**) α-Synuclein protein levels were quantified in CSF exosome preparations from PD patients (red bar) and healthy control patients (grey bar). Exosomes were purified from 500 µl CSF and protein levels were normalized to 1 ml. N = 76 PD patients, n = 58 healthy control patients, * $p < 0.05$, two-sided t-test. (**C**) The ratio of exosomal α-Synuclein to α-Synuclein present in total CSF was calculated in PD patient samples (red bar) and healthy control samples (grey bar) and is shown in %. No significant difference is detected. Exosomes were prepared from 500 µl CSF and α-Synuclein values were normalized to 1 ml for both, exosomes and total CSF. N = 76 PD patients, n = 58 healthy control patients, n.s. = not significant, two-sided t-test. All values are given as mean ± SEM.

3.1.4. Characterization of CSF exosomal α-Synuclein in PD, DLB, and non-α-Synuclein related disease controls

We next studied CSF exosomal α-Synuclein in more progressed PD stages. We obtained CSF samples from 37 patients diagnosed with PD according to UK Brain Bank criteria from the Kassel cohort. Selected subjects showed different grades of motor symptoms as assessed by Hoehn and Yahr staging (mean H&Y stage = 3.9, SEM = 0.20). These samples were further complemented with 35 patients suffering from DLB as a second α-Synuclein related disease with Parkinson syndrome and two different control groups. The first control group contained 15 patients with polyneuropathy (PNP) who presented with gait disturbances but, after thorough clinical assessment, were diagnosed with PNP and no Parkinson syndrome. The second control group consisted of 25 patients with progressive supranuclear palsy (PSP). These patients show a characteristic Parkinson syndrome caused by Tau pathology. All samples were randomly selected from the Kassel cohort (Mollenhauer et al., 2011). In addition, 3 DLB CSF samples were provided from the Göttingen cohort to increase sample size numbers. Demographic information of the selected samples is given in Table 6.2).

3.1.4.1. Comparison of CSF exosomal α-Synuclein levels in PD, DLB, PNP and PSP

When analyzing the absolute levels of α-Synuclein in exosome preparations derived from the same CSF volume after normalization to 1 ml, we did not observe significant differences between the PD, PNP and PSP groups (Figure 3.4A; PD mean = 17.20 pg α-Synuclein in exosomes derived from 1 ml CSF, SEM = 1.50 pg, n = 36; PNP mean = 17.20 pg in exosomes derived from 1 ml CSF, SEM = 2.97 pg, n = 15; PSP mean = 20.60 pg α-Synuclein in exosomes derived from 1 ml CSF, SEM = 4.56 pg, n = 25, one-way ANOVA $p = 0.000691$, Games-Howell post hoc test revealed no significant differences). Interestingly, this is in contrast to our findings from the DeNoPa cohort, where exosomal α-Synuclein levels were slightly lower in PD samples (see 3.1.3 and Figure 3.3B). We also measured total α-Synuclein amounts in exosome fractions from 35 DLB patients. Here, significant lower α-Synuclein levels were found compared to all other patient groups as depicted in Figure 3.4A (DLB mean = 7.92 pg α-Synuclein in exosomes derived from 1 ml CSF, SEM = 0.78 pg, one-way ANOVA $p = 0.000691$ followed by Games-Howell post hoc test, (*) $p = 0.05$, * $p < 0.05$, *** $p < 0.0005$). Additionally, α-Synuclein levels were determined in total CSF fractions of

the four different patients groups. As shown in Figure 3.4B, α-Synuclein was found to be significantly less abundant in DLB CSF than in total CSF of PD patients (DLB mean = 380.61 pg/ml, SEM = 27.55 pg/ml; PD mean = 602.42 pg/ml, SEM = 59.79 pg/ml; PNP mean = 615.86 pg/ml, SEM = 122.47 pg/ml; PSP mean = 467.65 pg/ml, SEM = 78.74 pg/ml, one-way ANOVA, p = 0.0202, followed by Games-Howell post hoc test, * p = 0.05). As already observed with α-Synuclein levels in exosomes (Figure 3.4A), total α-Synuclein levels in PD CSF did not differ significantly from those in CSF from control patients (PNP and PSP, Figure 3.4B). Again, this finding is in contrast to the small reduction of α-Synuclein protein level in total CSF from early-stage PD patients of the DeNoPa cohort (Figure 3.3A).

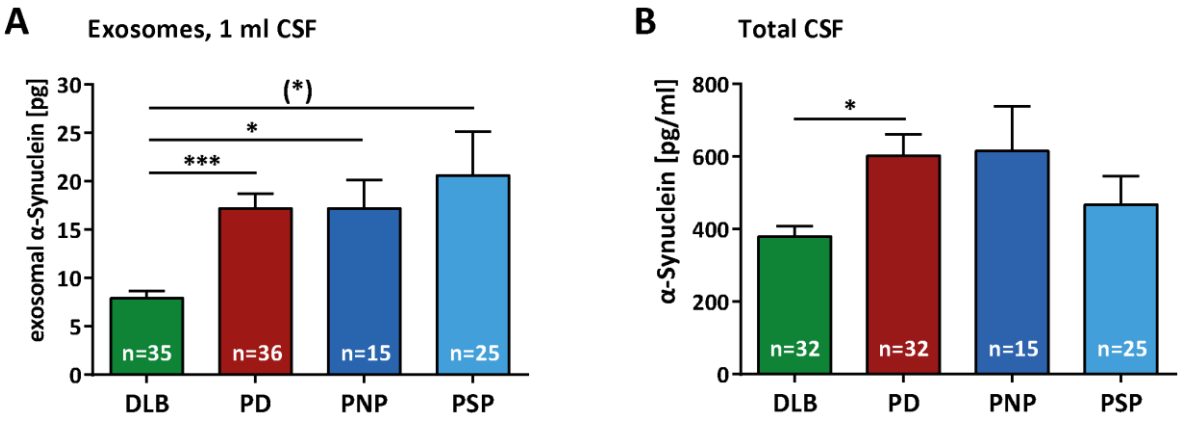

Figure 3.4: α-Synuclein levels in CSF exosomes and total CSF from patients with PD, DLB and non-α-Synuclein related disease controls in the Kassel cohort. (**A**) α-Synuclein protein levels were determined in exosomes prepared from 500 µl CSF from patients with DLB (green bar), PD (red bar), PNP (dark blue bar) and PSP (light blue bar). Protein values were then normalized to 1 ml, n = 35 DLB patients, n = 36 PD patients, n = 15 PNP patients and n = 25 PSP patients. DLB exosomes exhibit lower α-Synuclein levels compared to all other patients groups. One-way ANOVA indicated significant differences (p = 0.000691) and Games-Howell post hoc test was applied, (*) p = 0.05, * p < 0.05, *** p < 0.0005. (**B**) Quantification of α-Synuclein concentrations in total CSF from patients with DLB (green bar, n = 32), PD (red bar, n = 32), PNP (dark blue bar, n = 15) and PSP (light blue bar, n = 25). α-Synuclein is less abundant in DLB CSF compared to PD CSF, one-way ANOVA (p = 0.0202), Games-Howell post hoc test, * p = 0.05. All values are shown as mean ± SEM.

3.1.4.2. CSF exosomal α-Synuclein correlates with cognitive impairment in DLB patients

Next, we plotted CSF exosomal α-Synuclein levels against the Mini-mental State Examination (MMSE) scores. The MMSE is a screening test for dementia which covers different cognitive domains such as orientation, language, memory and visuoconstruction (Folstein et al., 1975) (see also Table 3.1.). A MMSE score between 0 – 10 indicates severe dementia, 11 – 20 moderate dementia and above 20 mild dementia. Test scores between 27 – 30 can be observed in non-demented individuals.

Table 3.1: Mini-mental State Examination after Folstein et al. (1975).

Maximum	Score	
		Orientation
5	( )	What is the (year) (season) (date) (day) (month)?
5	( )	Where are we (state) (country) (town) (hospital) (floor)?
		Registration
3	( )	name 3 objects: 1 second to say each. Then ask the patient all 3 after you have said them. Give 1 point for each correct answer. Then repeat them until he/she learns all 3. Count trials and record. Trials _____
		Attention and Calculation
5	( )	Serial 7`s. 1 point for each correct answer. Stop after 5 answers. Alternatively spell “world” backward.
		Recall
3	( )	Ask for the 3 objects repeated above. Give 1 point for each correct answer.
		Language
2	( )	Name a pencil and watch.
1	( )	Repeat the following “No ifs, ands, or buts”
3	( )	Follow a 3-stage command: “Take a paper in your hand, fold it half, and put it on the floor”
1	( )	Read and obey the following: CLOSE YOUR EYES
1	( )	Write a sentence.
1	( )	Copy the design

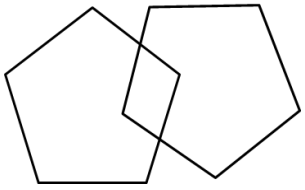

We found an inverse correlation of exosomal α-Synuclein levels and MMSE scores in 32 DLB patients (for 3 DLB subjects no MMSE data were available) indicating that higher α-Synuclein protein levels in exosomes are associated with lower MMSE scores and therefore with impaired cognitive function (Figure 3.5A, Pearson`s correlation coefficient $r = -0.382$, $p = 0.028$, two-tailed probability, $n = 32$). We next tested for a correlation of CSF exosomal α-Synuclein with CSF Tau levels, as CSF Tau is a general marker of neurodegeneration, presumably caused by an increased release of Tau from disintegrating neurons. We observed a strong positive correlation for the 17 DLB patients for whom both values were available (Figure 3.5B, Pearson`s correlation coefficient $r = 0.751$, $p = 0.0005$, two-tailed probability). These data demonstrate that higher α-Synuclein protein levels in CSF exosomes are associated with increased CSF Tau levels.

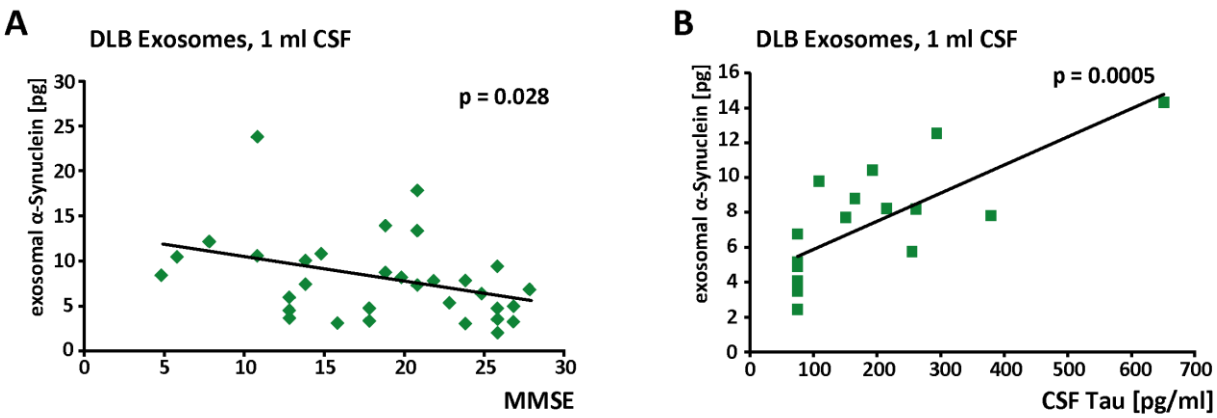

Figure 3.5: Exosomal α-Synuclein correlates with cognitive impairment and neurodegeneration in DLB patients. (**A**) Correlation of α-Synuclein levels in CSF exosomes with impaired cognitive function in DLB patients. Cognitive function was measured by Mini-Mental State Examination (MMSE) test with low scores indicating decreased cognitive function. N = 32, Pearson`s correlation was applied for statistical analysis, coefficient $r = -0.382$, $p = 0.028$, two-tailed probability. (**B**) α-Synuclein levels in CSF exosomes correlate with the increase of Tau protein levels in total CSF from DLB patients indicating progressive neurodegeneration. N = 17, Pearson`s correlation coefficient $r = 0.751$, $p = 0.0005$, two-tailed probability.

3.1.4.3. CSF exosomal α-Synuclein does not correlate with severity of motor symptoms in PD patients

To examine whether CSF exosomal α-Synuclein levels correlate with disease progression in PD, we plotted exosomal α-Synuclein values of 36 PD patients against their individual H&Y stage score. The H&Y score distinguishes the severity of motor symptoms on a scale from one to five, with higher scores reflecting more severe deficits (Hoehn and Yahr, 1967) (see also Table 3.2). As shown in Figure 3.6, no correlation was observed between exosomal α-Synuclein levels and motor deficits in PD patients (Pearsons`s correlation coefficient r = −0.011, p = 0.950, two-tailed probability, n = 36).

Table 3.2: Hoen and Yahr scale

Stage	H&Y Scale
1	Only unilateral involvement, usually with minimal or no functional disability
2	Bilateral or midline involvement without impairment of balance
3	Bilateral disease: mild to moderate disability with impaired postural reflexes; physically indpendent
4	Severly disabling disease, still able to walk or stand unassisted
5	Confinement to bed or wheelchair unless aided

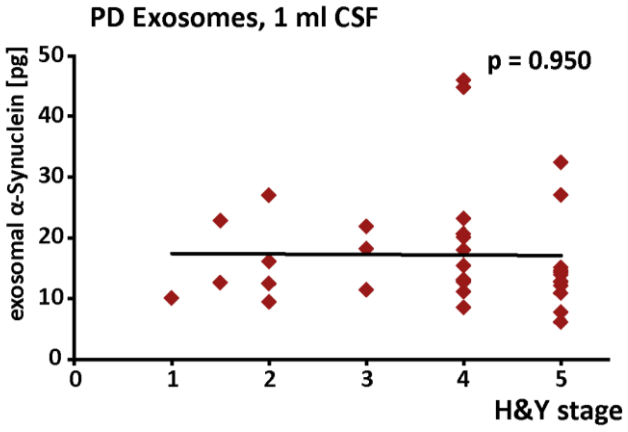

Figure 3.6: Exosomal α-Synuclein does not correlate with the severity of motor symptoms in PD patients. Correlation analysis of CSF exosomal α-Synuclein levels with motor symptoms in PD patients. Motor symptoms were classified by Hoen and Yahr staging (H&Y) with higher numbers indicating decreased motor performance. N = 36, Pearson`s correlation coefficient r = −0.011, p = 0.950, two-tailed probability.

3.1.4.4. CSF exosome numbers differ between the different diagnostic groups

We next measured exosome numbers normalized to the number of exosomes in 1 ml CSF in the different diagnostic groups. Figure 3.7 illustrates that the PD group revealed the highest number of exosomes among all groups with almost four-fold higher values as compared to the DLB group, which in turn exhibited the lowest number of exosomes (PD mean = 3.69×10^9 exosomes/ml CSF, SEM = 1.83×10^8 exosomes/ml CSF, n = 37; DLB mean = 1.08×10^9 exosomes/ml CSF, SEM = 1.83×10^8 exosomes/ml CSF, n = 30; one-way ANOVA $p < 0.0001$ followed by Games-Howell post hoc test, *** $p < 0.0005$). The number of exosomes was also two-fold higher in PD CSF as compared to the PNP and PSP control groups (PNP mean = 2.03×10^9 exosomes/ml CSF, SEM = 4.09×10^8 exosomes/ml CSF, n = 15; PSP mean = 1.39×10^9 exosomes/ml CSF, SEM = 5.23×10^8 exosomes/ml, n = 24; Games-Howell post hoc test, * $p < 0.05$). Between the PNP and PSP control groups, no significant differences were observed.

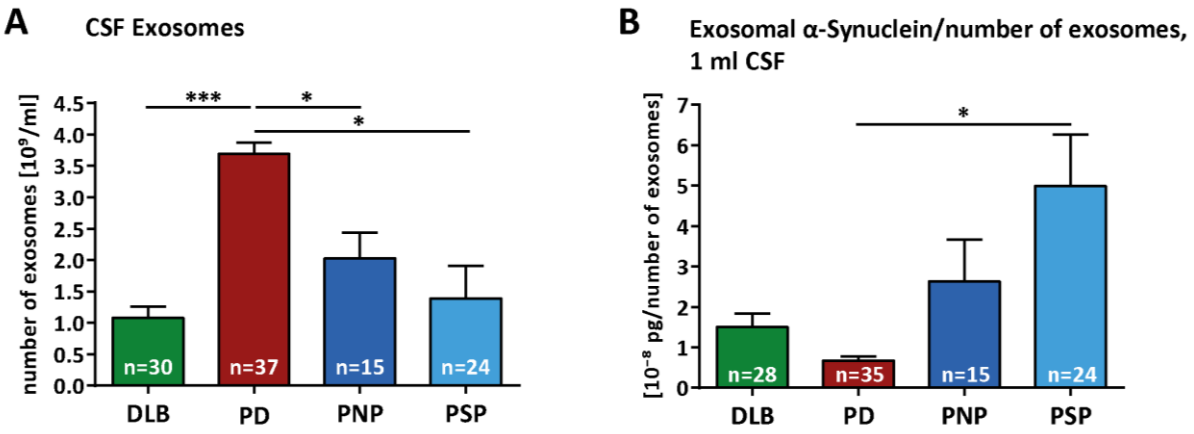

Figure 3.7: Characterization of CSF exosome numbers from DLB, PD, PNP and PSP patient groups. (**A**) Numbers of exosomes were determined by NTA followed by normalization to exosome numbers in 1 ml CSF. Exosome numbers differ highly between the groups; DLB (green bar, n = 30), PD (red bar, n = 37), PNP (dark blue bar, n = 15) and PSP (light blue bar, n = 24). For statistical analysis one-way ANOVA was applied ($p < 0.0001$) followed by Games-Howell post hoc test, * $p < 0.05$, *** $p < 0.0005$. (**B**) Ratio of exosomal α-Synuclein (CSF exosomal α-Synuclein levels are shown in Figure 3.4) to the number of exosomes in 1 ml CSF from patients with DLB (green bar, n = 28), PD (red bar, n = 35), PNP (dark blue bar, n = 15) and PSP (light blue bar, n = 24). One-way ANOVA revealed statistical significance ($p = 0.000377$) and Games-Howell post hoc test was applied, * $p < 0.05$. Values are given as mean ± SEM.

Furthermore, the ratio of exosomal α-Synuclein to the number of exosomes present in 1 ml starting volume of CSF was calculated for DLB, PD, PNP and PSP groups (Figure 3.7B). Here, we found a two- to three-fold lower ratio in PD CSF compared to the other groups, indicating that PD patients contain less α-Synuclein protein per exosomal particle than patients of all other groups (PD mean = 6.74×10^{-9} pg α-Synuclein/number of exosomes, SEM = 1.04×10^{-9} pg α-Synuclein/number of exosomes, n = 35; DLB mean = 1.50×10^{-8} pg α-Synuclein/number of exosomes, SEM = 3.37×10^{-9} pg α-Synuclein/number of exosomes, n = 28; PNP mean = 2.63×10^{-8} pg α-Synuclein/number of exosomes, SEM = 1.03×10^{-8} pg α-Synuclein/number of exosomes, n = 15; PNP mean = 4.99×10^{-8} pg α-Synuclein/number of exosomes, SEM = 1.27×10^{-8} pg α-Synuclein/number of exosomes, n = 24; one-way ANOVA revealed significant differences, p = 0.000377, Games-Howell post hoc test, * $p < 0.05$). We did not find significant differences between the PNP and PSP groups.

3.1.5. Diagnostic performance of CSF exosomal α-Synuclein as a potential biomarker in α-Synuclein related disorders

We next evaluated the diagnostic performance of CSF exosomal α-Synuclein and the ratio of exosomal α-Synuclein to the number of CSF exosomes as potential biomarkers in a preliminary trial (Figure 3.8). ROC curve analysis of exosomal α-Synuclein to distinguish DLB from PD revealed a sensitivity and specificity of 85.7% and 80.6% with a positive predicitive value of 81.1% and a negative predictive value of 85.3% (Table 3.3). ROC curve analysis of exosomal α-Synuclein to discriminate between DLB and PNP exhibited values of 85.7% for the sensitivity and 66.7% for specificity and positive and negative prediction were 83.3% and 64.3%, respectively (Table 3.3). The sensitivity and specificity for the distinction of DLB from PSP samples were 71.4% and 92.0% with positive and negative predictive values of 92.9% and 71.8% (Table 3.3). Calculated AUC values, indicating the overall quality of the test to distinguish between two diagnostic groups, were between 0.804 and 0.883 for exosomal α-Synuclein (Figure 3.8A,C,D).

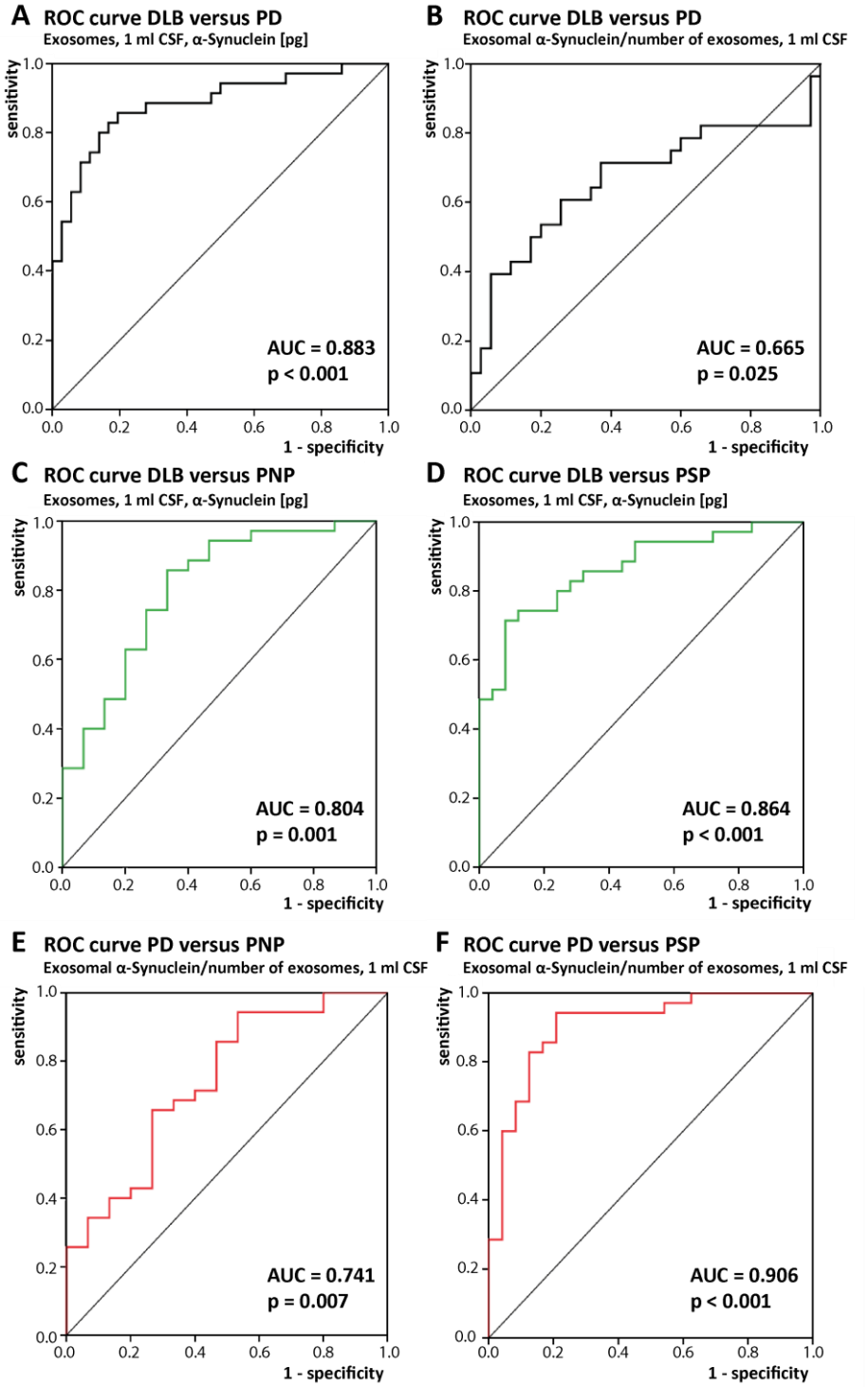

Figure 3.8: Diagnostic performance of CSF exosomal α-Synuclein and the ratio of CSF exosomal α-Synuclein to the number of exosomes. Receiver operating characteristics (ROC) curve analysis was performed to examine the diagnostic value of CSF exosomal α-Synuclein levels as well as of the ratio exosomal α-Synuclein to the number of exosomes. (**A**) ROC curve of exosomal α-Synuclein in CSF to distinguish DLB from PD, area under the curve (AUC) = 0.883, $p < 0.001$. (**B**) ROC curve of the ratio exosmal α-Synuclein to the number of exosomes to discriminate between DLB and PD, AUC = 0.665, $p = 0.025$. (**C**) ROC curve of α-Synuclein levels in exosomes to distinguish DLB from PNP, AUC = 0.804, $p = 0.001$ and (**D**) to distinguish DLB from PSP, AUC = 0.864, $p < 0.001$. (**E**) ROC curve of the ratio of exosomal α-Synuclein to the number of exosomes to discriminate between PD and PNP, AUC = 0.741, $p = 0.007$ and (**F**) to discriminate between PD and PSP, AUC = 0.906, $p < 0.001$. Values for sensitivity, specificity and prediction are listed in Table 3.3 and Table 3.4.

In addition, we performed ROC curve analysis of the ratio of exosomal α-Synuclein to the number of exsomes in CSF and we observed a sensitivity of 74.3% and a specificity of 60.7% for the discrimination of PD patients from DLB patients (Table 3.4). The sensitivity was high (94.3%) to distinguish PD from PNP, whereas the specifity was only 46.7% (Table 3.4). We also detected high values for the sensitivity (94.3%) and moderately high levels of specificity (79.2%) to differentiate between PD and PSP (Table 3.4). The positive and negative predictive values for this marker were between 68.4% and 82.1% for positive prediction and between 64.0% and 90.4% for negative prediction. Calculation of AUC values showed values between 0.665 for the discrimination of PD and DLB (Figure 3.8B), 0.741 for the discrimination of PS and PNP (Figure 3.8E) and 0.906 to distinguish PD from PSP (Figure 3.8F).

Table 3.3: Exosomal α-Synuclein [pg] in 1 ml CSF

	AUC	P-value	Cut-off Value (pg/ml)	Sensitivity (%)	Specificity (%)	Positive Predictive Value (%)	Negative Predictive Value (%)
DLB versus PD	0.883	< 0.001	11.34	85.7	80.6	81.1	85.3
DLB versus PNP	0.804	= 0.001	11.46	85.7	66.7	83.3	64.3
DLB versus PSP	0.864	< 0.001	9.23	71.4	92.0	92.9	71.8

Table 3.4: Exosomal α-Synuclein [pg]/number of exosomes, 1 ml CSF

	AUC	P-value	Cut-off Value (10^{-8} pg per particle)	Sensitivity (%)	Specificity (%)	Positive Predictive Value (%)	Negative Predictive Value (%)
PD versus DLB	0.665	0.025	0.75	74.3	60.7	68.4	64.0
PD versus PNP	0.741	0.007	1.30	94.3	46.7	80.5	77.8
PD versus PSP	0.906	< 0.001	1.27	94.3	79.2	82.1	90.4

3.1.6. CSF exosomes from PD and DLB patients induce the aggregation of α-Synuclein *in vitro*

We hypothesized that exosomes might contribute to the spreading of pathological α-Synuclein species by the transfer of aggregated α-Synuclein to healthy neurons. Here, they could act as a seed to induce the aggregation of soluble α-Synuclein. To study the potential of CSF exosomes to induce α-Synuclein aggregation we incubated CSF derived exosomes from patients with PD, DLB and neurological controls with a reporter cell line to detect α-Synuclein aggregation. In this *Gaussia* luciferase protein-fragment complementation assay split luciferase fragments [either N-terminal (S1) or C-terminal (S2) fragment], that are not active in their state, are fused to the C-terminus of α-Synuclein and were transiently expressed in H4 cells (Figure 3.9A). Physical interaction of the α-Synuclein molecules results in active luciferase due to the close proximity and complementation of the split fragments which can be measured as a luminescence signal in the presence of a luciferase substrate. The protein-fragment complementation assay was kindly performed by Prof. Dr. Karin Danzer`s research group (Department of Neurology, Ulm University).

To study the effect and seeding potential of CSF derived exosomes on the induction of aggregation of soluble α-Synuclein in cells, exosomes were purified from the same volume of CSF from patients with DLB, PD and neurological controls. All CSF specimens were randomly selected from the Kassel cohort and the control patient group consisted of 6 PNP patients, 1 patient with normal pressure hydrocephalus and 1 patient suffering from corticobasal degeneration. Previously transfected cells were then treated with purified CSF exosomes and the seeding capacity of exosomes was quantified. Quantification of α-Synuclein interaction was calculated as fold luminescence increase of the luminescence signal measured in α-Synuclein transfected and CSF exosome treated cells compared to mock treated control cells. Control cells were incubated with CSF exosomes but were not transfected with the two α-Synuclein constructs, only transfection reagent was added. To rule out unspecific interaction of both luciferase fragments, a series of control experiments was performed previously by Danzer et al. (2011). Here, no luciferase activity changes were reported for the co-transfection of α-Synuclein S1 with Aβ fused to the C-terminal luciferase fragment nor for the combination of α-Synuclein S2 with Aβ fused to the N-terminal fragment of luciferase.

As shown in Figure 3.9B, we observed an approximately two-fold increase of the luminescence signal in H4 cells treated with PD derived exosomes compared to cells treated with DLB and neurological control exosomes (DLB mean = 6.40 fold increase, SEM = 0.77 fold increase, n = 9; PD mean = 15.79 fold increase, SEM = 1.73 fold increase, n = 10 and neurological control mean = 8.79 fold increase, SEM = 1.58 fold increase, n = 7, one-way ANOVA, p = 0.000513, followed by Student`s two-sided t-test, * < 0.05). Thus, PD derived CSF exosomes exhibit a higher capacity to induce the aggregation of soluble α-Synuclein in cells.

As reported in sections 3.1.4.1 and 3.1.4.4, α-Synuclein levels and the number of exosomes are significantly decreased in CSF derived from DLB patients compared to PD and neurological controls. We therefore calculated the potential of CSF exosomes to induce aggregation of soluble α-Synuclein after normalizing for exosomal α-Synuclein content in each sample (Figure 3.9C). To this end, we calculated the ratio of fold luminescence increase to exosomal α-Synuclein content of each sample. Interestingly, after normalizing for exosomal α-Synuclein content, both, PD and DLB exosomes had a stronger aggregate inducing effect on α-Synuclein compared to neurological controls [DLB mean = 2.43 fold luminescence increase/pg exosomal α-Synuclein, SEM = 1.05 fold luminescence increase/pg exosomal α-Synuclein, n = 8; PD mean = 2.87 fold luminescence increase/pg exosomal α-Synuclein, SEM = 0.95 fold luminescence increase/pg exosomal α-Synuclein, n = 9; neurological control mean = 1.50 fold luminescence increase/pg exosomal α-Synuclein, n = 6; one-way ANOVA revealed significant difference, p = 0.00698, (*) p < 0.10 indicates strong statistical tendency due to the small sample size, * p < 0.05, Mann-Whitney U-test].

As shown in (Figure 3.9D), a strong correlation between exosomal α-Synuclein content and the potential to induce α-Synuclein aggregation was observed for exosomes from DLB (green diamonds, n = 8) and PD patients (red rectangles, n = 9) but not for exosomes from the control group (blue triangles, n = 6; Pearson`s correlation coefficient for DLB and PD: r = 0.85, p = 1.6×10^{-5}, n = 17; control group: r = −0.25, p = 0.64).

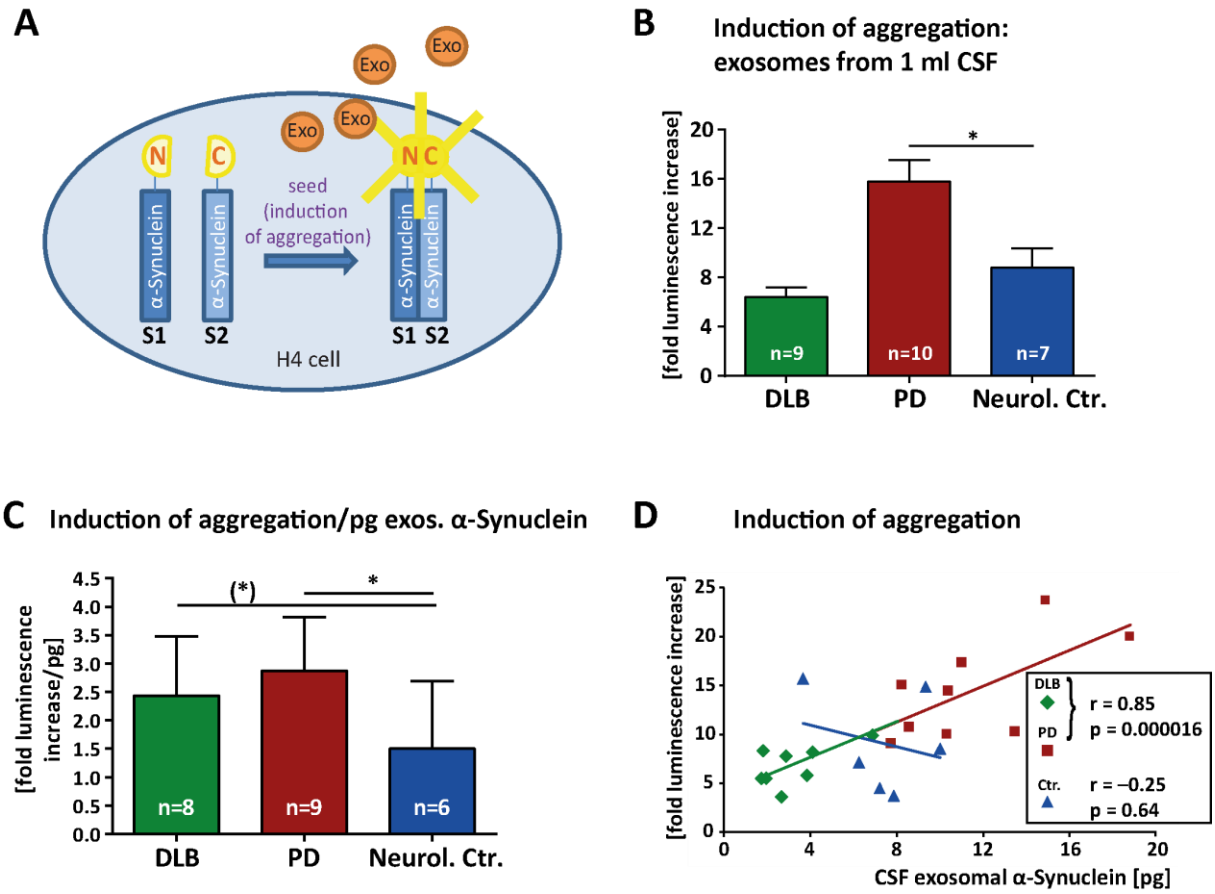

Figure 3.9: CSF exosomes from DLB and PD patients induce the aggregation of soluble α-Synuclein in a cell model. (**A**) Schematic cartoon of the split luciferase complementation assay. Human neuroglioma H4 cells are co-transfected with two α-Synuclein constructs, each fused to different luciferase fragments (S1: N-terminal part of luciferase, S2: C-terminal part of luciferase). When both luciferase fragments complement due to aggregation of α-Synuclein, a luminescence signal is measured indicating induced aggregation of α-Synuclein. (**B**) Transfected H4 cells exhibit a luminescence increase upon treatment with exosomes prepared from equal volumes of CSF. Exosomes were derived from patients with DLB (green bar, n = 9), PD (red bar, n = 10) and neurological controls (blue bar, n = 7). One-way ANOVA revealed significant difference ($p = 0.000513$) that was further specified by two-sided t-test, * $p < 0.05$. All measurements were peformed in duplicates. (**C**) Ratio of luminescence increase in H4 cells to α-Synuclein levels in CSF exosomes from patients with DLB (green bar, n = 8), PD (red bar, n = 9) and neurological controls (blue bar, n = 6). After normalizing for α-Synuclein content in exosomes, DLB and PD derived exosomes cause a significant increase of the luminescence signal in reporter cells. One-way ANOVA was applied ($p = 0.00698$) followed by two-tailed Mann-Whitney U-test, (*) $p < 0.10$, * $p < 0.05$. All measurements were performed in duplicates. (**D**) Correlation analysis of luminescence increase in H4 cells with CSF exosomal α-Synuclein levels prepared from 1 ml CSF; DLB: green diamonds, n = 8, PD: red rectangles, n = 9 and neurological controls: bue triangles, n = 6. Pearson`s correlation coefficient for DLB and PD: $r = 0.85$, $p = 1.6 \times 10^{-5}$ and neurological controls: $r = -0.25$, $p = 0.64$.

3.1.7. Characterization of exosomal α-Synuclein in plasma from patients with DLB, PD and neurological controls

Additionally to the characterization of exosomal α-Synuclein derived from CSF, we focused on exosomal α-Synuclein derived from plasma as another source of exosomes. Therefore, we selected plasma samples from DLB, PD and neurological control patients from the Kassel cohort and purified exosomes from 500 µl total plasma by UC. Further demographic information of the analyzed plasma samples is depicted in Table 6.3.

Exosomes were then analyzed for their α-Synuclein content by ECL assay. Figure 3.10A shows the quantification of α-Synuclein levels in exosomes normalized to 1 ml plasma as starting material. Here, we did not detect any significant differences in exosomal α-Synuclein content between DLB and control plasma or between PD and control plasma [DLB mean = 83.30 pg exosomal α-Synuclein, SEM = 29.32 pg exosomal α-Synuclein, n = 9; PD mean = 60.95 pg exosomal α-Synuclein, SEM = 12.04 pg exosomal α-Synuclein, n = 23 and neurological control mean = 59.73 pg exosomal α-Synuclein, SEM = 9.77 pg exosomal α-Synuclein, n = 23; one-way ANOVA revealed no significant differences (p = 0.5723)]. When we calculated the ratio of α-Synuclein in exosome preparations to α-Synuclein in total plasma, we observed that 0.2% – 0.3% of total plasma α-Synuclein is associated with exosomes with a tendency to a lower ratio in patients with DLB. However, no significant differences between the patient groups were detected (Figure 3.10B, DLB mean = 0.21%, SEM = 0.018%, n = 9; PD mean = 0.30%, SEM = 0.037%, n = 23 and neurological control mean = 0.30%, SEM = 0.038%, n = 22; p = 0.3065, one-way ANOVA).

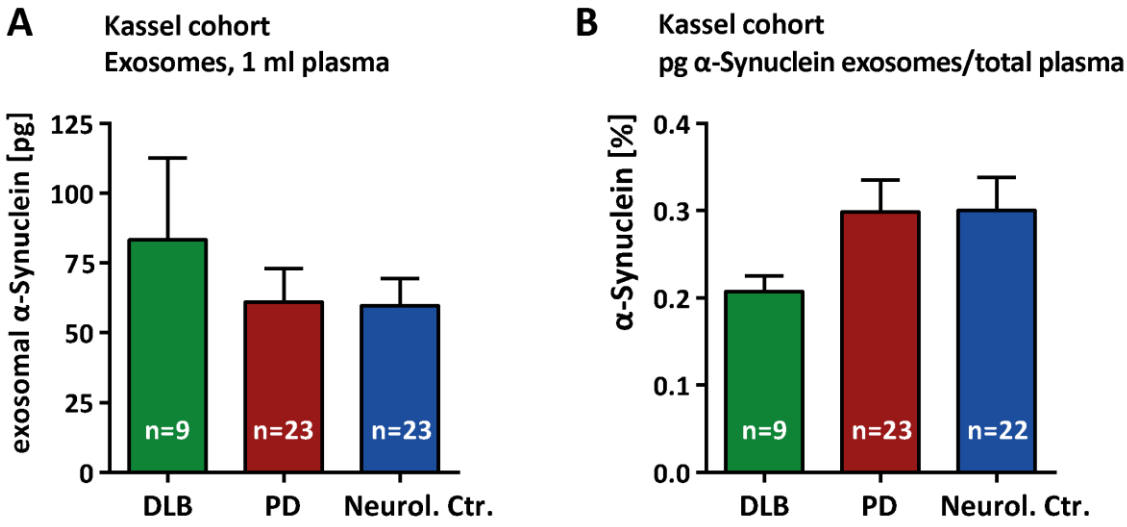

Figure 3.10: Characterization of exosomal α-Synuclein in plasma from patients with DLB, PD and neurological controls. (**A**) Quantification of plasma exosomal α-Synuclein derived from DLB, PD and neurological control samples, which were obtained from the Kassel cohort. DLB: green bar (n = 9), PD: red bar (n = 23) and neurological controls: blue bar (n = 23). One-way ANOVA (p = 0.5732) revealed no significant differences.
(**B**) Ratio (in %) of α-Synuclein levels in exosomes to α-Synuclein levels in total plasma in DLB patients (green bar, n = 9), PD patients (red bar, n = 23) and neurological controls (blue bar, n = 22). For statistical analysis, one-way ANOVA was applied, p = 0.3065 (n.s.). All values are given as mean ± SEM.

3.1.7.1. Plasma exosomes and exosomal α-Synuclein purified by SEC are suitable for quantitative analysis

In addition to the UC based isolation method, we used SEC purification as a second approach to isolate plasma exosomes since several disadvantages of the UC purification have been observed. A reliable quantification of exosome numbers in both, total plasma and the UC pellet is not possible by using NTA due to the abundance of lipoproteins and IgG complexes of similar size in total plasma which might be co-isolated with exosomal vesicles in the UC pellet (Boing et al., 2014), thus making it impossible to discriminate between protein complexes and exosomes. Furthermore, UC leads to aggregation of exosomes, which might interfere with the correct analysis of exosome concentrations in the pellet. Another challenge is the lack of purity of blood derived UC exosomes since they were found to be contaminated with albumin and protein complexes (Boing et al., 2014).

For SEC purification, 1 ml plasma was subjected to serial centrifugation rounds as described in section 2.2.3.2. The supernatant of the 10,000 x g step was loaded on the SEC column and 24 fractions (500 µl each) were collected and analyzed for particle numbers by NTA and their total protein content by NanoDrop spectrophotometer (Figure 3.11A). For the quantification of exosome numbers, fractions were measured six times in a 1:800 dilution. The majority of particles in the size range of exosomes (≤ 120 nm) eluted in SEC fractions 9 – 12 (red line) whereas total protein amounts started to increase from fraction 12 on and reached their highest levels in fractions 21 and 22 (blue line) (Figure 3.11A). This was further supported by WB analysis of SEC fractions derived from 1 ml plasma and immunostained against human IgG as an abundant protein in total plasma (Figure 3.11C). IgG was detected in total plasma and in SEC fractions 12 – 24 as well as in the UC pellet indicating partial co-purification of IgG via UC. In contrast, lower SEC fractions 7 – 11 were found to be free of IgG (Figure 3.11C). We therefore decided to collect fractions 8 – 11 as the purest fractions containing exosomes.

For α-Synuclein quantification fractions were pooled as follows: 1 – 4, 5 – 8, 9 – 12, 13 – 16 and 17 - 24. Quantification of α-Synuclein protein revealed a total of 11.6 pg in fraction pool 9 - 12, which was the exosome containing pool, compared to fractions 1 - 4 (0 pg α-Synuclein), fractions 5 – 8 (6.18 pg α-Synuclein) and fractions 13 – 16 (10.5 pg α-Synuclein) (Figure 3.11B). However, the highest level of α-Synuclein was measured in fraction pool 17 - 24 (422.8 pg α-Synuclein) indicating that the majority of α-Synuclein in total plasma is non-vesicle associated but rather consists of free α-Synuclein species which elute later and are therefore found in in higher SEC fractions. This was further confirmed by the ratio of exosomal α-Synuclein (fraction 8 – 11) to total plasma α-Synuclein content (Figure 3.11D). Only 0.27% (± 0.15%) of overall α-Synuclein in total plasma was found in association with exosomes. This ratio is comparable to our previous findings with plasma exosomes purified by UC (see also 3.1.7 and Figure 3.10B).

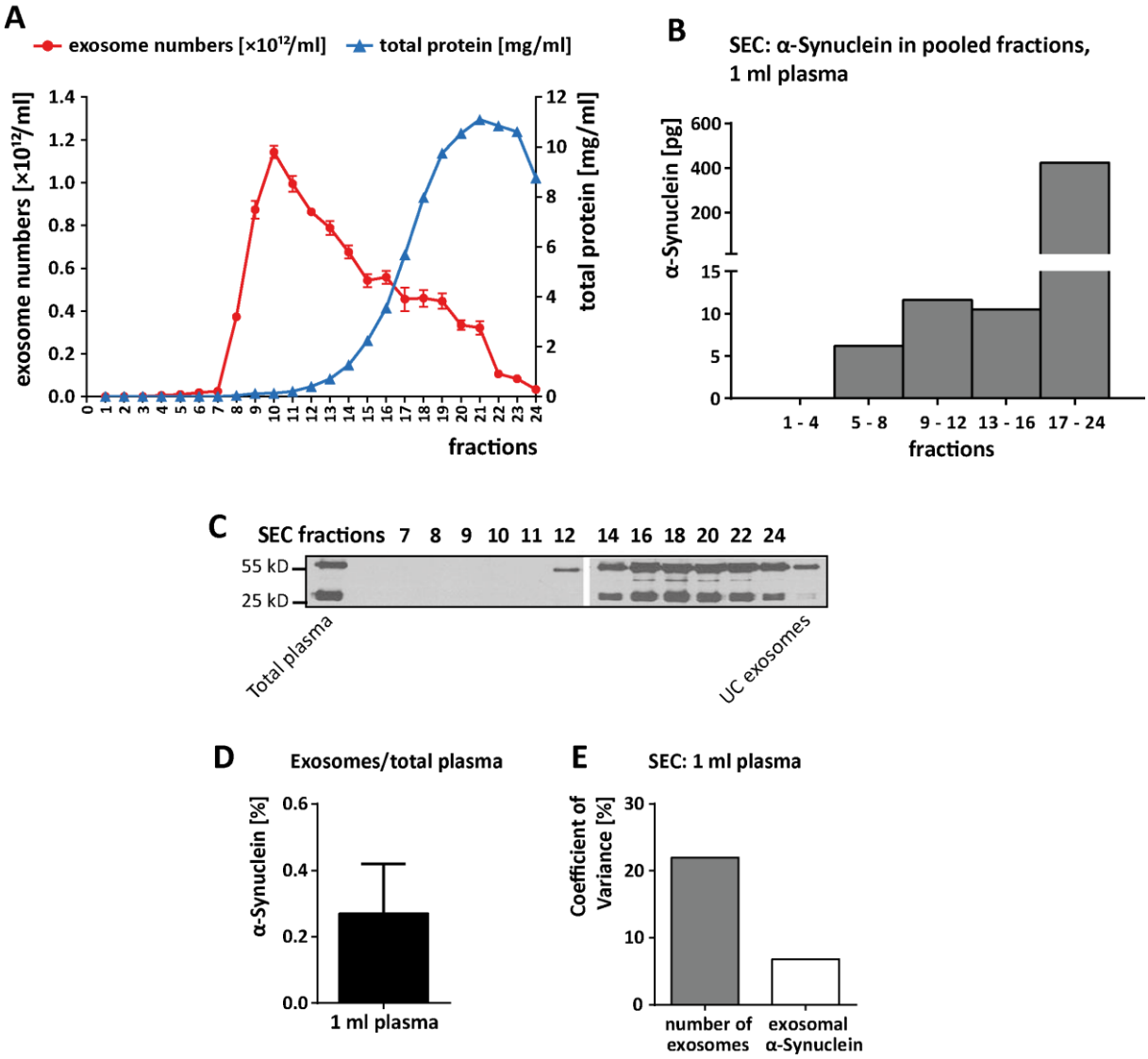

Figure 3.11: Purification of exosomes from plasma by size exclusion chromatography (SEC). (**A**) 1 ml plasma was first cleared from cellular debris and larger plasma membrane derived vesicles and then loaded on a SEC column. Particle numbers in the size range of exosomes of each SEC fraction were quantified by NTA (red line) and the total protein concentration of each fraction was measured by NanoDrop spectrophotometer (blue line). (**B**) α-Synuclein protein levels of pooled SEC fractions 1 – 4, 5 – 8, 9 – 12, 13 – 16 and 17 – 24 derived from 1 ml plasma were quantified by ECL assay with fractions 9 – 12 as the exosome pool according to NTA results in **A** . The y-axis was splitted into two segments due to the high α-Synuclein level in fraction pool 17 – 24. (**C**) WB analysis of SEC fractions derived from 1 ml plasma, total plasma and the UC preparation from 1 ml of the same sample. Samples were stained against the high abundant total plasma protein IgG to verify purity of the exosome pool (**D**) The ratio of α-Synuclein levels in exosomes purified by SEC (fractions 8 – 11) to α-Synuclein levels present in total plasma is given in %. (**E**) The CV was calculated for the number of exosomes and α-Synuclein protein levels in SEC purified exosome pool (fraction 8 – 11). Here, n = 5 biological replicates from one plasma donor were purified by SEC and analyzed on 5 different days. Values are given as mean or mean ± SEM.

As described above, accurate quantification of exosome numbers by NTA was challenging when using UC preparation due to the presence of lipoproteins displaying a similar size as exosomes. By using SEC, exosome numbers analyzed in the exosome containing fractions 8 - 11 resulted in a CV of 22% (Figure 3.11E, *left bar*) and the CV for exosomal α-Synuclein levels revealed a value of 6.84%. (Figure 3.11E, *right bar*). The CVs were calculated from 5 biological replicates of one plasma sample.

These findings indicate that exosomes purified via the SEC method now allow reliable quantification of exosome numbers and exosomal α-Synuclein levels.

3.2. Small ncRNAs in CSF exosomes as a potential biomarker in AD

In the second part of the study we evaluated the potential of CSF exosomal small ncRNA species to discriminate AD from controls without neurodegeneration. We first asked whether exosomal RNA reflects the intracellular RNA composition and may therefore be suitable as a potential biomarker candidate. The potential of CSF exosomal small ncRNAs as a diagnostic biomarker was tested with a cohort of AD patients and psychiatric controls without dementia or other neurodegenerative diseases.

Of note, since a patent application for CSF exosomal small ncRNAs as a biomarker in AD is in preparation, the small ncRNA signatures of exosomes derived from primary cortical and hippocampal neurons as well as from AD and neurological control CSF are not shown in this thesis.

3.2.1. Exosomal small ncRNA content reflects neuronal small ncRNA composition

First, we determined the small ncRNA composition in exosomes and compared it to that of the corresponding parent cell line. For this purpose, exosomes were purified from medium of primary mouse cortical or hippocampal neuronal cultures. Purification was performed according to the UC protocol (see section 2.2.3.1) and cell lysates were prepared in parallel (see section 2.2.5.3) followed by extraction of total RNA from exosome preparations and cell lysates using TriReagent based protocols. Samples were then subjected to small RNA NGS sequencing.

When plotting the small ncRNA expression levels in exosomes derived from cortical neurons against the cellular small ncRNA expression levels we found a strong correlation (Figure 3.12A, Pearson`s correlation $R^2 = 0.98$, $p < 10^{-5}$) indicating that the exosomal RNA composition is very similar to the intracellular RNA of the parental cell. Similar results were obtained in exosomes derived from hippocampal neuron cultures as depicted in Figure 3.12B (Pearson`s correlation $R^2 = 0.98$, $p < 10^{-5}$).

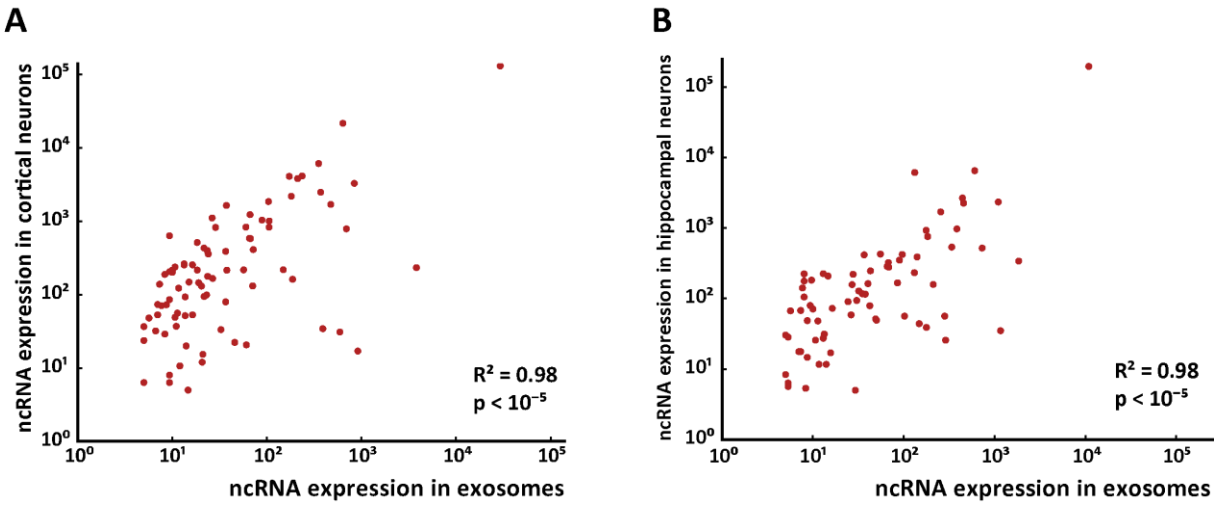

Figure 3.12: Small ncRNA composition in exosomes partially reflects that one of the parental cell. Scatterplots displaying correlations between small ncRNA expression levels in exosomes derived from primary cortical neurons and ncRNA expression levels in corresponding cells (**A**) or between small ncRNA expression levels in exosomes derived from primary hippocampal neurons and those of the parental cells (**B**). Each dot represents an individual small ncRNA and Pearson`s correlation was applied for statistical analysis. Correlation coefficient $R^2 = 0.98$, $p < 10^{-5}$ for (**A**) and correlation coefficient $R^2 = 0.98$, $p < 10^{-5}$ for (**B**).

Despite the fact that several small ncRNAs were found to be differentially expressed in exosomes compared to the parent cell (data not shown), the overall composition of small ncRNAs in exosomes represented that of the corresponding cell. Thus, exosomes might be suitable to reflect small ncRNA dysregulation in neurons.

3.2.2. CSF exosomal small ncRNA signatures as a potential diagnostic biomarker for AD

The next step was to test whether the exosomal RNA composition could be used for diagnostic purposes to distinguish between AD and controls. To this end, CSF exosomal small ncRNA from a cohort composed of 24 AD patients and 18 controls (for detailed description of the cohort refer to section 2.2.2.3 and Table 6.4) was sequencend followed by the analysis of differentially expressed small ncRNAs (Figure 3.13A for experimental design). Initially, the exosomal RNA of 31 AD and 19 control samples was sequenced but 7 AD and 1 control sample were not usable for bioinformatic analyses due to poor RNA quality. These samples were filtered out since their library size was below 100,000 reads.

Based on RNA expression levels, sample classification was performed by using machine learning algorithm approach in combination with statistical methods to achieve the selection of a specific combination of small ncRNAs. This set of selected small ncRNAs was further used to develop an algorithm that allows the discrimination of AD patients from controls. The final data set was then trained and tested with an independent replication cohort that comprised 21 AD and 20 control samples (for further information see section 2.2.2.3 and Table 6.5). The initial cohort comprised 37 AD and 34 control samples and was reduced to 21 AD and 20 control samples after quality filtering for library size.

The performance during training and testing is depicted in Figure 3.13B and resulted in an AUC value of 0.83 during testing indicating that the final small ncRNA signature achieved high accuracy (Figure 3.13C).

This indicates that the identified small ncRNA signature in human CSF may in principle be suitable to distinguish between AD patients and psychiatric controls with an accuracy similar to that of the approved diagnostic CSF markers Aβ42, Tau and phospho-Tau.

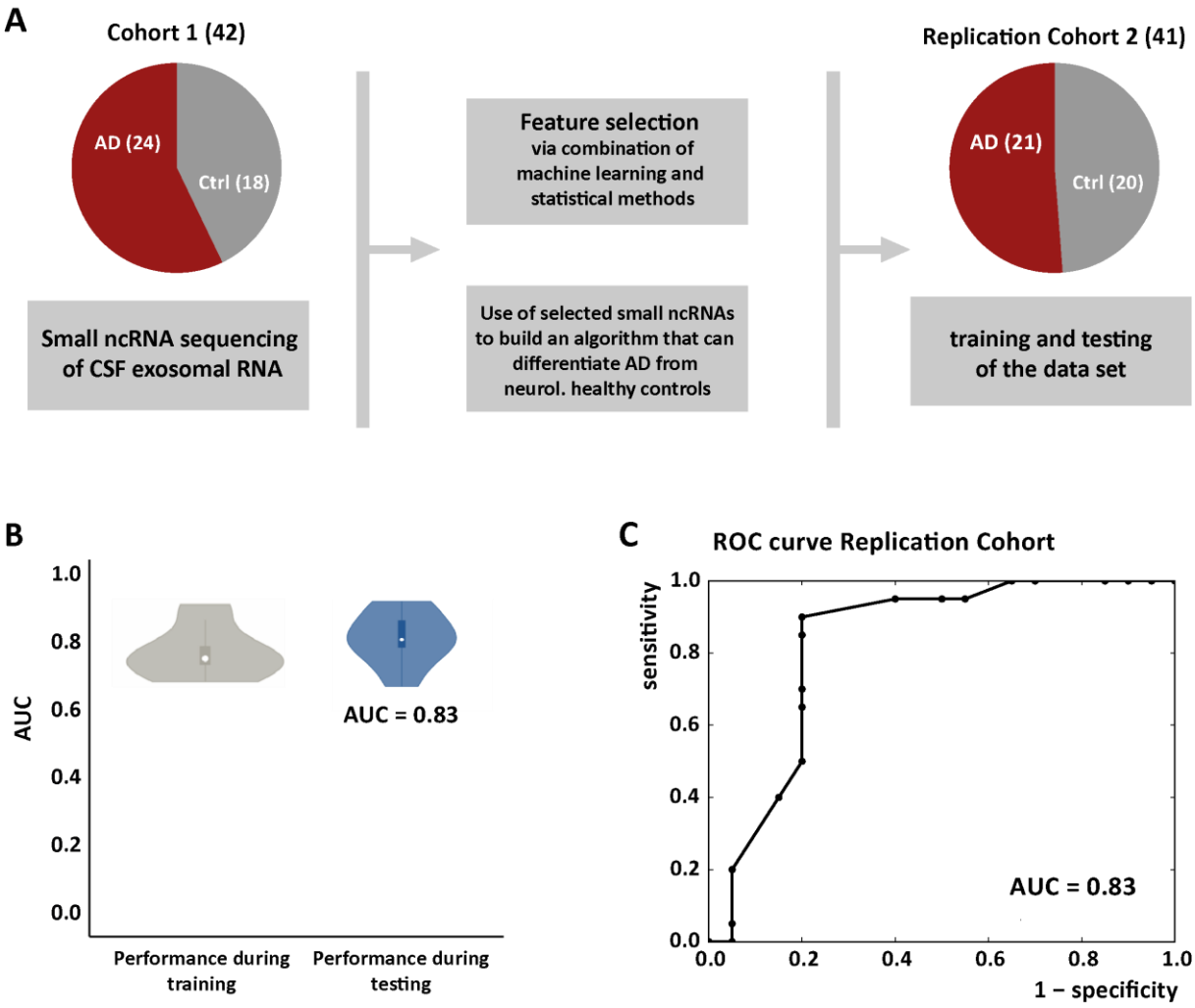

Figure 3.13: CSF exosomal small ncRNA signature to differentiate AD from controls. (A) Schematic overview of the generated pipeline to evaluate the potential of CSF exosomal small ncRNA signatures to distinguish between AD and controls. Bioinformatic analyses were developed and performed by Gaurav Jain (under supervision of Prof. Dr. André Fischer, DZNE Göttingen). (**B**) Violin plot demonstrating performance of the replication cohort during training and testing of the selected data set. (**C**) ROC curve analysis of the replication cohort was performed to examine the diagnostic performance of CSF exosomal small ncRNAs to discriminate between AD patients and controls and revealed an AUC value of 0.83.

4. Discussion

4.1. Characterization of CSF exosomal α-Synuclein in patients with α-Synuclein related neurodegeneration

In this study, we aimed to characterize exosomal α-Synuclein in different patient groups including α-Synuclein related neurodegeneration (PD and DLB), neurological controls with a non-α-Synuclein related Pakinson syndrome (PSP), and non-neurodegenerative controls by quantifying exosomal α-Synuclein levels and exosome numbers in CSF. Here, we provide evidence that CSF exosomal α-Synuclein may allow the discrimination between α-Synuclein related neurodegeneration and non-α-Synuclein related Parkinson syndrome. Therefore, exosomal α-Synuclein bears the potential as a diagnostic biomarker in the future, replication provided.

Moreover, we were able to show that CSF derived exosomes from patients with PD and DLB have an increased potential to cause the induction of α-Synuclein aggregation compared to those from neurological controls. This finding may provide more insight on the spreading of α-Synuclein pathology.

4.1.1. Induction of α-Synuclein aggregation by CSF exosomes

4.1.1.1. Exosomes as carriers for pathogenic proteins

It has been previously shown that exosome-like MVs can be enriched in aggregation-prone proteins such as PrP, Aβ, Tau, and α-Synuclein (Bellingham et al., 2012b; Fevrier et al., 2004; Saman et al., 2012; Sharples et al., 2008). Several *in vitro* studies demonstrated exosomal α-Synuclein release, transfer, and uptake into recipient cells (Danzer et al., 2012; Emmanouilidou et al., 2010). Recently, we were able to report that exosomal α-Synuclein is present in the CNS *in vivo* (Kunadt et al., 2015).

Within this study, we demonstrate that exosomal α-Synuclein can be isolated from human CSF where it is accessible for quantification (section 3.1.1 and Figure 3.2). By using a reporter cell assay, PD exosomes show a two-times higher aggregate inducing activity when exosomes prepared from equal CSF volumes were added to the reporter cells. Since we observed that CSF from DLB patients contains lower overall numbers of exosomes compared

to PD patients and neurological controls it was not surprising that DLB and control exosomes purified from equal CSF volumes do not differ in their α-Synuclein aggregate inducing activity (Figure 3.9B). However, when adjusting for exosomal α-Synuclein levels in the preparations, exosomes from PD and DLB patients exhibit a similar and approximately two times higher potential to induce aggregation of soluble α-Synuclein in recipient cells compared to exosomes from neurological controls. Moreover, exosomal α-Synuclein levels strongly correlate with their potential to induce α-Synuclein aggregation in the case of DLB and PD but not for exosomes derived from the control group. This indicates that exosomes from DLB and PD may contain a pathogenic species of α-Synuclein.

Our findings suggest (i) that exosomes isolated from human CSF carry bioactive α-Synuclein molecules, which are internalized into neuronal cells in an *in vitro* model and (ii) that exosomes from DLB and PD CSF contain a pathogenic α-Synuclein species that is able to induce aggregation of soluble α-Synuclein.

It was demonstrated previously *in vivo* that exosomes can be taken up into neurons where their cargo proteins and RNA molecules are functionally active (El Andaloussi et al., 2013; Fruhbeis et al., 2013). It is possible that a pathogenic misfolded α-Synuclein species is preferentially sorted into exosomes in DLB and PD followed by the exosomal transfer and uptake into a healthy neuron. Interestingly, it has been previously suggested that higher-order oligomerization targets proteins for EV release as demonstrated with the cytoplasmic protein TyA in Jurkat T cells (Fang et al., 2007). Moreover, antibody-induced aggregation of the transferrin receptor enhanced its sorting into MVBs in maturing reticulocytes (Vidal et al., 1997). Thus, in the case of PD and DLB, oligomerization and aggregation of misfolded α-Synuclein could favour its uptake into exosomes.

Observations from *in vitro* and *in vivo* studies could demonstrate that endogenous α-Synuclein can move to healthy neurons (Desplats et al., 2009), exogenous α-Synuclein oligomers and fibrils are taken up by recipient cells and cause seeding of neuronal α-Synuclein aggregation (Hansen et al., 2011; Luk et al., 2009; Volpicelli-Daley et al., 2011), suggesting intercellular propagation of pathogenic α-Synuclein in a prion-like manner. It is possible that pathogenic α-Synuclein aggregates may be released in exosomes and act as a seed for α-Synuclein aggregation in recipient cells. Importantly, Danzer et al. (2012) have provided evidence that oligomeric forms of α-Synuclein are even more efficiently internalized into neuronal cells when they are incorporated into exosomes.

Overall, cell-to-cell transfer of α-Synuclein via exosomes could contribute to the spreading of α-Synuclein pathology in a stereotypical anatomical pattern along axonal projections as observed in α-Synuclein related neurodegeneration (Braak et al., 2003; Lee et al., 2012; Luk et al., 2012; Ulusoy et al., 2013).

To date, the role of exosomes in neurodegeneration is still elusive and besides their proposed disease-driving role, exosomes are suggested to exhibit neuroprotective functions by acting as scavengers in order to remove pathogenic or harmful molecules from the cell under physiological as well as pathological circumstances. Interestingly, impairment of cellular degradation pathways, as autophagy, seems to play a role in insufficient α-Synuclein clearance in PD and DLB (Crews et al., 2010; Rockenstein et al., 2005). Furthermore, α-Synuclein release via exosomes was observed to be increased when the autophagy pathway is blocked *in vitro* (Alvarez-Erviti et al., 2011; Danzer et al., 2012).
Extracellular Aβ has been found to attach to the surface of exosomes *in vitro* (Rajendran et al., 2006) and N2a cell derived exosomes injected into mouse brains were reported to capture Aβ and further favor its clearance by microglia, thus suggesting a role of exosomes in Aβ clearance (Yuyama et al., 2014). The authors further suggest that extracellular Aβ might be trapped to exosomes by binding to glycosphingolipids expressed on the exosomal surface (Yuyama et al., 2014). However, this scenario is unlikely for pathogenic α-Synuclein since α-Synuclein was found to localize to the lumen of exosomes rather than being attached to the surface membrane (Kunadt et al., 2015). Nevertheless, neurons could release pathogenic α-Synuclein species via the exosomal pathway to protect cell integrity. Indeed, exosomes are able to eliminate toxins from cells and deliver these molecules to the extracellular space, e.g. as shown previously with the *Staphylococcus aureus* α-toxin (Husmann et al., 2009).

Thus, exosomes could represent an alternative route to relieve the cell of excess or toxic α-Synuclein molecules and deliver those to microglial cells. Notably, exosomes are more efficiently taken up by microglia than by neurons (Fitzner et al., 2011; Fruhbeis et al., 2013; Zhuang et al., 2011). However, possible microglia dysfunction, as observed in the course of many neurodegenerative diseases (Luo et al., 2010), could contribute to exosomal α-Synuclein spreading to other neurons rather than mediating its degradation via exosome uptake into microglia.

4.1.1.2. Seeding capacity of exosomes

By using the split-luciferase protein fragment complementation assay, we could demonstrate that isolated CSF exosomes from DLB and PD patients exhibit the capacity to induce aggregation of soluble α-Synuclein (Figure 3.9). Evidence of exosomal seeding activities on endogenous proteins was recently provided from studies on the dissemination of Tau pathology (Polanco et al., 2016). Here, the authors demonstrated that exosomes derived from Tau transgenic mice are enriched in mutant Tau and are able to initiate the aggregation of soluble Tau compared to exosomes derived from wild-type mice in a FRET biosensor cell model. Interestingly, induction of Tau aggregation seems to be threshold dependent as reflected by the observation that only cells with a high level of exosome uptake showed Tau aggregation.

We observe that the aggregation inducing activity of PD and DLB exosomes correlates linearily with the levels of exosomal α-Synuclein (Figure 3.9D). Additionally, we find that only a small portion of approximately 2% of CSF total α-Synuclein is associated with exosomes (Figure 3.3C). However, exosomal α-Synuclein aggregates were taken up into cells more efficiently than free extracellular α-Synuclein oligomers (Danzer et al., 2012) and a pathological confirmation of α-Synuclein could induce the templated conversion of soluble α-Synuclein in target cells. Moreover, exosomes were recently suggested to exhibit catalytic effects on the α-Synuclein aggregation process by reducing the lag time and therefore facilitating aggregation of synthetic α-Synuclein *in vitro* (Grey et al., 2015). Also, the authors claimed that gangliosides in the exosomal membrane are sufficient for catalyzing α-Synuclein aggregation. In fact, we cannot claim that the α-Synuclein aggregation inducing activity of PD and DLB exosomes exclusively depends on the exosomal α-Synuclein species.
Since exosomal α-Synuclein levels do not differ between PD and controls in the Kassel cohort (Figure 3.4), the difference in the aggregation inducing activity between PD and control exosomes could be due to a pathogenic α-Synuclein species in PD exosomes. According to our hypothesis, a pathogenic seed, whose actual nature is unknown, would be required in exosomes to initiate the aggregation of endogenous α-Synuclein in healthy cells. This assumption needs to be further investigated by experimental studies including identification of the α-Synuclein species in DLB and PD exosomes compared to control exosomes and

further analyses on whether this species can induce conversion of endogenous α-Synuclein monomers into a misfolded state.

4.1.2. CSF exosomal α-Synuclein as a potential biomarker for α-Synuclein related diseases

4.1.2.1. Quantification of exosomal α-Synuclein and exosome numbers

In this work, we show that exosomal α-Synuclein is present in CSF and that exosomal α-Synuclein levels and CSF exosome numbers can be quantified (Figure 3.2). Multiple studies have already focused on the quantification of α-Synuclein amount in total CSF and plasma in attempt to study this parameter as a potential marker to diagnose PD or other α-Synuclein related disorders. However, reports resulted in inconsistent observations and the diagnostic value was limited due to overlaps with α-Synuclein levels of control groups (Vella et al., 2016; Wennstrom et al., 2013).

When studying CSF α-Synuclein levels in patients with an early stage of PD, in the DeNoPa cohort, we find slightly reduced α-Synuclein levels in total CSF as well as in exosomes compared to healthy controls (Figure 3.3A,B). This finding is in contrast to our observation of more progressed disease stages in the Kassel cohort, where no differences are detected between the PD group and the control groups (compare Figure 3.4). The discrepancy in our two cohorts could be given by the different control groups, which consisted of healthy control patients who did not show any movement disorder in the case of the DeNoPa cohort and patients suffering from polyneuropathy in the Kassel cohort. Although the latter group was negatively tested for PD by clinical methods including standardized Levodopa testing, smell test and brainstem ultrasound, we cannot fully exclude that a minor part of these patients already had an early stage of PD. Moreover, some of the PNP patients also showed a tremor which has recently been shown to precede the clinical diagnosis of PD (Schrag et al., 2015). In addition, it might be possible that the relatively small sample number of the Kassel cohort controls (n = 15) compared to the sample number of the healthy control group of the DeNoPa cohort (n = 58) resulted in a lack of significant differences within exosomal α-Synuclein levels between PD and neurological controls.

The finding of significant lower exosomal α-Synuclein levels in DLB patients compared to PD and the two control groups (Figure 3.4A) is most likely caused by the reduced absolute number of exosomes in DLB CSF compared to all other tested groups (Figure 3.7A). However, we also detect decreased α-Synuclein protein concentrations in total CSF from DLB patients, which is in contrast to findings of other studies that report no differences between DLB, PD and controls (Aerts et al., 2012; Reesink et al., 2010).

Interestingly, the levels of exosomal α-Synuclein increase in more progressed stages of DLB, indicated by the finding that elevated exosomal α-Synuclein levels are paralleled by impaired cognitive function and elevated CSF levels of the neuronal injury marker Tau (Figure 3.5). Tau is an axonal enriched protein that stabilizes microtubules and therefore maintains the morphology of neurons (Ballatore et al., 2007). It is likely that damaged neurons release Tau proteins, which in turn can be transported to the CSF. Consequently, elevated CSF total Tau levels could mirror neuronal damage and are therefore considered as an unspecific marker for neurodegenerative processes, as reported for AD and DLB (Mollenhauer et al., 2005; Montine et al., 2010; Musiek and Holtzman, 2012). We suggest that higher levels of exosomal α-Synuclein in later disease stages could reflect an increased disease activity in DLB patients since it is possible that an increasing number of neurons contain pathogenic α-Synuclein species during the disease course, which in turn could be released within exosomes. As a consequence, the higher number of neurons bearing pathological α-Synuclein could then contribute to the rise of exosomal α-Synuclein levels in CSF. According to this, it would be important to study whether neurons release more exosomes enriched with α-Synuclein during disease progression compared to control neurons. However, a correlation between disease progression and CSF exosomal α-Synuclein levels is not observed in PD. Here, exosomal α-Synuclein levels do not correlate with the severity of motor symptoms (Figure 3.6).

The correlation between increasing exosomal α-Synuclein levels with disease progression and neurodegeneration is in contrast with the finding of overall lower exosomal α-Synuclein levels in the DLB group compared to all other groups. We hypothesize that exosome numbers and hence exosomal α-Synuclein levels in DLB CSF decrease at the beginning or in early stages of the disease and increase again during later stages. The initially low levels of exosomal α-Synuclein and exosome numbers could display a cellular clearance deficit for

α-Synuclein in DLB, which could further contribute to the formation of intracellular α-Synuclein deposits.

4.1.2.2. Preliminary evaluation of CSF exosomal α-Synuclein as a biomarker

By using exosomal α-Synuclein levels as well as the ratio of exosomal α-Synuclein levels to the number of exosomes we are able to discriminate between α-Synuclein related Parkinson syndrome and neurological controls, in a small pilot study. Specificity and sensitivity for the discrimination of DLB, PD and controls are high as demonstrated by ROC curve analysis (Figure 3.8, Table 3.3 and Table 3.4). Of note, since we additionally find that increasing CSF exosomal α-Synuclein levels in DLB are strongly paralleled by cognitive decline and neurodegeneration in later disease stages, we suggest that CSF exosomal α-Synuclein could also display a potential surrogate marker to monitor disease progression in DLB patients. Such markers are still missing, nevertheless longitudinal observations are clearly needed to evaluate the prognostic performance of exosomal α-Synuclein in DLB CSF.

Overall, we provide here the first evaluation of exosomal α-Synuclein as a CSF biomarker for PD and DLB. Since patient numbers are relatively low in the cohort used for analysis, the cohort was monocentric and an independent validation cohort is missing, replication in a larger cohort, ideally derived from different centers, is required for further analysis to define the diagnostic potential of exosomal α-Synuclein.

4.1.3. Methodological considerations regarding EV purification for α-Synuclein quantification in CSF and plasma

A prerequisite before an application as a clinical biomarker for patient stratification or outcome measurement is (i) to further optimize and validate a sample preparation technique which allows easy, fast and reliable purification and quantification of exosomes with low intertest and intersite variability, (ii) the validation of our previous findings in a larger and independent cohort and (iii) to expand our approach to plasma in addition to CSF.

The preparation of plasma exosomes with the most commonly used UC method has so far been hampered by a high variation of exosome yields and a tremendous difficulty to quantify exosome numbers in the resulting vesicle fraction, due to clogging of the vesicles after UC. In addition, blood derived exosome preparations lack a satisfying purity and contain contaminants of lipoproteins, albumin and protein complexes. To overcome these obstacles, we have established size exclusion chromatography preparations from CSF and plasma exosomes, using commercially available SEC columns (qEV, Izon) which are based on Boing et al. (2014).

This approach results in preparations of superior purity, gives highly reproducible results and can be performed without expensive equipment and with the settings of a routine diagnostic laboratory. Another major advantage of the SEC method is the possibility to directly quantify exosome yields of the preparations by standardized NTA. In contrast, the previously employed UC method did not allow the measurement of exosome yields and we had to refer to exosome numbers of the unprocessed CSF. Thus, in the previous approach, employing the UC method, we could not correct for differences in exosome preparation yields, which added another factor of variation. Of note, the coefficient of variance of this method was 22% (Figure 3.2C), which can now be considerably improved by the SEC approach.

When we used the UC method to isolate exosomes from human plasma, we do not detect differences of exosomal α-Synuclein levels between DLB, PD and neurological control patients selected from the Kassel cohort (Figure 3.10A). Quantification of exosome numbers by using NTA was not possible due to the presence of lipoproteins and protein complexes that are indistinguishable from exosomes by common particle quantification methods. In contrast, SEC purification of plasma exosomes results in exosome preparations of high purity with low non-exosomal protein contaminations (Figure 3.11A,C).

In contrast to CSF, where approximately 2% of total CSF α-Synuclein is localized to the exosome fraction, only 0.3% of total plasma α-Synuclein is found in exosomes (Figure 3.11D). This ratio is comparable to our findings obtained from UC exosome preparations (Figure 3.10B). Importantly, we demonstrate that SEC plasma exosomes are suitable for quantification of exosome numbers as well as exosomal α-Synuclein levels. The coefficient of variance calculated from five biological replicates reveals values of 6.8% for exosomal α-Synuclein content and 22% for the quantification of exosome numbers in the pure exosome fraction (Figure 3.11E).

In conclusion, we provide evidence that the SEC approach allows reliable purification and further quantification of plasma exosomes to better characterize exosomal α-Synuclein in patients with α-Synuclein related neurodegeneration compared to controls.

4.2. Preliminary evaluation of CSF exosomal small ncRNAs as a biomarker for AD

In the second study, we investigated the small ncRNA composition of CSF derived exosomes to test whether exosomal ncRNAs could be used to distinguish AD from cognitively healthy controls.

4.2.1. Exosomes partially mirror the cellular small ncRNA composition

Experimental studies from brain tissue or body fluids have provided evidence that the expression pattern of small ncRNAs is dysregulated in neurodegenerative diseases including AD and PD, suggesting that these RNA species play an important regulatory role in disease onset and progression (Goodall et al., 2013; Kumar et al., 2013; Schipper et al., 2007; Smith et al., 2011). Hence, CSF and blood have been screened for changes in miRNA expression levels in AD patients compared to controls in order to use identified miRNA profiles as a diagnostic or prognostic biomarker (Alexandrov et al., 2012; Burgos et al., 2014; Danborg et al., 2014; Geekiyanage et al., 2012; Leidinger et al., 2013). Although some 'AD specific' miRNAs have been identified, analyses of differentially expressed miRNAs generally result in different signatures among studies with a lack of overlap. Challenges and variabilities are most likely caused by sample collection, handling, processing, and storing conditions, which were suggested to cause differences in the expression levels of specific miRNAs (Femminella et al., 2015). Thus, widely used standard operating procedures (SOPs) for sample processing, including standardized RNA extraction, are required to minimize intersite variability.

Since small ncRNA species are also detectable in exosomes that are secreted into body fluids, exosomes could provide important information of intracellular processes. Exosomal small ncRNA compositions in CSF or plasma could even represent more reliable signatures than free small ncRNAs since the exosome content is enclosed by the lipid bilayer membrane and therefore protected from degradation, for instance by extracellular RNAses. Moreover, the exosomal membrane seems to be highly stable in storing conditions even over long time periods (Kalra et al., 2013), consequently providing excellent protection of the encapsulated RNA cargo.

By using NGS we were able to identify small ncRNA profiles of primary cortical and hippocampal neurons and their secreted exosomes. Here, we find that the exosomal RNA profile partially overlaps with that of the parental cell and expression levels of a small ncRNA subset in exosomes highly correlate with those of the exosome releasing cell (Figure 3.12). Thus, small ncRNAs transported into exosomes partially reflect the intracellular ncRNA content and could be used as a biomarker. This finding is in contrast to other reports which stated that the miRNA expression pattern found in exosomes does not significantly correlate with the miRNA composition of the parental cell as described for $CD4^+$ T cells (de Candia et al., 2014), Jurkat T cells, and primary DCs (Mittelbrunn et al., 2011).

4.2.2. Selected CSF small ncRNA profile distinguishes between AD and controls

Recently, Cheng et al. (2015) reported a signature of 17 differentially expressed miRNAs in serum derived exosomes from AD patients obtained by NGS sequencing. Further validation by quantitative real-time PCR resulted in a set of 16 dysregulated miRNAs in AD compared to controls. This miRNA set could predict AD with 87% sensitivity and 77% specificity when risk factors as age and apolipoprotein ε4 allele status were included in the analysis (Cheng et al., 2015), suggesting that miRNA signatures in exosomes could be used as a biomarker.

Our algorithm, based on the selection of a specific small ncRNA set expressed in CSF exosomes, is able to distinguish AD from controls in our replication cohort with high accuracy (Figure 3.13). Thus, our data provide evidence that the final set of exosomal small ncRNAs has the potential of a “disease signature” for AD that however still needs to be replicated in an independent larger validation study.
Moreover, it is important to study to what extend exosomal small ncRNAs expression levels depend on SOPs between different laboratories.

An ultimate aim is the identification of markers which could predict subsequent AD dementia already during preclinical or prodromal disease stages in order to enable treatment at the earliest possible time point. Therefore, it is of high interest to study CSF exosomal small ncRNA signatures in MCI patients with and without a later conversion to AD dementia and to compare their profiles to those found in AD patients.

4.3. Conclusions

4.3.1. Characterization of CSF exosomal α-Synuclein

The work from section 3.1 presents a comprehensive analysis of α-Synuclein in CSF exosomes from different diseases with α-Synuclein related and non-related neurodegeneration. CSF exosomes from patients with α-Synuclein related neurodegeneration (DLB and PD) exhibit the capacity to induce aggregation of soluble α-Synuclein in an *in vitro* model. We therefore suggest that DLB and PD exosomes contain a pathogenic α-Synuclein species. The ability to induce α-Synuclein aggregation correlates linearily with the α-Synuclein content in CSF exosomes from these patients, which is not the case for control derived exosomes. This supports the hypothesis that exosomes might function as carriers for interneuronal transmission of α-Synuclein pathology in synucleinopathies. Taken together, these data might shed light on the mechanism of α-Synuclein transmission between cells in PD and DLB and are therefore relevant for disease pathogenesis. To expand our findings, further studies are needed, including analysis of the α-Synculein species in DLB and PD exosomes compared to exosomes from controls.

In addition, we showed that the measurement of three parameters, exosomal α-Synuclein, exosome numbers and the ratio of exosomal α-Synuclein to exosome numbers is necessary to characterize disesase specific differences. Importantly, the amount of CSF exosomal α-Synuclein correlates with impaired cognitive function and increased CSF Tau levels as a general marker for neurodegeneration in patients with DLB. Hence, we suggest that CSF exosomal α-Synuclein levels and the number of CSF exosomes can be used as (i) a diagnostic marker to distinguish between DLB, PD and neurological controls and as (ii) a progressive marker to monitor disease course in DLB. The diagnostic performance has to be validated in a larger and independent cohort for any further biomarker applications.

Moreover, by using SEC purification, it is now possible to study and characterize α-Synuclein in exosomes derived from plasma of patients with α-Synuclein related neurodegeneration and neurological controls.

4.3.2. CSF exosomal small ncRNAs as a potential biomarker in AD

The experimental study described in section 3.2 aimed to investigate whether small ncRNA content isolated from CSF derived exosomes could be suitable to differentiate AD from cognitively healthy psychiatric controls.

First, we show that small ncRNA profiles found in exosomes partially reflect the small ncRNA composition of parental cells, demonstrating that identification of exosomal small ncRNAs provides insight into intracellular processes, which could be relevant for the pathogenesis of neurodegenerative diseases such as AD. Moreover, we demonstrate that CSF exosomal small ncRNAs can be used to differentiate patients with AD from control subjects with no signs of neurodegeneration by applying a newly developed statistical model that is entirely based on a specific set of differentially expressed exosomal small ncRNAs. A small patient cohort was used for testing and training of the model which revealed a high AUC value. To further elucidate its potential impact as a diagnostic biomarker in AD, this model needs to be further validated in a larger and independent patient cohort.

5. References

Abramowicz A., Widlak P., and Pietrowska M. (2016). Proteomic analysis of exosomal cargo: the challenge of high purity vesicle isolation. Molecular bioSystems.

Aerts M.B., Esselink R.A., Abdo W.F., Bloem B.R., and Verbeek M.M. (2012). CSF alpha-synuclein does not differentiate between parkinsonian disorders. Neurobiology of aging *33*, 430 e431-433.

Albert M.S., DeKosky S.T., Dickson D., Dubois B., Feldman H.H., Fox N.C., Gamst A., Holtzman D.M., Jagust W.J., Petersen R.C., Snyder P.J., Carrillo M.C., Thies B., and Phelps C.H. (2011). The diagnosis of mild cognitive impairment due to Alzheimer's disease: recommendations from the National Institute on Aging-Alzheimer's Association workgroups on diagnostic guidelines for Alzheimer's disease. Alzheimer's & dementia : the journal of the Alzheimer's Association *7*, 270-279.

Alexandrov P.N., Dua P., Hill J.M., Bhattacharjee S., Zhao Y., and Lukiw W.J. (2012). microRNA (miRNA) speciation in Alzheimer's disease (AD) cerebrospinal fluid (CSF) and extracellular fluid (ECF). International journal of biochemistry and molecular biology *3*, 365-373.

Alvarez-Erviti L., Seow Y., Schapira A.H., Gardiner C., Sargent I.L., Wood M.J., and Cooper J.M. (2011). Lysosomal dysfunction increases exosome-mediated alpha-synuclein release and transmission. Neurobiology of disease *42*, 360-367.

Alvarez-Erviti L., Seow Y., Schapira A.H., Rodriguez-Oroz M.C., Obeso J.A., and Cooper J.M. (2013). Influence of microRNA deregulation on chaperone-mediated autophagy and alpha-synuclein pathology in Parkinson's disease. Cell death & disease *4*, e545.

Babst M. (2011). MVB vesicle formation: ESCRT-dependent, ESCRT-independent and everything in between. Current opinion in cell biology *23*, 452-457.

Babst M., Katzmann D.J., Estepa-Sabal E.J., Meerloo T., and Emr S.D. (2002a). Escrt-III: an endosome-associated heterooligomeric protein complex required for mvb sorting. Developmental cell *3*, 271-282.

Babst M., Katzmann D.J., Snyder W.B., Wendland B., and Emr S.D. (2002b). Endosome-associated complex, ESCRT-II, recruits transport machinery for protein sorting at the multivesicular body. Developmental cell *3*, 283-289.

Baietti M.F., Zhang Z., Mortier E., Melchior A., Degeest G., Geeraerts A., Ivarsson Y., Depoortere F., Coomans C., Vermeiren E., Zimmermann P., and David G. (2012). Syndecan-syntenin-ALIX regulates the biogenesis of exosomes. Nature cell biology *14*, 677-685.

Bakhti M., Winter C., and Simons M. (2011). Inhibition of myelin membrane sheath formation by oligodendrocyte-derived exosome-like vesicles. The Journal of biological chemistry *286*, 787-796.

Ballatore C., Lee V.M., and Trojanowski J.Q. (2007). Tau-mediated neurodegeneration in Alzheimer's disease and related disorders. Nature reviews Neuroscience *8*, 663-672.

Bartels T., Choi J.G., and Selkoe D.J. (2011). alpha-Synuclein occurs physiologically as a helically folded tetramer that resists aggregation. Nature *477*, 107-110.

Batagov A.O., Kuznetsov V.A., and Kurochkin I.V. (2011). Identification of nucleotide patterns enriched in secreted RNAs as putative cis-acting elements targeting them to exosome nano-vesicles. BMC genomics *12 Suppl 3*, S18.

Beckett K., Monier S., Palmer L., Alexandre C., Green H., Bonneil E., Raposo G., Thibault P., Le Borgne R., and Vincent J.P. (2013). Drosophila S2 cells secrete wingless on exosome-like vesicles but the wingless gradient forms independently of exosomes. Traffic *14*, 82-96.

Bellingham S.A., Coleman B.M., and Hill A.F. (2012a). Small RNA deep sequencing reveals a distinct miRNA signature released in exosomes from prion-infected neuronal cells. Nucleic acids research *40*, 10937-10949.

Bellingham S.A., Guo B.B., Coleman B.M., and Hill A.F. (2012b). Exosomes: vehicles for the transfer of toxic proteins associated with neurodegenerative diseases? Frontiers in physiology *3*, 124.

Benskey M.J., Perez R.G., and Manfredsson F.P. (2016). The contribution of alpha synuclein to neuronal survival and function - Implications for Parkinson's disease. Journal of neurochemistry *137*, 331-359.

Blennow K., de Leon M.J., and Zetterberg H. (2006). Alzheimer's disease. Lancet *368*, 387-403.

Bodles A.M., Guthrie D.J., Greer B., and Irvine G.B. (2001). Identification of the region of non-Abeta component (NAC) of Alzheimer's disease amyloid responsible for its aggregation and toxicity. Journal of neurochemistry *78*, 384-395.

Boing A.N., van der Pol E., Grootemaat A.E., Coumans F.A., Sturk A., and Nieuwland R. (2014). Single-step isolation of extracellular vesicles by size-exclusion chromatography. Journal of extracellular vesicles *3*.

Bonifati V., Rizzu P., Squitieri F., Krieger E., Vanacore N., van Swieten J.C., Brice A., van Duijn C.M., Oostra B., Meco G., and Heutink P. (2003). DJ-1(PARK7), a novel gene for autosomal recessive, early onset parkinsonism. Neurological sciences : official journal of the Italian Neurological Society and of the Italian Society of Clinical Neurophysiology *24*, 159-160.

Borghi R., Marchese R., Negro A., Marinelli L., Forloni G., Zaccheo D., Abbruzzese G., and Tabaton M. (2000). Full length alpha-synuclein is present in cerebrospinal fluid from Parkinson's disease and normal subjects. Neuroscience letters *287*, 65-67.

Boukouris S., and Mathivanan S. (2015). Exosomes in bodily fluids are a highly stable resource of disease biomarkers. Proteomics Clinical applications *9*, 358-367.

Braak H., and Braak E. (1991). Neuropathological stageing of Alzheimer-related changes. Acta neuropathologica *82*, 239-259.

Braak H., Del Tredici K., Rub U., de Vos R.A., Jansen Steur E.N., and Braak E. (2003). Staging of brain pathology related to sporadic Parkinson's disease. Neurobiology of aging *24*, 197-211.

Brettschneider J., Del Tredici K., Lee V.M., and Trojanowski J.Q. (2015). Spreading of pathology in neurodegenerative diseases: a focus on human studies. Nature reviews Neuroscience *16*, 109-120.

Bulloj A., Leal M.C., Xu H., Castano E.M., and Morelli L. (2010). Insulin-degrading enzyme sorting in exosomes: a secretory pathway for a key brain amyloid-beta degrading protease. Journal of Alzheimer's disease : JAD *19*, 79-95.

Burgos K., Malenica I., Metpally R., Courtright A., Rakela B., Beach T., Shill H., Adler C., Sabbagh M., Villa S., Tembe W., Craig D., and Van Keuren-Jensen K. (2014). Profiles of extracellular miRNA in cerebrospinal fluid and serum from patients with Alzheimer's and Parkinson's diseases correlate with disease status and features of pathology. PloS one *9*, e94839.

Burre J., Vivona S., Diao J., Sharma M., Brunger A.T., and Sudhof T.C. (2013). Properties of native brain alpha-synuclein. Nature *498*, E4-6; discussion E6-7.

Caby M.P., Lankar D., Vincendeau-Scherrer C., Raposo G., and Bonnerot C. (2005). Exosomal-like vesicles are present in human blood plasma. International immunology *17*, 879-887.

Capece V., Garcia Vizcaino J.C., Vidal R., Rahman R.U., Pena Centeno T., Shomroni O., Suberviola I., Fischer A., and Bonn S. (2015). Oasis: online analysis of small RNA deep sequencing data. Bioinformatics *31*, 2205-2207.

Cardo L.F., Coto E., de Mena L., Ribacoba R., Moris G., Menendez M., and Alvarez V. (2013). Profile of microRNAs in the plasma of Parkinson's disease patients and healthy controls. Journal of neurology *260*, 1420-1422.

Cardo L.F., Coto E., Ribacoba R., Menendez M., Moris G., Suarez E., and Alvarez V. (2014). MiRNA profile in the substantia nigra of Parkinson's disease and healthy subjects. Journal of molecular neuroscience : MN *54*, 830-836.

Cheng L., Doecke J.D., Sharples R.A., Villemagne V.L., Fowler C.J., Rembach A., Martins R.N., Rowe C.C., Macaulay S.L., Masters C.L., and Hill A.F. (2015). Prognostic serum miRNA biomarkers associated with Alzheimer's disease shows concordance with neuropsychological and neuroimaging assessment. Molecular psychiatry *20*, 1188-1196.

Cheng L., Sharples R.A., Scicluna B.J., and Hill A.F. (2014a). Exosomes provide a protective and enriched source of miRNA for biomarker profiling compared to intracellular and cell-free blood. Journal of extracellular vesicles *3*.

Cheng L., Sun X., Scicluna B.J., Coleman B.M., and Hill A.F. (2014b). Characterization and deep sequencing analysis of exosomal and non-exosomal miRNA in human urine. Kidney international *86*, 433-444.

Chitambar C.R., Loebel A.L., and Noble N.A. (1991). Shedding of transferrin receptor from rat reticulocytes during maturation in vitro: soluble transferrin receptor is derived from receptor shed in vesicles. Blood *78*, 2444-2450.

Coart E., Barrado L.G., Duits F.H., Scheltens P., van der Flier W.M., Teunissen C.E., van der Vies S.M., and Burzykowski T. (2015). Correcting for the Absence of a Gold Standard Improves Diagnostic Accuracy of Biomarkers in Alzheimer's Disease. Journal of Alzheimer's disease : JAD *46*, 889-899.

Cogswell J.P., Ward J., Taylor I.A., Waters M., Shi Y., Cannon B., Kelnar K., Kemppainen J., Brown D., Chen C., Prinjha R.K., Richardson J.C., Saunders A.M., Roses A.D., and Richards C.A. (2008). Identification of miRNA changes in Alzheimer's disease brain and CSF yields putative biomarkers and insights into disease pathways. Journal of Alzheimer's disease : JAD *14*, 27-41.

Colombo M., Raposo G., and Thery C. (2014). Biogenesis, secretion, and intercellular interactions of exosomes and other extracellular vesicles. Annual review of cell and developmental biology *30*, 255-289.

Conde-Vancells J., Rodriguez-Suarez E., Embade N., Gil D., Matthiesen R., Valle M., Elortza F., Lu S.C., Mato J.M., and Falcon-Perez J.M. (2008). Characterization and comprehensive proteome profiling of exosomes secreted by hepatocytes. Journal of proteome research *7*, 5157-5166.

Crews L., Spencer B., Desplats P., Patrick C., Paulino A., Rockenstein E., Hansen L., Adame A., Galasko D., and Masliah E. (2010). Selective molecular alterations in the autophagy pathway in patients with Lewy body disease and in models of alpha-synucleinopathy. PloS one *5*, e9313.

Cummings J.L., Doody R., and Clark C. (2007). Disease-modifying therapies for Alzheimer disease: challenges to early intervention. Neurology *69*, 1622-1634.

Damme M., Suntio T., Saftig P., and Eskelinen E.L. (2015). Autophagy in neuronal cells: general principles and physiological and pathological functions. Acta neuropathologica *129*, 337-362.

Danborg P.B., Simonsen A.H., Waldemar G., and Heegaard N.H. (2014). The potential of microRNAs as biofluid markers of neurodegenerative diseases--a systematic review. Biomarkers : biochemical indicators of exposure, response, and susceptibility to chemicals *19*, 259-268.

Danzer K.M., Kranich L.R., Ruf W.P., Cagsal-Getkin O., Winslow A.R., Zhu L., Vanderburg C.R., and McLean P.J. (2012). Exosomal cell-to-cell transmission of alpha synuclein oligomers. Molecular neurodegeneration *7*, 42.

Danzer K.M., Ruf W.P., Putcha P., Joyner D., Hashimoto T., Glabe C., Hyman B.T., and McLean P.J. (2011). Heat-shock protein 70 modulates toxic extracellular alpha-synuclein oligomers and rescues trans-synaptic toxicity. FASEB journal : official publication of the Federation of American Societies for Experimental Biology *25*, 326-336.

Davidson W.S., Jonas A., Clayton D.F., and George J.M. (1998). Stabilization of alpha-synuclein secondary structure upon binding to synthetic membranes. The Journal of biological chemistry *273*, 9443-9449.

de Candia P., Torri A., Pagani M., and Abrignani S. (2014). Serum microRNAs as Biomarkers of Human Lymphocyte Activation in Health and Disease. Frontiers in immunology *5*, 43.

de Gassart A., Geminard C., Fevrier B., Raposo G., and Vidal M. (2003). Lipid raft-associated protein sorting in exosomes. Blood *102*, 4336-4344.

de Lau L.M., and Breteler M.M. (2006). Epidemiology of Parkinson's disease. The Lancet Neurology *5*, 525-535.

Dehay B., Ramirez A., Martinez-Vicente M., Perier C., Canron M.H., Doudnikoff E., Vital A., Vila M., Klein C., and Bezard E. (2012). Loss of P-type ATPase ATP13A2/PARK9 function induces general lysosomal deficiency and leads to Parkinson disease neurodegeneration. Proceedings of the National Academy of Sciences of the United States of America *109*, 9611-9616.

Deregibus M.C., Cantaluppi V., Calogero R., Lo Iacono M., Tetta C., Biancone L., Bruno S., Bussolati B., and Camussi G. (2007). Endothelial progenitor cell derived microvesicles activate an angiogenic program in endothelial cells by a horizontal transfer of mRNA. Blood *110*, 2440-2448.

Desplats P., Lee H.J., Bae E.J., Patrick C., Rockenstein E., Crews L., Spencer B., Masliah E., and Lee S.J. (2009). Inclusion formation and neuronal cell death through neuron-to-neuron transmission of alpha-synuclein. Proceedings of the National Academy of Sciences of the United States of America *106*, 13010-13015.

Dettmer U., Newman A.J., von Saucken V.E., Bartels T., and Selkoe D. (2015). KTKEGV repeat motifs are key mediators of normal alpha-synuclein tetramerization: Their mutation causes excess monomers and neurotoxicity. Proceedings of the National Academy of Sciences of the United States of America *112*, 9596-9601.

Dinkins M.B., Dasgupta S., Wang G., Zhu G., and Bieberich E. (2014). Exosome reduction in vivo is associated with lower amyloid plaque load in the 5XFAD mouse model of Alzheimer's disease. Neurobiology of aging *35*, 1792-1800.

Dragovic R.A., Gardiner C., Brooks A.S., Tannetta D.S., Ferguson D.J., Hole P., Carr B., Redman C.W., Harris A.L., Dobson P.J., Harrison P., and Sargent I.L. (2011). Sizing and phenotyping of cellular vesicles using Nanoparticle Tracking Analysis. Nanomedicine : nanotechnology, biology, and medicine *7*, 780-788.

Duran R., Barrero F.J., Morales B., Luna J.D., Ramirez M., and Vives F. (2010). Plasma alpha-synuclein in patients with Parkinson's disease with and without treatment. Movement disorders : official journal of the Movement Disorder Society *25*, 489-493.

El-Agnaf O.M., Salem S.A., Paleologou K.E., Cooper L.J., Fullwood N.J., Gibson M.J., Curran M.D., Court J.A., Mann D.M., Ikeda S., Cookson M.R., Hardy J., and Allsop D. (2003). Alpha-synuclein implicated in Parkinson's disease is present in extracellular biological fluids, including human plasma. FASEB journal : official publication of the Federation of American Societies for Experimental Biology *17*, 1945-1947.

El-Agnaf O.M., Salem S.A., Paleologou K.E., Curran M.D., Gibson M.J., Court J.A., Schlossmacher M.G., and Allsop D. (2006). Detection of oligomeric forms of alpha-synuclein protein in human plasma as a potential biomarker for Parkinson's disease. FASEB journal : official publication of the Federation of American Societies for Experimental Biology *20*, 419-425.

El Andaloussi S., Lakhal S., Mager I., and Wood M.J. (2013). Exosomes for targeted siRNA delivery across biological barriers. Advanced drug delivery reviews *65*, 391-397.

Eliezer D., Kutluay E., Bussell R., Jr., and Browne G. (2001). Conformational properties of alpha-synuclein in its free and lipid-associated states. Journal of molecular biology *307*, 1061-1073.

Emmanouilidou E., Elenis D., Papasilekas T., Stranjalis G., Gerozissis K., Ioannou P.C., and Vekrellis K. (2011). Assessment of alpha-synuclein secretion in mouse and human brain parenchyma. PloS one *6*, e22225.

Emmanouilidou E., Melachroinou K., Roumeliotis T., Garbis S.D., Ntzouni M., Margaritis L.H., Stefanis L., and Vekrellis K. (2010). Cell-produced alpha-synuclein is secreted in a calcium-dependent manner by exosomes and impacts neuronal survival. The Journal of neuroscience : the official journal of the Society for Neuroscience *30*, 6838-6851.

Esteller M. (2011). Non-coding RNAs in human disease. Nature reviews Genetics *12*, 861-874.

Fader C.M., Sanchez D., Furlan M., and Colombo M.I. (2008). Induction of autophagy promotes fusion of multivesicular bodies with autophagic vacuoles in k562 cells. Traffic *9*, 230-250.

Fader C.M., Sanchez D.G., Mestre M.B., and Colombo M.I. (2009). TI-VAMP/VAMP7 and VAMP3/cellubrevin: two v-SNARE proteins involved in specific steps of the autophagy/multivesicular body pathways. Biochimica et biophysica acta *1793*, 1901-1916.

Fahn S. (2003). Description of Parkinson's disease as a clinical syndrome. Annals of the New York Academy of Sciences *991*, 1-14.

Fang Y., Wu N., Gan X., Yan W., Morrell J.C., and Gould S.J. (2007). Higher-order oligomerization targets plasma membrane proteins and HIV gag to exosomes. PLoS biology *5*, e158.

Faure J., Lachenal G., Court M., Hirrlinger J., Chatellard-Causse C., Blot B., Grange J., Schoehn G., Goldberg Y., Boyer V., Kirchhoff F., Raposo G., Garin J., and Sadoul R. (2006). Exosomes are released by cultured cortical neurones. Molecular and cellular neurosciences *31*, 642-648.

Fauvet B., Mbefo M.K., Fares M.B., Desobry C., Michael S., Ardah M.T., Tsika E., Coune P., Prudent M., Lion N., Eliezer D., Moore D.J., Schneider B., Aebischer P., El-Agnaf O.M., et al. (2012). alpha-Synuclein in central nervous system and from erythrocytes, mammalian cells, and Escherichia coli exists predominantly as disordered monomer. The Journal of biological chemistry *287*, 15345-15364.

Femminella G.D., Ferrara N., and Rengo G. (2015). The emerging role of microRNAs in Alzheimer's disease. Frontiers in physiology *6*, 40.

Fevrier B., Vilette D., Archer F., Loew D., Faigle W., Vidal M., Laude H., and Raposo G. (2004). Cells release prions in association with exosomes. Proceedings of the National Academy of Sciences of the United States of America *101*, 9683-9688.

Fiandaca M.S., Kapogiannis D., Mapstone M., Boxer A., Eitan E., Schwartz J.B., Abner E.L., Petersen R.C., Federoff H.J., Miller B.L., and Goetzl E.J. (2015). Identification of preclinical Alzheimer's disease by a profile of pathogenic proteins in neurally derived blood exosomes: A case-control study. Alzheimer's & dementia : the journal of the Alzheimer's Association *11*, 600-607 e601.

Fitzner D., Schnaars M., van Rossum D., Krishnamoorthy G., Dibaj P., Bakhti M., Regen T., Hanisch U.K., and Simons M. (2011). Selective transfer of exosomes from oligodendrocytes to microglia by macropinocytosis. Journal of cell science *124*, 447-458.

Folstein M.F., Folstein S.E., and McHugh P.R. (1975). "Mini-mental state". A practical method for grading the cognitive state of patients for the clinician. Journal of psychiatric research *12*, 189-198.

Fruhbeis C., Frohlich D., Kuo W.P., Amphornrat J., Thilemann S., Saab A.S., Kirchhoff F., Mobius W., Goebbels S., Nave K.A., Schneider A., Simons M., Klugmann M., Trotter J., and Kramer-Albers E.M. (2013). Neurotransmitter-triggered transfer of exosomes mediates oligodendrocyte-neuron communication. PLoS biology *11*, e1001604.

Gao L., Tang H., Nie K., Wang L., Zhao J., Gan R., Huang J., Zhu R., Feng S., Duan Z., and Zhang Y. (2015). Cerebrospinal fluid alpha-synuclein as a biomarker for Parkinson's disease diagnosis: a systematic review and meta-analysis. The International journal of neuroscience *125*, 645-654.

Geekiyanage H., and Chan C. (2011). MicroRNA-137/181c regulates serine palmitoyltransferase and in turn amyloid beta, novel targets in sporadic Alzheimer's disease. The Journal of neuroscience : the official journal of the Society for Neuroscience *31*, 14820-14830.

Geekiyanage H., Jicha G.A., Nelson P.T., and Chan C. (2012). Blood serum miRNA: non-invasive biomarkers for Alzheimer's disease. Experimental neurology *235*, 491-496.

Geminard C., De Gassart A., Blanc L., and Vidal M. (2004). Degradation of AP2 during reticulocyte maturation enhances binding of hsc70 and Alix to a common site on TFR for sorting into exosomes. Traffic *5*, 181-193.

George J.M. (2002). The synucleins. Genome biology *3*, REVIEWS3002.

Giasson B.I., Murray I.V., Trojanowski J.Q., and Lee V.M. (2001). A hydrophobic stretch of 12 amino acid residues in the middle of alpha-synuclein is essential for filament assembly. The Journal of biological chemistry *276*, 2380-2386.

Goedert M. (2001). Alpha-synuclein and neurodegenerative diseases. Nature reviews Neuroscience *2*, 492-501.

Gomes C., Keller S., Altevogt P., and Costa J. (2007). Evidence for secretion of Cu,Zn superoxide dismutase via exosomes from a cell model of amyotrophic lateral sclerosis. Neuroscience letters *428*, 43-46.

Goodall E.F., Heath P.R., Bandmann O., Kirby J., and Shaw P.J. (2013). Neuronal dark matter: the emerging role of microRNAs in neurodegeneration. Frontiers in cellular neuroscience *7*, 178.

Gould G.W., and Lippincott-Schwartz J. (2009). New roles for endosomes: from vesicular carriers to multi-purpose platforms. Nature reviews Molecular cell biology *10*, 287-292.

Grey M., Dunning C.J., Gaspar R., Grey C., Brundin P., Sparr E., and Linse S. (2015). Acceleration of alpha-synuclein aggregation by exosomes. The Journal of biological chemistry *290*, 2969-2982.

Gross J.C., Chaudhary V., Bartscherer K., and Boutros M. (2012). Active Wnt proteins are secreted on exosomes. Nature cell biology *14*, 1036-1045.

Guduric-Fuchs J., O'Connor A., Camp B., O'Neill C.L., Medina R.J., and Simpson D.A. (2012). Selective extracellular vesicle-mediated export of an overlapping set of microRNAs from multiple cell types. BMC genomics *13*, 357.

Gui Y., Liu H., Zhang L., Lv W., and Hu X. (2015). Altered microRNA profiles in cerebrospinal fluid exosome in Parkinson disease and Alzheimer disease. Oncotarget *6*, 37043-37053.

Hansen C., Angot E., Bergstrom A.L., Steiner J.A., Pieri L., Paul G., Outeiro T.F., Melki R., Kallunki P., Fog K., Li J.Y., and Brundin P. (2011). alpha-Synuclein propagates from mouse brain to grafted dopaminergic neurons and seeds aggregation in cultured human cells. The Journal of clinical investigation *121*, 715-725.

Harding C., Heuser J., and Stahl P. (1983). Receptor-mediated endocytosis of transferrin and recycling of the transferrin receptor in rat reticulocytes. The Journal of cell biology *97*, 329-339.

Henne W.M., Buchkovich N.J., and Emr S.D. (2011). The ESCRT pathway. Developmental cell *21*, 77-91.

Hoehn M.M., and Yahr M.D. (1967). Parkinsonism: onset, progression and mortality. Neurology *17*, 427-442.

Hsu C., Morohashi Y., Yoshimura S., Manrique-Hoyos N., Jung S., Lauterbach M.A., Bakhti M., Gronborg M., Mobius W., Rhee J., Barr F.A., and Simons M. (2010). Regulation of exosome secretion by Rab35 and its GTPase-activating proteins TBC1D10A-C. The Journal of cell biology *189*, 223-232.

Huang X., Yuan T., Tschannen M., Sun Z., Jacob H., Du M., Liang M., Dittmar R.L., Liu Y., Kohli M., Thibodeau S.N., Boardman L., and Wang L. (2013). Characterization of human plasma-derived exosomal RNAs by deep sequencing. BMC genomics *14*, 319.

Hulka B.S., and Wilcosky T. (1988). Biological markers in epidemiologic research. Archives of environmental health *43*, 83-89.

Husmann M., Beckmann E., Boller K., Kloft N., Tenzer S., Bobkiewicz W., Neukirch C., Bayley H., and Bhakdi S. (2009). Elimination of a bacterial pore-forming toxin by sequential endocytosis and exocytosis. FEBS letters *583*, 337-344.

Huttenhofer A., Schattner P., and Polacek N. (2005). Non-coding RNAs: hope or hype? Trends in genetics : TIG *21*, 289-297.

Ishii R., Tokuda T., Tatebe H., Ohmichi T., Kasai T., Nakagawa M., Mizuno T., and El-Agnaf O.M. (2015). Decrease in plasma levels of alpha-synuclein is evident in patients with Parkinson's disease after elimination of heterophilic antibody interference. PloS one *10*, e0123162.

Iwai A., Masliah E., Yoshimoto M., Ge N., Flanagan L., de Silva H.A., Kittel A., and Saitoh T. (1995). The precursor protein of non-A beta component of Alzheimer's disease amyloid is a presynaptic protein of the central nervous system. Neuron *14*, 467-475.

Jack C.R., Jr., and Holtzman D.M. (2013). Biomarker modeling of Alzheimer's disease. Neuron *80*, 1347-1358.

Janas T., Janas M.M., and Sapon K. (2015). Mechanisms of RNA loading into exosomes. FEBS letters *589*, 1391-1398.

Janas T., and Yarus M. (2012). Human tRNA(Sec) associates with HeLa membranes, cell lipid liposomes, and synthetic lipid bilayers. RNA *18*, 2260-2268.

Jankovic J. (2008). Parkinson's disease: clinical features and diagnosis. Journal of neurology, neurosurgery, and psychiatry *79*, 368-376.

Jo E., McLaurin J., Yip C.M., St George-Hyslop P., and Fraser P.E. (2000). alpha-Synuclein membrane interactions and lipid specificity. The Journal of biological chemistry *275*, 34328-34334.

Johnstone R.M., Adam M., Hammond J.R., Orr L., and Turbide C. (1987). Vesicle formation during reticulocyte maturation. Association of plasma membrane activities with released vesicles (exosomes). The Journal of biological chemistry *262*, 9412-9420.

Kaether C., Schmitt S., Willem M., and Haass C. (2006). Amyloid precursor protein and Notch intracellular domains are generated after transport of their precursors to the cell surface. Traffic *7*, 408-415.

Kalra H., Adda C.G., Liem M., Ang C.S., Mechler A., Simpson R.J., Hulett M.D., and Mathivanan S. (2013). Comparative proteomics evaluation of plasma exosome isolation techniques and assessment of the stability of exosomes in normal human blood plasma. Proteomics *13*, 3354-3364.

Kapranov P., Cheng J., Dike S., Nix D.A., Duttagupta R., Willingham A.T., Stadler P.F., Hertel J., Hackermuller J., Hofacker I.L., Bell I., Cheung E., Drenkow J., Dumais E., Patel S., et al. (2007).

RNA maps reveal new RNA classes and a possible function for pervasive transcription. Science *316*, 1484-1488.

Katzmann D.J., Babst M., and Emr S.D. (2001). Ubiquitin-dependent sorting into the multivesicular body pathway requires the function of a conserved endosomal protein sorting complex, ESCRT-I. Cell *106*, 145-155.

Khoo S.K., Petillo D., Kang U.J., Resau J.H., Berryhill B., Linder J., Forsgren L., Neuman L.A., and Tan A.C. (2012). Plasma-based circulating MicroRNA biomarkers for Parkinson's disease. Journal of Parkinson's disease *2*, 321-331.

Kim Y.K., and Kim V.N. (2007). Processing of intronic microRNAs. The EMBO journal *26*, 775-783.

Kitada T., Asakawa S., Hattori N., Matsumine H., Yamamura Y., Minoshima S., Yokochi M., Mizuno Y., and Shimizu N. (1998). Mutations in the parkin gene cause autosomal recessive juvenile parkinsonism. Nature *392*, 605-608.

Kong S.M., Chan B.K., Park J.S., Hill K.J., Aitken J.B., Cottle L., Farghaian H., Cole A.R., Lay P.A., Sue C.M., and Cooper A.A. (2014). Parkinson's disease-linked human PARK9/ATP13A2 maintains zinc homeostasis and promotes alpha-Synuclein externalization via exosomes. Human molecular genetics *23*, 2816-2833.

Kosaka K. (1990). Diffuse Lewy body disease in Japan. Journal of neurology *237*, 197-204.

Kowal J., Tkach M., and Thery C. (2014). Biogenesis and secretion of exosomes. Current opinion in cell biology *29*, 116-125.

Kramer-Albers E.M., Bretz N., Tenzer S., Winterstein C., Mobius W., Berger H., Nave K.A., Schild H., and Trotter J. (2007). Oligodendrocytes secrete exosomes containing major myelin and stress-protective proteins: Trophic support for axons? Proteomics Clinical applications *1*, 1446-1461.

Kruger R., Kuhn W., Muller T., Woitalla D., Graeber M., Kosel S., Przuntek H., Epplen J.T., Schols L., and Riess O. (1998). Ala30Pro mutation in the gene encoding alpha-synuclein in Parkinson's disease. Nature genetics *18*, 106-108.

Kruse N., Schulz-Schaeffer W.J., Schlossmacher M.G., and Mollenhauer B. (2012). Development of electrochemiluminescence-based singleplex and multiplex assays for the quantification of alpha-synuclein and other proteins in cerebrospinal fluid. Methods *56*, 514-518.

Kumar P., Dezso Z., MacKenzie C., Oestreicher J., Agoulnik S., Byrne M., Bernier F., Yanagimachi M., Aoshima K., and Oda Y. (2013). Circulating miRNA biomarkers for Alzheimer's disease. PloS one *8*, e69807.

Kunadt M., Eckermann K., Stuendl A., Gong J., Russo B., Strauss K., Rai S., Kugler S., Falomir Lockhart L., Schwalbe M., Krumova P., Oliveira L.M., Bahr M., Mobius W., Levin J., et al. (2015). Extracellular vesicle sorting of alpha-Synuclein is regulated by sumoylation. Acta neuropathologica *129*, 695-713.

Lachenal G., Pernet-Gallay K., Chivet M., Hemming F.J., Belly A., Bodon G., Blot B., Haase G., Goldberg Y., and Sadoul R. (2011). Release of exosomes from differentiated neurons and its regulation by synaptic glutamatergic activity. Molecular and cellular neurosciences *46*, 409-418.

Laemmli U.K. (1970). Cleavage of structural proteins during the assembly of the head of bacteriophage T4. Nature *227*, 680-685.

Lander E.S., Linton L.M., Birren B., Nusbaum C., Zody M.C., Baldwin J., Devon K., Dewar K., Doyle M., FitzHugh W., Funke R., Gage D., Harris K., Heaford A., Howland J., et al. (2001). Initial sequencing and analysis of the human genome. Nature *409*, 860-921.

Lang A.E., and Lozano A.M. (1998). Parkinson's disease. First of two parts. The New England journal of medicine *339*, 1044-1053.

Lee H.J., Patel S., and Lee S.J. (2005). Intravesicular localization and exocytosis of alpha-synuclein and its aggregates. The Journal of neuroscience : the official journal of the Society for Neuroscience *25*, 6016-6024.

Lee P.H., Lee G., Park H.J., Bang O.Y., Joo I.S., and Huh K. (2006). The plasma alpha-synuclein levels in patients with Parkinson's disease and multiple system atrophy. J Neural Transm (Vienna) *113*, 1435-1439.

Lee S.J., Desplats P., Lee H.J., Spencer B., and Masliah E. (2012). Cell-to-cell transmission of alpha-synuclein aggregates. Methods Mol Biol *849*, 347-359.

Leidinger P., Backes C., Deutscher S., Schmitt K., Mueller S.C., Frese K., Haas J., Ruprecht K., Paul F., Stahler C., Lang C.J., Meder B., Bartfai T., Meese E., and Keller A. (2013). A blood based 12-miRNA signature of Alzheimer disease patients. Genome biology *14*, R78.

Li Q.X., Mok S.S., Laughton K.M., McLean C.A., Cappai R., Masters C.L., Culvenor J.G., and Horne M.K. (2007). Plasma alpha-synuclein is decreased in subjects with Parkinson's disease. Experimental neurology *204*, 583-588.

Litvan I., Agid Y., Calne D., Campbell G., Dubois B., Duvoisin R.C., Goetz C.G., Golbe L.I., Grafman J., Growdon J.H., Hallett M., Jankovic J., Quinn N.P., Tolosa E., and Zee D.S. (1996). Clinical research criteria for the diagnosis of progressive supranuclear palsy (Steele-Richardson-Olszewski syndrome): report of the NINDS-SPSP international workshop. Neurology *47*, 1-9.

Lleo A., Cavedo E., Parnetti L., Vanderstichele H., Herukka S.K., Andreasen N., Ghidoni R., Lewczuk P., Jeromin A., Winblad B., Tsolaki M., Mroczko B., Visser P.J., Santana I., Svenningsson P., et al. (2015). Cerebrospinal fluid biomarkers in trials for Alzheimer and Parkinson diseases. Nature reviews Neurology *11*, 41-55.

Luga V., Zhang L., Viloria-Petit A.M., Ogunjimi A.A., Inanlou M.R., Chiu E., Buchanan M., Hosein A.N., Basik M., and Wrana J.L. (2012). Exosomes mediate stromal mobilization of autocrine Wnt-PCP signaling in breast cancer cell migration. Cell *151*, 1542-1556.

Luk K.C., Kehm V., Carroll J., Zhang B., O'Brien P., Trojanowski J.Q., and Lee V.M. (2012). Pathological alpha-synuclein transmission initiates Parkinson-like neurodegeneration in nontransgenic mice. Science *338*, 949-953.

Luk K.C., Song C., O'Brien P., Stieber A., Branch J.R., Brunden K.R., Trojanowski J.Q., and Lee V.M. (2009). Exogenous alpha-synuclein fibrils seed the formation of Lewy body-like intracellular inclusions in cultured cells. Proceedings of the National Academy of Sciences of the United States of America *106*, 20051-20056.

Lundblad M., Decressac M., Mattsson B., and Bjorklund A. (2012). Impaired neurotransmission caused by overexpression of alpha-synuclein in nigral dopamine neurons. Proceedings of the National Academy of Sciences of the United States of America *109*, 3213-3219.

Luo X.G., Ding J.Q., and Chen S.D. (2010). Microglia in the aging brain: relevance to neurodegeneration. Molecular neurodegeneration *5*, 12.

Margis R., and Rieder C.R. (2011). Identification of blood microRNAs associated to Parkinsonis disease. Journal of biotechnology *152*, 96-101.

Maroteaux L., and Scheller R.H. (1991). The rat brain synucleins; family of proteins transiently associated with neuronal membrane. Brain research Molecular brain research *11*, 335-343.

Mayers J.R., Fyfe I., Schuh A.L., Chapman E.R., Edwardson J.M., and Audhya A. (2011). ESCRT-0 assembles as a heterotetrameric complex on membranes and binds multiple ubiquitinylated cargoes simultaneously. The Journal of biological chemistry *286*, 9636-9645.

McKeith I.G., Dickson D.W., Lowe J., Emre M., O'Brien J.T., Feldman H., Cummings J., Duda J.E., Lippa C., Perry E.K., Aarsland D., Arai H., Ballard C.G., Boeve B., Burn D.J., et al. (2005). Diagnosis and management of dementia with Lewy bodies: third report of the DLB Consortium. Neurology *65*, 1863-1872.

McKhann G., Drachman D., Folstein M., Katzman R., Price D., and Stadlan E.M. (1984). Clinical diagnosis of Alzheimer's disease: report of the NINCDS-ADRDA Work Group under the auspices of Department of Health and Human Services Task Force on Alzheimer's Disease. Neurology *34*, 939-944.

Mittelbrunn M., Gutierrez-Vazquez C., Villarroya-Beltri C., Gonzalez S., Sanchez-Cabo F., Gonzalez M.A., Bernad A., and Sanchez-Madrid F. (2011). Unidirectional transfer of microRNA-loaded exosomes from T cells to antigen-presenting cells. Nature communications *2*, 282.

Mollenhauer B., Cepek L., Bibl M., Wiltfang J., Schulz-Schaeffer W.J., Ciesielczyk B., Neumann M., Steinacker P., Kretzschmar H.A., Poser S., Trenkwalder C., and Otto M. (2005). Tau protein, Abeta42 and S-100B protein in cerebrospinal fluid of patients with dementia with Lewy bodies. Dementia and geriatric cognitive disorders *19*, 164-170.

Mollenhauer B., El-Agnaf O.M., Marcus K., Trenkwalder C., and Schlossmacher M.G. (2010). Quantification of alpha-synuclein in cerebrospinal fluid as a biomarker candidate: review of the literature and considerations for future studies. Biomarkers in medicine *4*, 683-699.

Mollenhauer B., Locascio J.J., Schulz-Schaeffer W., Sixel-Doring F., Trenkwalder C., and Schlossmacher M.G. (2011). alpha-Synuclein and tau concentrations in cerebrospinal fluid of patients presenting with parkinsonism: a cohort study. The Lancet Neurology *10*, 230-240.

Mollenhauer B., Trautmann E., Sixel-Doring F., Wicke T., Ebentheuer J., Schaumburg M., Lang E., Focke N.K., Kumar K.R., Lohmann K., Klein C., Schlossmacher M.G., Kohnen R., Friede T., and Trenkwalder C. (2013a). Nonmotor and diagnostic findings in subjects with de novo Parkinson disease of the DeNoPa cohort. Neurology *81*, 1226-1234.

Mollenhauer B., Trautmann E., Taylor P., Manninger P., Sixel-Doring F., Ebentheuer J., Trenkwalder C., and Schlossmacher M.G. (2013b). Total CSF alpha-synuclein is lower in de novo Parkinson patients than in healthy subjects. Neuroscience letters *532*, 44-48.

Montecalvo A., Larregina A.T., Shufesky W.J., Stolz D.B., Sullivan M.L., Karlsson J.M., Baty C.J., Gibson G.A., Erdos G., Wang Z., Milosevic J., Tkacheva O.A., Divito S.J., Jordan R., Lyons-Weiler J., et al. (2012). Mechanism of transfer of functional microRNAs between mouse dendritic cells via exosomes. Blood *119*, 756-766.

Montine T.J., Shi M., Quinn J.F., Peskind E.R., Craft S., Ginghina C., Chung K.A., Kim H., Galasko D.R., Jankovic J., Zabetian C.P., Leverenz J.B., and Zhang J. (2010). CSF Abeta(42) and tau in Parkinson's disease with cognitive impairment. Movement disorders : official journal of the Movement Disorder Society *25*, 2682-2685.

Morel L., Regan M., Higashimori H., Ng S.K., Esau C., Vidensky S., Rothstein J., and Yang Y. (2013). Neuronal exosomal miRNA-dependent translational regulation of astroglial glutamate transporter GLT1. The Journal of biological chemistry *288*, 7105-7116.

Muller L., Hong C.S., Stolz D.B., Watkins S.C., and Whiteside T.L. (2014). Isolation of biologically-active exosomes from human plasma. Journal of immunological methods *411*, 55-65.

Muntasell A., Berger A.C., and Roche P.A. (2007). T cell-induced secretion of MHC class II-peptide complexes on B cell exosomes. The EMBO journal *26*, 4263-4272.

Murray I.V., Giasson B.I., Quinn S.M., Koppaka V., Axelsen P.H., Ischiropoulos H., Trojanowski J.Q., and Lee V.M. (2003). Role of alpha-synuclein carboxy-terminus on fibril formation in vitro. Biochemistry *42*, 8530-8540.

Musiek E.S., and Holtzman D.M. (2012). Origins of Alzheimer's disease: reconciling cerebrospinal fluid biomarker and neuropathology data regarding the temporal sequence of amyloid-beta and tau involvement. Current opinion in neurology *25*, 715-720.

Nazarenko I., Rana S., Baumann A., McAlear J., Hellwig A., Trendelenburg M., Lochnit G., Preissner K.T., and Zoller M. (2010). Cell surface tetraspanin Tspan8 contributes to molecular pathways of exosome-induced endothelial cell activation. Cancer research *70*, 1668-1678.

Nemani V.M., Lu W., Berge V., Nakamura K., Onoa B., Lee M.K., Chaudhry F.A., Nicoll R.A., and Edwards R.H. (2010). Increased expression of alpha-synuclein reduces neurotransmitter release by inhibiting synaptic vesicle reclustering after endocytosis. Neuron *65*, 66-79.

Noguchi-Shinohara M., Tokuda T., Yoshita M., Kasai T., Ono K., Nakagawa M., El-Agnaf O.M., and Yamada M. (2009). CSF alpha-synuclein levels in dementia with Lewy bodies and Alzheimer's disease. Brain research *1251*, 1-6.

Nolte-'t Hoen E.N., Buermans H.P., Waasdorp M., Stoorvogel W., Wauben M.H., and t Hoen P.A. (2012). Deep sequencing of RNA from immune cell-derived vesicles uncovers the selective incorporation of small non-coding RNA biotypes with potential regulatory functions. Nucleic acids research *40*, 9272-9285.

Ostrowski M., Carmo N.B., Krumeich S., Fanget I., Raposo G., Savina A., Moita C.F., Schauer K., Hume A.N., Freitas R.P., Goud B., Benaroch P., Hacohen N., Fukuda M., Desnos C., et al. (2010). Rab27a and Rab27b control different steps of the exosome secretion pathway. Nature cell biology *12*, 19-30; sup pp 11-13.

Outeiro T.F., Putcha P., Tetzlaff J.E., Spoelgen R., Koker M., Carvalho F., Hyman B.T., and McLean P.J. (2008). Formation of toxic oligomeric alpha-synuclein species in living cells. PloS one *3*, e1867.

Palanisamy V., Sharma S., Deshpande A., Zhou H., Gimzewski J., and Wong D.T. (2010). Nanostructural and transcriptomic analyses of human saliva derived exosomes. PloS one *5*, e8577.

Pan B.T., Teng K., Wu C., Adam M., and Johnstone R.M. (1985). Electron microscopic evidence for externalization of the transferrin receptor in vesicular form in sheep reticulocytes. The Journal of cell biology *101*, 942-948.

Parnetti L., Chiasserini D., Bellomo G., Giannandrea D., De Carlo C., Qureshi M.M., Ardah M.T., Varghese S., Bonanni L., Borroni B., Tambasco N., Eusebi P., Rossi A., Onofrj M., Padovani A., et al. (2011). Cerebrospinal fluid Tau/alpha-synuclein ratio in Parkinson's disease and degenerative dementias. Movement disorders : official journal of the Movement Disorder Society *26*, 1428-1435.

Perez-Gonzalez R., Gauthier S.A., Kumar A., and Levy E. (2012). The exosome secretory pathway transports amyloid precursor protein carboxyl-terminal fragments from the cell into the brain extracellular space. The Journal of biological chemistry *287*, 43108-43115.

Perez-Hernandez D., Gutierrez-Vazquez C., Jorge I., Lopez-Martin S., Ursa A., Sanchez-Madrid F., Vazquez J., and Yanez-Mo M. (2013). The intracellular interactome of tetraspanin-enriched microdomains reveals their function as sorting machineries toward exosomes. The Journal of biological chemistry *288*, 11649-11661.

Perrin R.J., Woods W.S., Clayton D.F., and George J.M. (2000). Interaction of human alpha-Synuclein and Parkinson's disease variants with phospholipids. Structural analysis using site-directed mutagenesis. The Journal of biological chemistry *275*, 34393-34398.

Petersen R.C. (2004). Mild cognitive impairment as a diagnostic entity. Journal of internal medicine *256*, 183-194.

Pisitkun T., Shen R.F., and Knepper M.A. (2004). Identification and proteomic profiling of exosomes in human urine. Proceedings of the National Academy of Sciences of the United States of America *101*, 13368-13373.

Poehler A.M., Xiang W., Spitzer P., May V.E., Meixner H., Rockenstein E., Chutna O., Outeiro T.F., Winkler J., Masliah E., and Klucken J. (2014). Autophagy modulates SNCA/alpha-synuclein release, thereby generating a hostile microenvironment. Autophagy *10*, 2171-2192.

Polanco J.C., Scicluna B.J., Hill A.F., and Gotz J. (2016). Extracellular vesicles isolated from brains of rTg4510 mice seed tau aggregation in a threshold-dependent manner. The Journal of biological chemistry.

Polymeropoulos M.H., Lavedan C., Leroy E., Ide S.E., Dehejia A., Dutra A., Pike B., Root H., Rubenstein J., Boyer R., Stenroos E.S., Chandrasekharappa S., Athanassiadou A., Papapetropoulos T., Johnson W.G., et al. (1997). Mutation in the alpha-synuclein gene identified in families with Parkinson's disease. Science *276*, 2045-2047.

Postuma R.B., Berg D., Stern M., Poewe W., Olanow C.W., Oertel W., Obeso J., Marek K., Litvan I., Lang A.E., Halliday G., Goetz C.G., Gasser T., Dubois B., Chan P., et al. (2015). MDS clinical diagnostic criteria for Parkinson's disease. Movement disorders : official journal of the Movement Disorder Society *30*, 1591-1601.

Rajendran L., Honsho M., Zahn T.R., Keller P., Geiger K.D., Verkade P., and Simons K. (2006). Alzheimer's disease beta-amyloid peptides are released in association with exosomes. Proceedings of the National Academy of Sciences of the United States of America *103*, 11172-11177.

Ramirez A., Heimbach A., Grundemann J., Stiller B., Hampshire D., Cid L.P., Goebel I., Mubaidin A.F., Wriekat A.L., Roeper J., Al-Din A., Hillmer A.M., Karsak M., Liss B., Woods C.G., et al. (2006). Hereditary parkinsonism with dementia is caused by mutations in ATP13A2, encoding a lysosomal type 5 P-type ATPase. Nature genetics *38*, 1184-1191.

Raposo G., Nijman H.W., Stoorvogel W., Liejendekker R., Harding C.V., Melief C.J., and Geuze H.J. (1996). B lymphocytes secrete antigen-presenting vesicles. The Journal of experimental medicine *183*, 1161-1172.

Raposo G., and Stoorvogel W. (2013). Extracellular vesicles: exosomes, microvesicles, and friends. The Journal of cell biology *200*, 373-383.

Ratajczak J., Miekus K., Kucia M., Zhang J., Reca R., Dvorak P., and Ratajczak M.Z. (2006). Embryonic stem cell-derived microvesicles reprogram hematopoietic progenitors: evidence for horizontal transfer of mRNA and protein delivery. Leukemia *20*, 847-856.

Reesink F.E., Lemstra A.W., van Dijk K.D., Berendse H.W., van de Berg W.D., Klein M., Blankenstein M.A., Scheltens P., Verbeek M.M., and van der Flier W.M. (2010). CSF alpha-

synuclein does not discriminate dementia with Lewy bodies from Alzheimer's disease. Journal of Alzheimer's disease : JAD *22*, 87-95.

Rockenstein E., Schwach G., Ingolic E., Adame A., Crews L., Mante M., Pfragner R., Schreiner E., Windisch M., and Masliah E. (2005). Lysosomal pathology associated with alpha-synuclein accumulation in transgenic models using an eGFP fusion protein. Journal of neuroscience research *80*, 247-259.

Saman S., Kim W., Raya M., Visnick Y., Miro S., Jackson B., McKee A.C., Alvarez V.E., Lee N.C., and Hall G.F. (2012). Exosome-associated tau is secreted in tauopathy models and is selectively phosphorylated in cerebrospinal fluid in early Alzheimer disease. The Journal of biological chemistry *287*, 3842-3849.

Savina A., Fader C.M., Damiani M.T., and Colombo M.I. (2005). Rab11 promotes docking and fusion of multivesicular bodies in a calcium-dependent manner. Traffic *6*, 131-143.

Savina A., Vidal M., and Colombo M.I. (2002). The exosome pathway in K562 cells is regulated by Rab11. Journal of cell science *115*, 2505-2515.

Scheltens P., Blennow K., Breteler M.M., de Strooper B., Frisoni G.B., Salloway S., and Van der Flier W.M. (2016). Alzheimer's disease. Lancet.

Schipper H.M., Maes O.C., Chertkow H.M., and Wang E. (2007). MicroRNA expression in Alzheimer blood mononuclear cells. Gene regulation and systems biology *1*, 263-274.

Schneider A., and Simons M. (2013). Exosomes: vesicular carriers for intercellular communication in neurodegenerative disorders. Cell and tissue research *352*, 33-47.

Schrag A., Horsfall L., Walters K., Noyce A., and Petersen I. (2015). Prediagnostic presentations of Parkinson's disease in primary care: a case-control study. The Lancet Neurology *14*, 57-64.

Scott D., and Roy S. (2012). alpha-Synuclein inhibits intersynaptic vesicle mobility and maintains recycling-pool homeostasis. The Journal of neuroscience : the official journal of the Society for Neuroscience *32*, 10129-10135.

Sharples R.A., Vella L.J., Nisbet R.M., Naylor R., Perez K., Barnham K.J., Masters C.L., and Hill A.F. (2008). Inhibition of gamma-secretase causes increased secretion of amyloid precursor protein C-terminal fragments in association with exosomes. FASEB journal : official publication of the Federation of American Societies for Experimental Biology *22*, 1469-1478.

Shi M., Liu C., Cook T.J., Bullock K.M., Zhao Y., Ginghina C., Li Y., Aro P., Dator R., He C., Hipp M.J., Zabetian C.P., Peskind E.R., Hu S.C., Quinn J.F., et al. (2014). Plasma exosomal alpha-synuclein is likely CNS-derived and increased in Parkinson's disease. Acta neuropathologica *128*, 639-650.

Shi M., Zabetian C.P., Hancock A.M., Ginghina C., Hong Z., Yearout D., Chung K.A., Quinn J.F., Peskind E.R., Galasko D., Jankovic J., Leverenz J.B., and Zhang J. (2010). Significance and confounders of peripheral DJ-1 and alpha-synuclein in Parkinson's disease. Neuroscience letters *480*, 78-82.

Shioya M., Obayashi S., Tabunoki H., Arima K., Saito Y., Ishida T., and Satoh J. (2010). Aberrant microRNA expression in the brains of neurodegenerative diseases: miR-29a decreased in Alzheimer disease brains targets neurone navigator 3. Neuropathology and applied neurobiology *36*, 320-330.

Simon D., Garcia-Garcia E., Royo F., Falcon-Perez J.M., and Avila J. (2012). Proteostasis of tau. Tau overexpression results in its secretion via membrane vesicles. FEBS letters *586*, 47-54.

Singleton A.B., Farrer M., Johnson J., Singleton A., Hague S., Kachergus J., Hulihan M., Peuralinna T., Dutra A., Nussbaum R., Lincoln S., Crawley A., Hanson M., Maraganore D., Adler C., et al. (2003). alpha-Synuclein locus triplication causes Parkinson's disease. Science *302*, 841.

Skog J., Wurdinger T., van Rijn S., Meijer D.H., Gainche L., Sena-Esteves M., Curry W.T., Jr., Carter B.S., Krichevsky A.M., and Breakefield X.O. (2008). Glioblastoma microvesicles transport RNA and proteins that promote tumour growth and provide diagnostic biomarkers. Nature cell biology *10*, 1470-1476.

Smith P., Al Hashimi A., Girard J., Delay C., and Hebert S.S. (2011). In vivo regulation of amyloid precursor protein neuronal splicing by microRNAs. Journal of neurochemistry *116*, 240-247.

Spies P.E., Melis R.J., Sjogren M.J., Rikkert M.G., and Verbeek M.M. (2009). Cerebrospinal fluid alpha-synuclein does not discriminate between dementia disorders. Journal of Alzheimer's disease : JAD *16*, 363-369.

Spillantini M.G., Crowther R.A., Jakes R., Hasegawa M., and Goedert M. (1998). alpha-Synuclein in filamentous inclusions of Lewy bodies from Parkinson's disease and dementia with lewy bodies. Proceedings of the National Academy of Sciences of the United States of America *95*, 6469-6473.

Spillantini M.G., Schmidt M.L., Lee V.M., Trojanowski J.Q., Jakes R., and Goedert M. (1997). Alpha-synuclein in Lewy bodies. Nature *388*, 839-840.

Stenmark H. (2009). Rab GTPases as coordinators of vesicle traffic. Nature reviews Molecular cell biology *10*, 513-525.

Stoorvogel W., Strous G.J., Geuze H.J., Oorschot V., and Schwartz A.L. (1991). Late endosomes derive from early endosomes by maturation. Cell *65*, 417-427.

Strauss K., Goebel C., Runz H., Mobius W., Weiss S., Feussner I., Simons M., and Schneider A. (2010). Exosome secretion ameliorates lysosomal storage of cholesterol in Niemann-Pick type C disease. The Journal of biological chemistry *285*, 26279-26288.

Street J.M., Barran P.E., Mackay C.L., Weidt S., Balmforth C., Walsh T.S., Chalmers R.T., Webb D.J., and Dear J.W. (2012). Identification and proteomic profiling of exosomes in human cerebrospinal fluid. Journal of translational medicine *10*, 5.

Stuendl A., Kunadt M., Kruse N., Bartels C., Moebius W., Danzer K.M., Mollenhauer B., and Schneider A. (2016). Induction of alpha-synuclein aggregate formation by CSF exosomes from patients with Parkinson's disease and dementia with Lewy bodies. Brain : a journal of neurology *139*, 481-494.

Stuffers S., Sem Wegner C., Stenmark H., and Brech A. (2009). Multivesicular endosome biogenesis in the absence of ESCRTs. Traffic *10*, 925-937.

Thery C., Amigorena S., Raposo G., and Clayton A. (2006). Isolation and characterization of exosomes from cell culture supernatants and biological fluids. Current protocols in cell biology / editorial board, Juan S Bonifacino [et al] *Chapter 3*, Unit 3 22.

Thery C., Boussac M., Veron P., Ricciardi-Castagnoli P., Raposo G., Garin J., and Amigorena S. (2001). Proteomic analysis of dendritic cell-derived exosomes: a secreted subcellular compartment distinct from apoptotic vesicles. J Immunol *166*, 7309-7318.

Thery C., Ostrowski M., and Segura E. (2009). Membrane vesicles as conveyors of immune responses. Nature reviews Immunology *9*, 581-593.

Tokuda T., Qureshi M.M., Ardah M.T., Varghese S., Shehab S.A., Kasai T., Ishigami N., Tamaoka A., Nakagawa M., and El-Agnaf O.M. (2010). Detection of elevated levels of alpha-synuclein oligomers in CSF from patients with Parkinson disease. Neurology *75*, 1766-1772.

Tokuda T., Salem S.A., Allsop D., Mizuno T., Nakagawa M., Qureshi M.M., Locascio J.J., Schlossmacher M.G., and El-Agnaf O.M. (2006). Decreased alpha-synuclein in cerebrospinal fluid of aged individuals and subjects with Parkinson's disease. Biochemical and biophysical research communications *349*, 162-166.

Tomlinson C.L., Stowe R., Patel S., Rick C., Gray R., and Clarke C.E. (2010). Systematic review of levodopa dose equivalency reporting in Parkinson's disease. Movement disorders : official journal of the Movement Disorder Society *25*, 2649-2653.

Trajkovic K., Hsu C., Chiantia S., Rajendran L., Wenzel D., Wieland F., Schwille P., Brugger B., and Simons M. (2008). Ceramide triggers budding of exosome vesicles into multivesicular endosomes. Science *319*, 1244-1247.

Tsunemi T., Hamada K., and Krainc D. (2014). ATP13A2/PARK9 regulates secretion of exosomes and alpha-synuclein. The Journal of neuroscience : the official journal of the Society for Neuroscience *34*, 15281-15287.

Ulusoy A., Rusconi R., Perez-Revuelta B.I., Musgrove R.E., Helwig M., Winzen-Reichert B., and Di Monte D.A. (2013). Caudo-rostral brain spreading of alpha-synuclein through vagal connections. EMBO molecular medicine *5*, 1051-1059.

Valadi H., Ekstrom K., Bossios A., Sjostrand M., Lee J.J., and Lotvall J.O. (2007). Exosome-mediated transfer of mRNAs and microRNAs is a novel mechanism of genetic exchange between cells. Nature cell biology *9*, 654-659.

Vallelunga A., Ragusa M., Di Mauro S., Iannitti T., Pilleri M., Biundo R., Weis L., Di Pietro C., De Iuliis A., Nicoletti A., Zappia M., Purrello M., and Antonini A. (2014). Identification of

circulating microRNAs for the differential diagnosis of Parkinson's disease and Multiple System Atrophy. Frontiers in cellular neuroscience *8*, 156.

van Niel G., Charrin S., Simoes S., Romao M., Rochin L., Saftig P., Marks M.S., Rubinstein E., and Raposo G. (2011). The tetraspanin CD63 regulates ESCRT-independent and -dependent endosomal sorting during melanogenesis. Developmental cell *21*, 708-721.

van Niel G., Raposo G., Candalh C., Boussac M., Hershberg R., Cerf-Bensussan N., and Heyman M. (2001). Intestinal epithelial cells secrete exosome-like vesicles. Gastroenterology *121*, 337-349.

Vargas K.J., Makani S., Davis T., Westphal C.H., Castillo P.E., and Chandra S.S. (2014). Synucleins regulate the kinetics of synaptic vesicle endocytosis. The Journal of neuroscience : the official journal of the Society for Neuroscience *34*, 9364-9376.

Vella L.J., Hill A.F., and Cheng L. (2016). Focus on Extracellular Vesicles: Exosomes and Their Role in Protein Trafficking and Biomarker Potential in Alzheimer's and Parkinson's Disease. International journal of molecular sciences *17*.

Vidal M., Mangeat P., and Hoekstra D. (1997). Aggregation reroutes molecules from a recycling to a vesicle-mediated secretion pathway during reticulocyte maturation. Journal of cell science *110 (Pt 16)*, 1867-1877.

Villarroya-Beltri C., Gutierrez-Vazquez C., Sanchez-Cabo F., Perez-Hernandez D., Vazquez J., Martin-Cofreces N., Martinez-Herrera D.J., Pascual-Montano A., Mittelbrunn M., and Sanchez-Madrid F. (2013). Sumoylated hnRNPA2B1 controls the sorting of miRNAs into exosomes through binding to specific motifs. Nature communications *4*, 2980.

Vingtdeux V., Hamdane M., Loyens A., Gele P., Drobeck H., Begard S., Galas M.C., Delacourte A., Beauvillain J.C., Buee L., and Sergeant N. (2007). Alkalizing drugs induce accumulation of amyloid precursor protein by-products in luminal vesicles of multivesicular bodies. The Journal of biological chemistry *282*, 18197-18205.

Volpicelli-Daley L.A., Luk K.C., Patel T.P., Tanik S.A., Riddle D.M., Stieber A., Meaney D.F., Trojanowski J.Q., and Lee V.M. (2011). Exogenous alpha-synuclein fibrils induce Lewy body pathology leading to synaptic dysfunction and neuron death. Neuron *72*, 57-71.

Wang S., Cesca F., Loers G., Schweizer M., Buck F., Benfenati F., Schachner M., and Kleene R. (2011). Synapsin I is an oligomannose-carrying glycoprotein, acts as an oligomannose-binding lectin, and promotes neurite outgrowth and neuronal survival when released via glia-derived exosomes. The Journal of neuroscience : the official journal of the Society for Neuroscience *31*, 7275-7290.

Weinreb P.H., Zhen W., Poon A.W., Conway K.A., and Lansbury P.T., Jr. (1996). NACP, a protein implicated in Alzheimer's disease and learning, is natively unfolded. Biochemistry *35*, 13709-13715.

Wennstrom M., Surova Y., Hall S., Nilsson C., Minthon L., Bostrom F., Hansson O., and Nielsen H.M. (2013). Low CSF levels of both alpha-synuclein and the alpha-synuclein cleaving enzyme neurosin in patients with synucleinopathy. PloS one *8*, e53250.

Williams R.L., and Urbe S. (2007). The emerging shape of the ESCRT machinery. Nature reviews Molecular cell biology *8*, 355-368.

Winblad B., Palmer K., Kivipelto M., Jelic V., Fratiglioni L., Wahlund L.O., Nordberg A., Backman L., Albert M., Almkvist O., Arai H., Basun H., Blennow K., de Leon M., DeCarli C., et al. (2004). Mild cognitive impairment--beyond controversies, towards a consensus: report of the International Working Group on Mild Cognitive Impairment. Journal of internal medicine *256*, 240-246.

Yuyama K., Sun H., Mitsutake S., and Igarashi Y. (2012). Sphingolipid-modulated exosome secretion promotes clearance of amyloid-beta by microglia. The Journal of biological chemistry *287*, 10977-10989.

Yuyama K., Sun H., Sakai S., Mitsutake S., Okada M., Tahara H., Furukawa J., Fujitani N., Shinohara Y., and Igarashi Y. (2014). Decreased amyloid-beta pathologies by intracerebral loading of glycosphingolipid-enriched exosomes in Alzheimer model mice. The Journal of biological chemistry *289*, 24488-24498.

Zarranz J.J., Alegre J., Gomez-Esteban J.C., Lezcano E., Ros R., Ampuero I., Vidal L., Hoenicka J., Rodriguez O., Atares B., Llorens V., Gomez Tortosa E., del Ser T., Munoz D.G., and de Yebenes J.G. (2004). The new mutation, E46K, of alpha-synuclein causes Parkinson and Lewy body dementia. Annals of neurology *55*, 164-173.

Zhang Z., Qin Y.W., Brewer G., and Jing Q. (2012). MicroRNA degradation and turnover: regulating the regulators. Wiley interdisciplinary reviews RNA *3*, 593-600.

Zhuang X., Xiang X., Grizzle W., Sun D., Zhang S., Axtell R.C., Ju S., Mu J., Zhang L., Steinman L., Miller D., and Zhang H.G. (2011). Treatment of brain inflammatory diseases by delivering exosome encapsulated anti-inflammatory drugs from the nasal region to the brain. Molecular therapy : the journal of the American Society of Gene Therapy *19*, 1769-1779.

Zitvogel L., Regnault A., Lozier A., Wolfers J., Flament C., Tenza D., Ricciardi-Castagnoli P., Raposo G., and Amigorena S. (1998). Eradication of established murine tumors using a novel cell-free vaccine: dendritic cell-derived exosomes. Nature medicine *4*, 594-600.

6. Appendix

6.1. Demographics of CSF and plasma samples used for the analysis of α-Synuclein in exosomes

Table 6.1: Demographics of analyzed CSF samples of the DeNoPa cohort

Mean ± standard deviation (range)	**Parkinson`s disease**	**healthy Controls**
numbers	76	58
age (years)	65 ± 8.8 (40–84)	66 ± 6.4 (52–84)
gender (female/total)	0.65	0.65
duration of disease (months)	22 ± 27 (4–210)	not defined
Hoehn and Yahr stage	1.7 ± 0.6 (1–3)	not defined
Mini-Mental State Examination (MMSE)	28.6 ± 1.3 (23–30)	28.7 ± 1.2 (26–30)

Table 6.2: Demographics of analyzed CSF samples of the Kassel cohort

Mean ± standard deviation (range)	**PD**	**PNP**	**PSP**	**DLB[1]**
numbers	37	15	25	35
age (years)	73 ± 7.9 (51–84)	67 ± 14 (34–84)	70 ± 7 (59–83)	72 ± 6.85 (55–84)
gender (female/total)	0.7	0.4	0.8	0.4
duration of disease (months)	77 ± 71 (10–300)	69 ± 79 (9–240)	53 ± 36 (12–120)	60 ± 80 (12–140)
Hoehn and Yahr stage	3.9 ± 1.2 (1–5)	not defined	not defined	not defined
Levodopaequivalent dosage (mg)[2]	557 ± 496 (0–2000)	not defined	not defined	not defined
Mini-Mental State Examination (MMSE)	not defined	not defined	not defined	18 ± 6.73 (5–27)

[1] 3 of 35 CSF samples were collected at the Göttingen site

[2] Tomlinson et al. (2010): Systematic review of levodopa dose equivalency reporting in Parkinson's disease

Table 6.3: Demographics of analyzed plasma samples of the Kassel cohort

Mean ± standard deviation (range)	**PD**	**DLB**	**Neurol. Controls**
numbers	23	9	23
age (years)	73 ± 8.3 (51–83)	73 ± 6.3 (63–84)	70 ± 10.8 (34–84)
gender (female/total)	0.3	0.7	0.4
duration of disease (months)	98 ± 85 (11–336)	60 ± 20 (24–96)	71 ± 60 (24–240)
Hoehn and Yahr stage	3.6 ± 1.2 (1–5)	3.6 ± 0.8 (3–5)	not defined
Mini-Mental State Examination (MMSE)	22.2 ± 7.5 (5–29)	21.8 ± 5.1 (13–27)	not defined

6.2. Demographics of CSF samples used for small RNA sequencing

Table 6.4: Demographics of analyzed CSF samples of the test cohort

Mean ± standard deviation (range)	**Alzeimer`s disease**	**Controls**
numbers	24	18
age (years)	72 ± 6.4 (60–84)	61 ± 8.4 (48–77)
gender (female/total)	0.5	0.67
Mini-Mental State Examination (MMSE)	22.6 ± 5.0 (8–28)	not defined
Depression/total	not defined	0.61

Table 6.5: Demographics of analyzed CSF samples of the replication cohort

Mean ± standard deviation (range)	**Alzeimer`s disease[1]**	**Controls[2,3]**
numbers	21	20
age (years)	71 ± 7.9 (53–81)	67 ± 9.7 (53–84)
gender (female/total)	0.33	0.55
Mini-Mental State Examination (MMSE)	23.7 ± 2.7 (17–28)	not defined
Depression/total	not defined	0.45

[1] 2 of 21 CSF samples were collected at the Tübingen site

[2] 4 of 20 CSF samples were collected at the Tübingen site and 6 samples at the Kassel site

[3] 7 controls were obtained from healthy subjects without any neurological disorder.

Curriculum vitae

Anne-Katrin Stündl

Date of birth	27. April 1986
Place of birth	Giessen

Education

06/2012 – present	**Georg-August University Göttingen, Germany** **GGNB PhD program "Molecular Physiology of the Brain"** PhD Thesis in the Department of Psychiatry, University Medical Center Göttingen and German Center for Neurodegenerative Diseases (DZNE) Göttingen under supervision of Prof. Dr. Anja Schneider
10/2006 – 12/2011	**Philipps-University Marburg, Germany** Diploma degree in Human Biology/Biomedical Sciences with the major subject *Neurosciences* and minor subject *Human Genetics*
08/1996 – 07/2005	**Landgraf-Ludwigs-Gymnasium Giessen, Germany** Graduation „Allgemeine Hochschulreife"

Publications

Stuendl A., Kunadt M., Kruse N., Bartels C., Moebius W., Danzer K.M., Mollenhauer B., and Schneider A. (2016). Induction of alpha-synuclein aggregate formation by CSF exosomes from patients with Parkinson's disease and dementia with Lewy bodies. Brain: a journal of neurology *139*, 481-494.

Kunadt M., Eckermann K., **Stuendl A.**, Gong J., Russo B., Strauss K., Rai S., Kugler S., Falomir Lockhart L., Schwalbe M., Krumova P., Oliveira L.M., Bahr M., Mobius W., (…), Weishaupt J.H., Schneider A. (2015). Extracellular vesicle sorting of alpha-Synuclein is regulated by sumoylation. Acta neuropathologica *129*, 695-713.

Rezaei-Ghaleh N., Amininasab M., Giller K., Kumar S., **Stündl A.**, Schneider A., Becker S., Walter J., Zweckstetter M. (2014). Turn plasticity distinguishes different modes of amyloid-β aggregation. J. Am. Chem. Soc. *136*, 4913-4919.

Roeder AM., Roettger Y., **Stündl A.**, Dodel R., Geyer A. (2013). Synthetic dimeric Aβ(28-40) mimics the complex epitope of human anti-Aβ autoantibodies against toxic Aβ oligomers. J. Biol. Chem. *288*, 27638-27645.